Mitigation of Seismic Risk pertaining to Non-Ductile Reinforced Concrete Buildings using Seismic Risk Maps

Matthew J. Zahr
University of California, Berkeley

Nicolas Luco
Research Structural Engineer
USGS Geologic Hazards Science Center
Golden, CO

Hyeuk Ryu
Postdoctoral Researcher
Stanford University

ABSTRACT

This report discusses the creation, improvement, and application of a web-based seismic risk map tool developed at the USGS in Golden, CO.

Reinforced concrete buildings built in the western United States prior to implementation of modern seismic code standards in 1976 typically behave in a non-ductile manner under seismic loading, which can lead to catastrophic failure. The high degree of seismic hazard in the western United States makes retrofitting such non-ductile concrete buildings a necessity. Due to the associated cost and time, it is virtually impossible to exhaustively mitigate the seismic risk created by these older concrete buildings. This has motivated the development and improvement of a web-based seismic risk map tool as a way to prioritize retrofits. This tool provides a means to quickly identify the regions of the US where non-ductile concrete buildings are at a high risk of failure. Furthermore, with an inventory of non-ductile concrete buildings for a particular area, the buildings at the highest risk in that area can be pinpointed for seismic retrofit.

Keywords/Phrases: seismic hazard, fragility, vulnerability, risk, HAZUS, risk maps, general risk maps, difference maps, inventory-specific risk maps, non-ductile concrete buildings, loss ratio, damage state, code level, structural type, catastrophic failure, site class, inventory, mean annual frequency of exceedance (MAFE), United States Geologic Survey (USGS)

CONTENTS

1 INTRODUCTION

In 1971, an earthquake in the San Fernando area caused a excessive amount of damage, in terms of monetary loss and casualties, due mainly to the collapse of some older concrete buildings. The most notable collapse, which resulted in the greatest number of casualties, was the concrete Veteran's Administration Hospital (http://www.data.scec.org/chrono_index/sanfer.html). Post-earthquake investigations revealed that a vast majority of the concrete buildings that collapsed were built with too much spacing between stirrups and inadequate flexural reinforcement, which caused them to behave in a non-ductile manner and fail catastrophically. In response to the damage and casualties resulting from the 1971 San Fernando earthquake, building codes were updated to increase the ductility of concrete buildings during the cyclic loading caused by earthquakes. Therefore, concrete buildings constructed after 1976 have a relatively high degree of ductility, which lessens their risk of catastrophic failure (Faison 2008). However, the non-ductile concrete problem still exists with buildings constructed prior to the building code revisions. Retrofitting all of these buildings to an acceptable level of seismic protection consistent with the current building code is an insurmountable task due to the sheer number of substandard buildings and the costs of retrofitting.

"50% of the casualties are coming from 5% of the buildings"

Kircher et al., "Estimated Losses due to a Repeat of the 1908 San Francisco Earthquake," Earthquake Spectra, 2006

Due to the high costs of retrofitting buildings, it is necessary to answer a few important questions that can be posed in relation to the quote above:

- ❖ Which buildings make up the 5%? How do we pinpoint the most problematic and risky buildings?
- ❖ Once we identify the 5%, which ones should we retrofit first?
- ❖ If we do these retrofits, how much will they really reduce the risk of damage and loss?

These questions, among others, have motivated the creation and improvement of a web-based seismic risk map tool.

Before presenting case studies that portray the utility and functionality of the risk maps, it is helpful to discuss the various components of risk and how they are combined. Risk can be thought of as a combination of four components: Hazard, Exposure to Hazard, Fragility/Vulnerability, and Resilience, all but one of which will be described next. Exposure to hazard, or inventory of buildings considered, whether hypothetical or real, is described later within Sections 2 and 3.

1.1 Hazard

Probabilistic hazard pertaining to earthquake risk is most typically presented in the form of a seismic hazard curve at a particular location. A hazard curve provides the mean annual frequency of exceedance (MAFE)[1] for each in an array of ground motion levels (spectral acceleration values at a particular period of oscillation). As shown in Figure 1 for an example, hazard curves are usually plotted on a logarithmic scale on the abscissa and ordinate.

[1] For the rest of this report, probability of exceedance in 1 year will be used interchangeably with mean annual frequency of exceedance (MAFE); numerically these two quantities are approximately equal when they are both small, under the assumption of a Poisson process described later in the report.

The USGS computes hazard curves on a grid of 0.05 latitude and longitude units covering the continental US, as well as Alaska, Hawaii, and Puerto Rico and the Virgin Islands. While the USGS computes hazard curves for reference ground characteristics, or a reference site class, hazard curves are highly dependent on the ground characteristics that exist at its location, which will be discussed in the next section.

Figure 1: Example Hazard Curve for a location in the San Francisco Bay Area and a spectral period of 1s

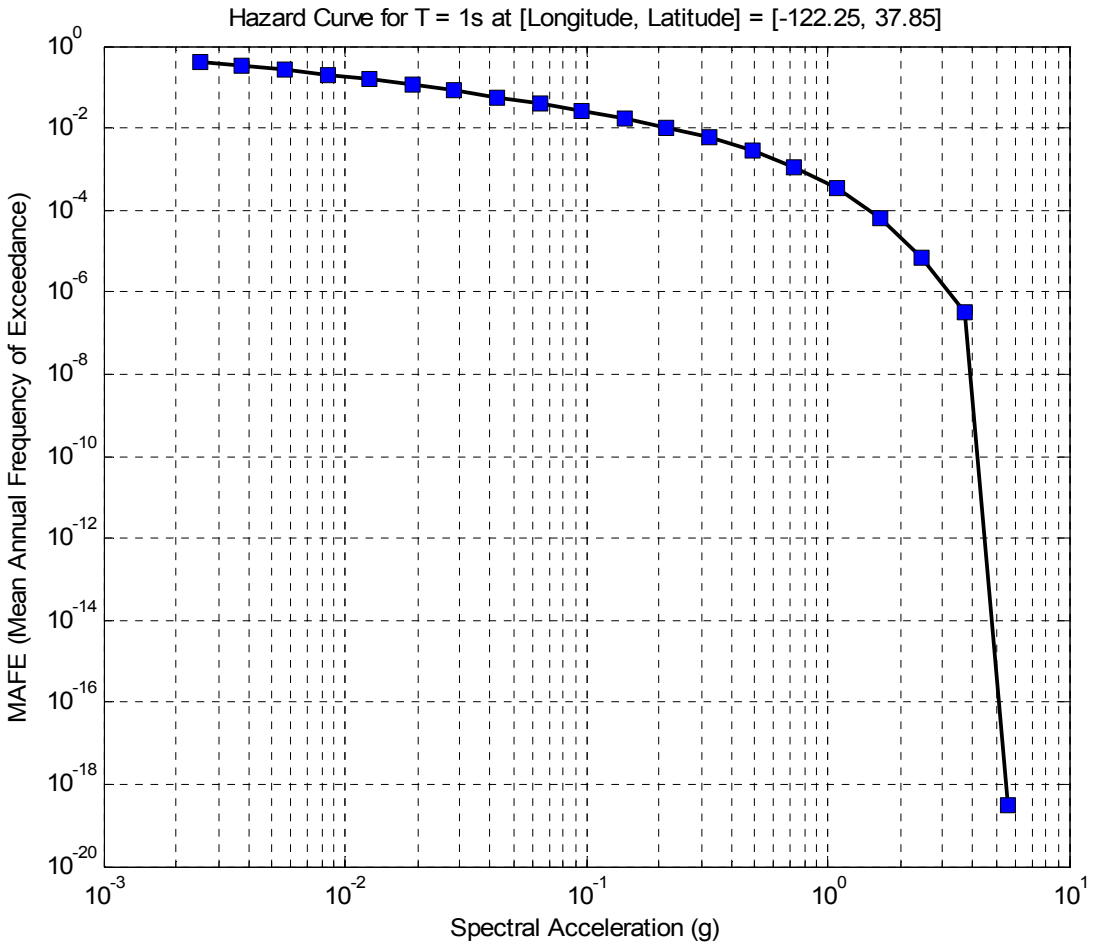

1.1.1 Site Class

The National Earthquake Hazards Reduction Program (NEHRP) *Recommended Provisions for Seismic Regulations for New Buildings and Other Structures* specifies five site classes in order to easily categorize and generalize ground characteristics.. The five

site classes are listed in Table 1, along with the V_S30 ranges that can be used to define each of them. V_S30 is the average shear-wave velocity over a depth of 30 meters below the surface. Wald and Allen (2007) have estimated V_S30 values for all of the continental United States based on topography, which we have used to determine a site classe for each point on the USGS grid covering the continental US. Figure 2 is a map of the results.

Table 1: Site Class descriptions and their V_S30 ranges

Site Class	Soil Profile Name	Soil shear wave velocity, V_S30 (m/s)
A	Hard rock	$V_S30 > 1500$
B	Rock	$1500 \geq V_S30 \geq 760$
C	Very dense soil and soft rock	$760 > V_S30 > 360$
D	Stiff soil profile	$360 \geq V_S30 > 180$
E	Soft soil profile	$180 \geq V_S30$

Figure 2: Site class distribution in the continental US

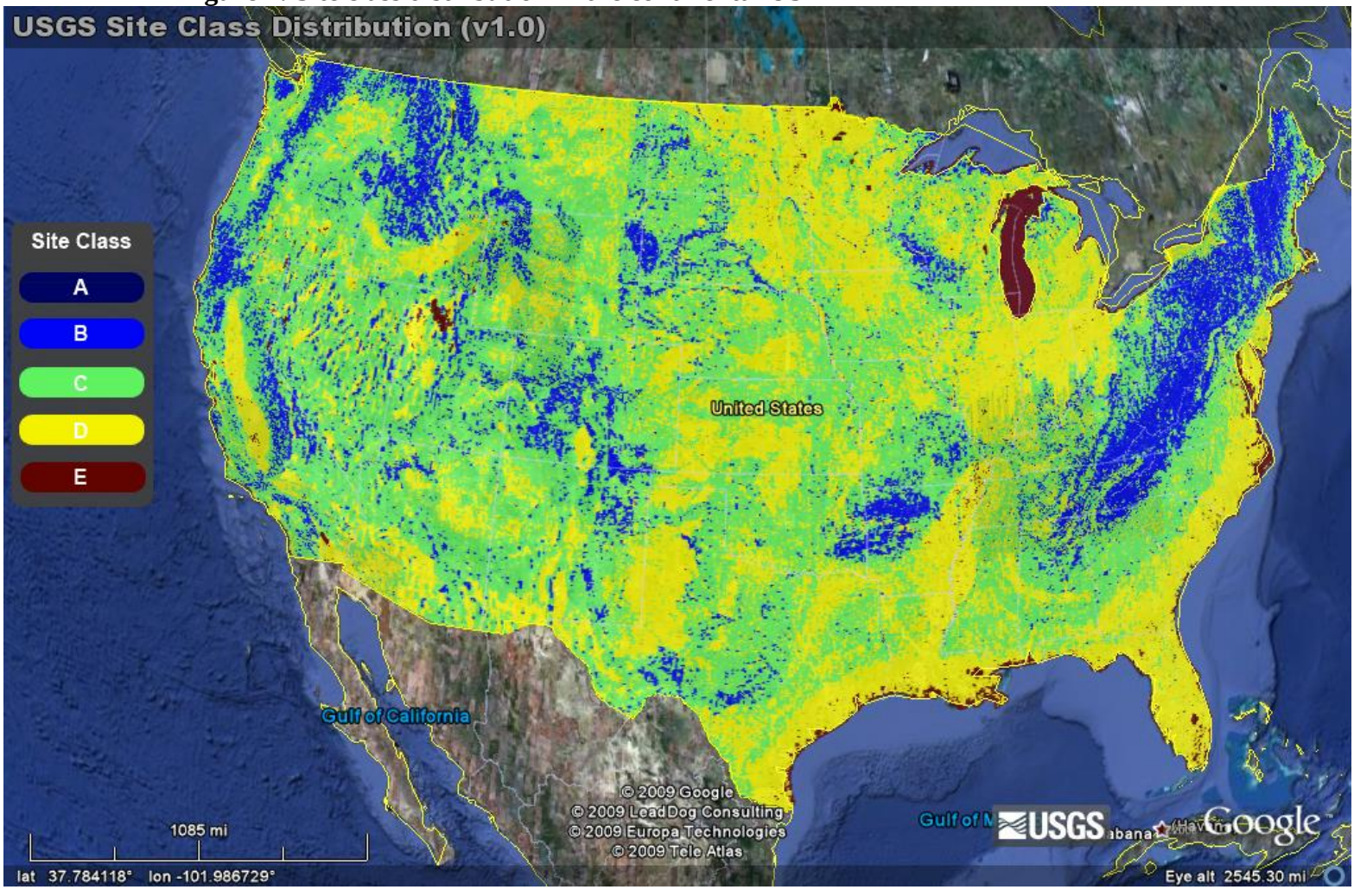

1.1.2 Site Class Effects on Hazard

As alluded to above, the USGS hazard curves have been computed for V_S30=760m/s, the boundary between site classes B and C. This was necessary because hazard curves for smaller V_S30 values (e.g., site calss D) could not be computed for the entire continental US given the available ground motion prediction models used. Obviously, though, the reference V_S30 is not an accurate representation of the site class distribution in the continental US.

Using the site class map shown in Figure 2, we have adjusted the USGS hazard curves (for V_S30=760m/s) for the site class at each location. The NEHRP *Recommended Provisions* defines two different tables (Tables 2 and 3 below) of coefficients for adjusting ground motions based on site class, albeit approximately. The coefficients in Table 2 are specific to spectral response acceleration at short periods and are denoted as F_a values. Table 3 is to be used for spectral response acceleration at longer periods, denoted as F_v values. For simplicity, we have used a period of 0.5 seconds as the cut-off between the "short" and "long" periods (i.e. $T \leq 0.5$ seconds are short periods and $T > 0.5$ seconds are long periods). Note that the site coefficients are further categorized based on spectral acceleration. For spectral acceleration values in between those specified in Tables 2 and 3, it is standard to linearly interpolate the coefficients.

Table 2: 2003 NEHRP *Provisions* site class coefficients for short periods

Site Class	VALUES OF SITE COEFFICIENT F_a				
	MAPPED SPECTRAL RESPONSE ACCELERATION AT SHORT PERIOD				
	SA ≤ 0.25	SA = 0.50	SA = 0.75	SA = 1.00	SA ≥ 1.25
A	0.8	0.8	0.8	0.8	0.8
B	1.0	1.0	1.0	1.0	1.0
C	1.2	1.2	1.1	1.0	1.0
D	1.6	1.4	1.2	1.1	1.0
E	2.5	1.7	1.2	0.9	0.9

Table 3: 2003 NEHRP *Provisions* site class coefficients for long periods

Site Class	VALUES OF SITE COEFFICIENT F_v				
	MAPPED SPECTRAL RESPONSE ACCELERATION AT 1s PERIOD				
	SA ≤ 0.25	SA = 0.50	SA = 0.75	SA = 1.00	SA ≥ 1.25
A	0.8	0.8	0.8	0.8	0.8
B	1.0	1.0	1.0	1.0	1.0
C	1.7	1.6	1.5	1.4	1.3
D	2.4	2.0	1.8	1.6	1.5
E	3.5	3.2	2.8	2.4	2.4

To adjust the USGS hazard curves, these coefficients are applied to the spectral acceleration values of the curves, not the MAFE values. The procedure used to adjust for site class can be broken down into the following 6 steps:

1) Determine the site class at the location of interest using V_S30 values and Table 1.
2) Based on the period of spectral response acceleration of interest, determine whether to use coefficients from Table 2 or 3.
3) Multiply each spectral acceleration value of the hazard curve on the abscissa by the appropriate coefficient based on Table 2 or 3.
4) Using the original MAFE values and the adjusted spectral acceleration values from Step 3, linearly interpolate (in log-log scale) to calculate new MAFE values that correspond to the original spectral acceleration values.
5) These new MAFE values and the original spectral acceleration values define the new site-adjusted hazard curve for the location of interest.

Using this process, five new hazard curves files were generated from the existing USGS hazard curves for the continental US. Four of the five hazard files are similar to the existing file in the sense that they are for a single site class. However, each new file was adjusted for a different site class, resulting in what we call "site-general" hazard data for the continental US for each of the five site classes (A-E). Using these five site-general

files in conjunction with the V_S30 values in Figure 2 and corresponding site classes defined in Table 1, a single hazard curve file was created that contains the adjusted hazard curve at each location based on the site class that exists there.

1.2 Fragility/Vulnerability

The fragility/vulnerability component of risk will be described in Sections 1.2.2 (fragility) and 1.2.3 (vulnerability) below, but described first are the HAZUS building types for which generic fragility/vulnerability curves have been, and are being developed by the USGS..

1.2.1 HAZUS Building Types

The USGS has developed (e.g., Karaca & Luco, 2009), and continues to develop (e.g., Ryu et al, 2008), fragility/vulnerability models for the generic building types defined in the multi-hazard risk analysis methodology, HAZUS. HAZUS designates 36 structural types, 4 code levels, and 33 occupancy types. The different structural types correspond to various building heights, construction materials, and lateral force-resisting systems, such as those in Table 4. The 4 code levels correspond to the levels of seismic design, as listed in Table 5.. Finally, the 33 occupancy types correspond to different uses of buildings, e.g., offices. In HAZUS, buildings are composed of three components: structural, drift-sensitive nonstructural, and acceleration-sensitive nonstructural. The vulnerability models we use in this report include all three components, whereas we focus on the structural components for the fragility curves.

The focus of this project report is risk associated with non-ductile concrete structures, but HAZUS does not have an explicit structural type corresponding to non-ductile concrete. For the remainder of this report, it is assumed that all concrete structures in HAZUS are considered non-ductile when built at pre-code levels. Concrete structures

built at high-code specifications will be considered ductile, while the low- and moderate-code levels will be de-emphasized as transitions between ductile and non-ductile. A limited summary of the HAZUS concrete structures is provided in Tables 4 –6. For more information on the HAZUS building types, including occupancy type descriptions, refer to the HAZUS-MH MR3 Technical Manual.

Table 4: Summary of HAZUS Concrete Structural Types

Label	Description	Height	
		Name	# Stories
C1L	Concrete Moment Frame	Low-Rise	1 - 3
C1M		Mid-Rise	4 - 7
C1H		High-Rise	8+
C2L	Concrete Shear Walls	Low-Rise	1 - 3
C2M		Mid-Rise	4 - 7
C2H		High-Rise	8+
C3L	Concrete Frame with Unreinforced Masonry Infill Walls	Low-Rise	1 - 3
C3M		Mid-Rise	4 - 7
C3H		High-Rise	8+

Table 5: Summary of HAZUS Levels of Seismic Design (i.e. Code Levels)

Seismic Level of Design	Description	Affect on HAZUS Concrete Structures
Pre-Code	Minimal Strength Minimal Ductility	Non-Ductile
Low-Code	Low Strength Low Ductility	Fairly Non-Ductile
Moderate-Code*	Moderate Strength Moderate Ductility	Fairly Ductile
High-Code*	High Strength High Ductility	Ductile

*Note: These code levels do not exist for C3L, C3M, and C3H structural types

1.2.2 Fragility

Fragility, pertaining to earthquake risk, is the conditional probability of exceeding a particular damage state in a structure given a certain ground motion (spectral acceleration at a particular period of oscillation). The fragilities developed by the USGS are for a specific HAZUS building type, height, and code level. Four damage states defined in HAZUS are considered: Slight, Moderate, Extensive, and Complete; each damage state corresponds to different visual levels of damage and an approximate ratio of repair cost to replacement cost (defined as the loss ratio). For the concrete building types in HAZUS, descriptions of the four damage states are provided in Table 6..

The USGS fragility functions derived by Karaca and Luco (2008) are considered generic in that they are derived using generic structural properties and are loosely based on the past performance of buildings with similar structural designs. These fragility curves were developed by first using probabilistic estimation of inelastic spectral displacement for a range of spectral acceleration values to define building response. Then, building performance was estimated in terms of damage state exceedance for a given building response. The final fragility curves were created by properly combining this information. Unlike hazard curves, fragilities are not defined at a particular point on a grid; each fragility exists for all structures of the same structural type, height, and code level. While fragilities are often lognormal cumulative distribution functions, those derived by Karaca and Luco (2008) are non-parametric.

Figure 3 displays the fragility curves for the HAZUS concrete structural types sustaining complete damage. That is, Figure 3 displays the probability of exceeding the complete damage as a function of spectral acceleration for a given concrete lateral force-

resisting system, height, and seismic level of design. By plotting the fragilities for different code levels on a single graph, ductile versus non-ductile affects on fragility become apparent. In Figure 3 and for the remainder of the report, a 0.5-second period of spectral acceleration is used for low-rise building fragilities, a 1.0-second period is used for mid-rise buildings, and 2.0 seconds is used for high-rise buildings. The fragility functions in Figure 3 are specific to the structural components (STR) of the various concrete structural systems.

Table 6: Summary of HAZUS Damage States for Concrete Buildings

Damage State	Description	Quantification
Slight	Flexural or Shear hairline cracks in some beams/columns near or within joints	~0%-5% of Replacement Cost
Moderate	Most beams/columns exhibit hairline cracks. Some larger cracks indicating yield capacity has been exceeded.	~5%-25% of Replacement Cost
Extensive	Some elements have large flexural cracks and spalling indicating ultimate strength has been reached. Some shear failures. Partial collapse may result.	~25%-100% of Replacement Cost
Complete	Structure is collapsed or in imminent danger of collapse due to brittle failure of non-ductile elements.	~100% of Replacement Cost

Figure 3: Concrete Fragility Curves for Complete Damage State

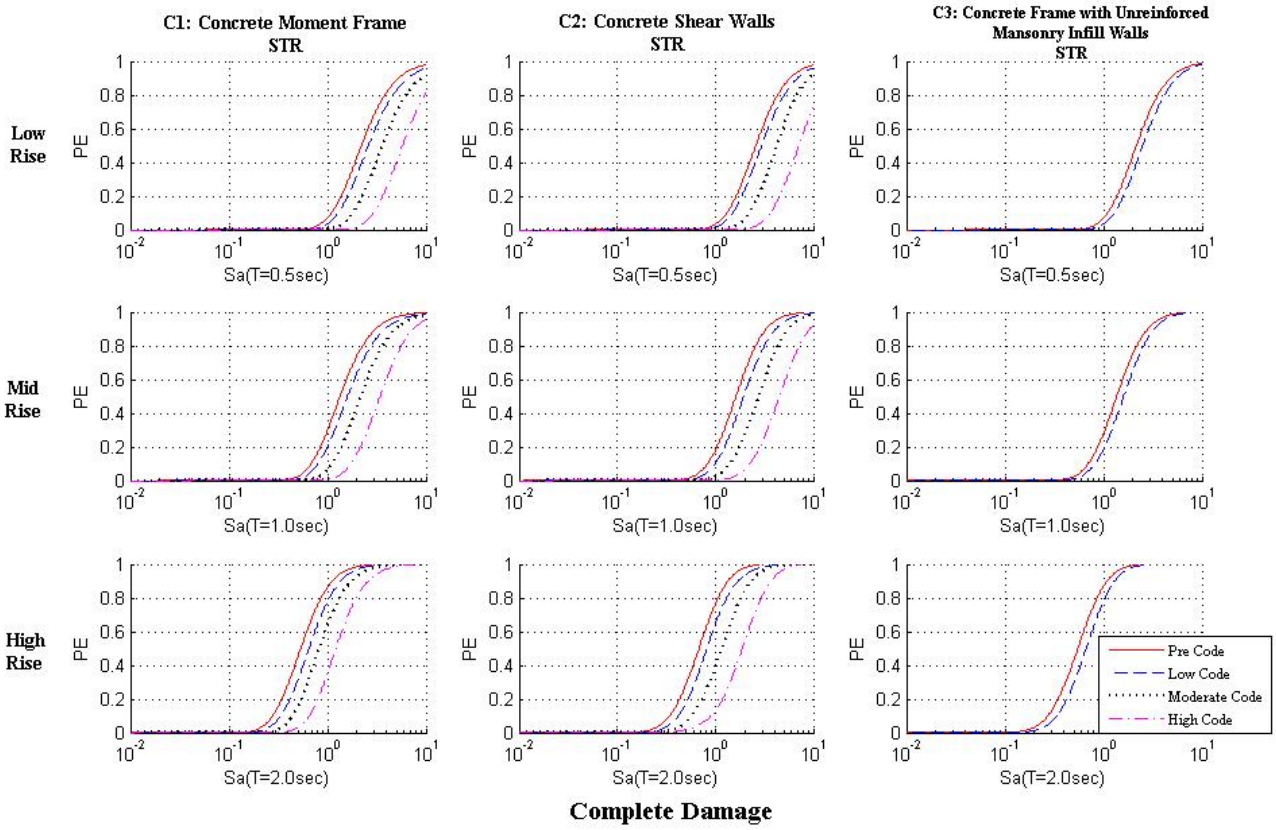

1.2.3 Vulnerability

A vulnerability curve provides the expected value of loss ratio for a given spectral acceleration. In effect, a vulnerability curve is a weighted summation of the loss for all damage states, where the weights are from the fragilities described in the preceding section. Vulnerability curves differs from fragility curves in that they are for a given occupancy type, since the loss ratio for a given damage state depends on the use of a building,. Like fragility curves, the vulnerabilities are for a given structural type, height, and code level. They are calculated as the sum of the expected loss to each building component. Randomness about this expected value can be considered (e.g., see Karaca and Luco, 2008), but has not been in this project. Vulnerability is similar to fragility in

that it contains no information about the location of the building (and therefore no hazard information).

Similar to Figure 3, Figure 4 provides for a direct comparison between the vulnerabilities of ductile (high-code) and non-ductile (pre-code) concrete structures. Figure 4 presents the vulnerabilities for concrete office buildings (i.e. C1, C2, or C3 structural type and COM4 occupation type).

Figure 4: Concrete Vulnerability Functions for COM4 (Offices) Occupancy Type

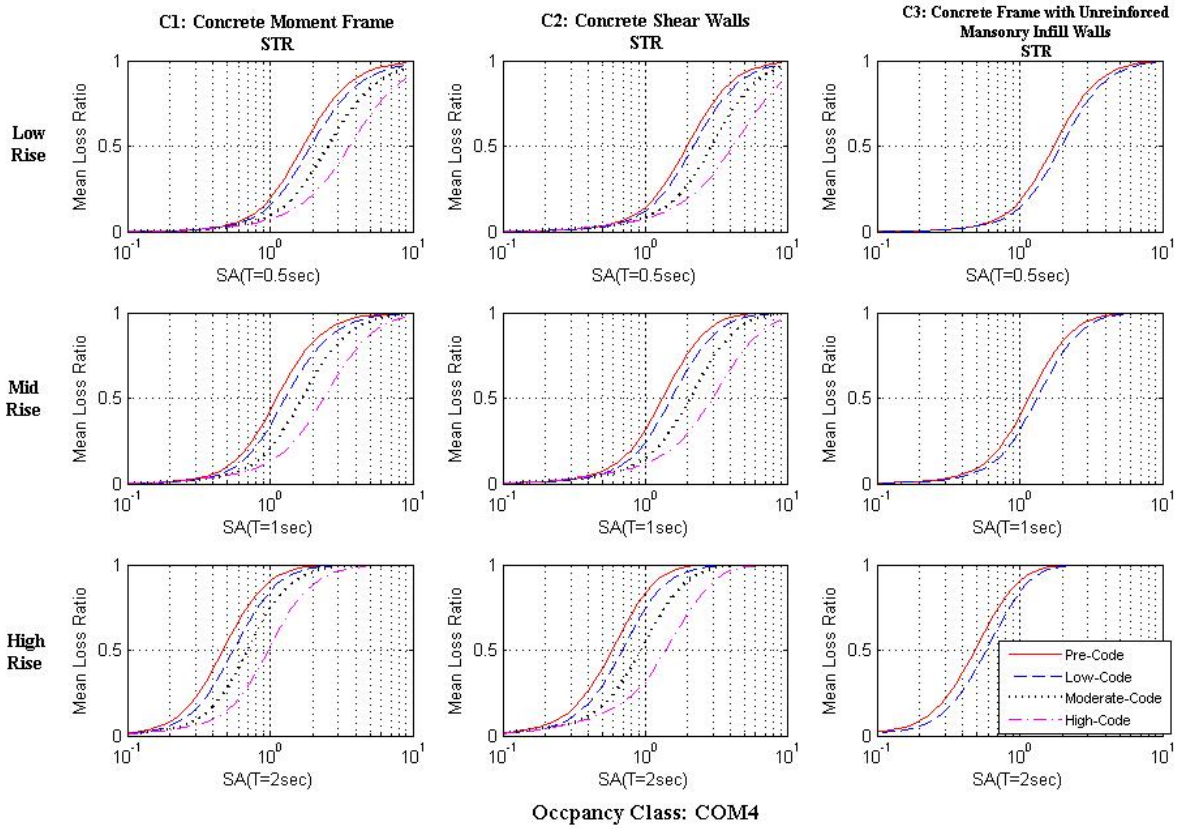

The trend that dominates the graphs in Figures 3 and 4 is that the curves representing lower code levels lie above those for higher code levels. Physically this means that for a given ground motion (spectral acceleration in this case), lower code levels will have a

higher probability of exceeding a certain damage state (for fragility) or a higher average loss ratio (for vulnerability). This makes intuitive sense because one would expect buildings at lower levels of seismic design to be more fragile/vulnerable for given ground motion values than those at higher code levels.

1.3 Resilience

Resilience pertaining to earthquake risk can be defined as a particular community's ability to cope with damage and associated loss. In many ways, this is more of a social science issue than an engineering issue because it involves socio-economic, political, and historical factors. This component of risk was not taken into consideration in the development of the seismic risk maps; it was only included for completeness of the discussion of risk.

1.4 Risk

Risk as pertaining to earthquake analysis is, in this report, either: 1) the probability that a certain damage state will be exceeded in a specified number of years, or 2) the expected value of loss ratio in one year. The first form of risk utilizes fragility, while the second is specific to vulnerability. In either form, risk combines ground motion hazard in a particular area and the fragility/vulnerability of a particular building. The two are combined via the so-called risk integral (an application of the Total Probability Theorem), applied here in the form of a summation since we seek numerical solutions. Equation 1 is used to combine a fragility curve and a hazard curve to determine the probability of exceeding damage state i (DS_i) in, here, 1 year. Equation 2 combines vulnerability and hazard information to determine the expected annual loss ratio.

Equation 1: Risk Summation using Fragility Functions

$$P[DS_i] = \sum_{0}^{\infty} \underbrace{P[DS_i|SA = a]}_{\text{Fragility}} |\underbrace{\Delta(P[SA > a])}_{\text{Hazard}}|$$

Equation 2: Risk Summation using Vulnerability Functions

$$E[LR] = \sum_{0}^{\infty} \underbrace{E[LR|SA = a]}_{\text{Vulnerability}} |\underbrace{\Delta(P[SA > a])}_{\text{Hazard}}|$$

Since the risk of collapse (or exceeding the complete damage state), for example, is typically very small in a given year, it is helpful to extend the risk calculations to a larger time period. To do this, we assume a Poisson Process governs earthquake risk. Inherent in this assumption are the assumptions that damage/loss are randomly occurring and statistically independent, the probability of damage/loss in a small time interval, Δt, is proportional to Δt, and the probability of two or more occurrences of damage/loss in a small time interval is negligible. Therefore, to extend the time interval of the probability of exceeding a certain damage state to the planning horizon, t, Equation 3 was used. Notice that Equation 3 is used with the output from Equation 1, but not Equation 2. For vulnerability-based risk, this report will only focus on the expected annual loss ratio, which eliminates the necessity of extending the time interval.

Equation 3: Poisson Process to extend Planning Horizon to t years (Fragility)

$$P(DS \geq ds \text{ in } t \text{ years}) = 1 - \exp(-\lambda t)$$

where: λ = mean annual frequency of exceedance (MAFE)

At this point in the discussion of risk, it is apparent that risk can be quantified in several ways. The first descriptor of risk is the probability of exceeding a certain damage state in some time period. As a point of reference, upcoming building codes will aim to

result in structural designs that pose less a 1% risk of collapse in 50 years. The two other quantifications of risk that will be discussed are expected annual loss ratio and expected annual loss. Expected annual loss ratio is a unitless measure of total damage to a building relative to its replacement cost. Expected annual loss, computed by multiplying the expected annual loss ratio by the value of a building, is the absolute damage to a structure in monetary units.

An important aspect of earthquake risk is that high hazard or fragility/vulnerability alone does not necessarily equate to high risk. If a particularly fragile building exists in a very low-hazard area, then it may have a low risk of sustaining damage. The converse is also true: very strong, earthquake-resistant buildings in high-hazard areas that often experience large ground motion can be at a low risk of damage or collapse. Fragile buildings located in areas of high hazard – e.g., non-ductile concrete buildings in the western United States – pose the greatest threat because they are at high levels of risk.

2 RISK MAP TOOL

2.1 Introduction to the USGS Risk Map Tool

The risk maps being developed at the USGS are contour plots of the risk of earthquake damage in a certain time period. These risk maps are saved as KML files and observed through Google Earth. The original Risk Map tool currently on the USGS website is powerful, yet fairly generic. The user specifies a building height, construction material, structural system, seismic design level, damage state, and time period, at which point the tool accesses a pre-computed risk map that places the user-specified building at every point on a grid covering the continental US. These maps will be referred to as general risk maps for the remainder of the report to distinguish them from inventory-specific

maps, which will be introduced later. Also, for the remainder of this report, two versions of the USGS Risk Map Web Tool will be discussed. The first version, referred to as the original web tool, is currently on the web (http://earthquake.usgs.gov/riskmaps) and is briefly outlined above. The second version, referred to as the updated web tool, exists only as a series of MATLAB functions at this point, but will be on the web soon.

2.2 Limitations of the Original Risk Map Tool

An array of limitations associated with the original risk maps tool has prompted the implementation of several generalizing updates. First, the original tool uses hazard data specific to a site class on the B/C boundary when calculating risk, as opposed to hazard data specific to a site class that is estimated for each location on the map. Figure 5 below presents the general risk map, specific to a site class on the B/C boundary, for a high-rise concrete shear wall structure (C2H) designed a pre-code level experiencing complete damage. All of the general risk maps presented in this report are specific to high-rise structures for consistency with the majority of structures in the sample inventory for the Los Angeles area that is presented later.

Figure 5: Risk Map specific to Site Class on B/C Boundary

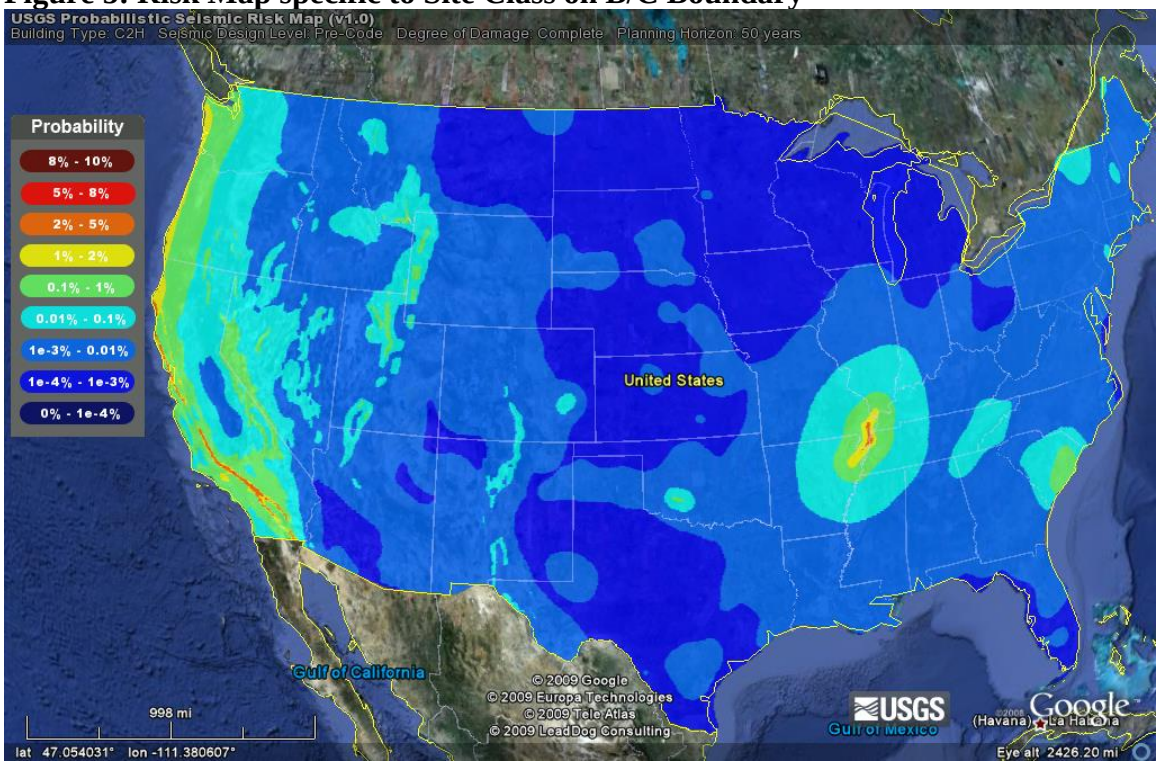

A second limitation of the original tool is related to the logistics of risk computation and map generation. The original tool uses risk maps that were developed a priori and saved as KML files. When a user inputs their specifications of interest, the tool simply accesses the appropriate risk map. This is efficient with respect to run time, but very limiting with regards to total possible combinations of user-specified parameters. This also limits users to the generic USGS fragility functions (Karaca and Luco 2008) used in the a priori risk computations. By performing risk computations a priori, it is impossible to use more specialized, user-specified fragility functions. Thirdly, the original risk map tool cannot create a risk map for a specific inventory of buildings, only for a uniform distribution of a particular building throughout the continental US. Allowing user-specified inventories will greatly bolster the overall utility of the web tool. Finally, the original tool presentes risk calculations based solely on fragility functions, where risk is

defined in terms of the probability of exceeding a certain damage state in a user-specified time horizon. Recall from earlier in the report that hazard and vulnerability can also be combined to quantify risk in terms of the expected annual loss or loss ratio. The ability to quantify risk in similar, yet different terms may be advantageous to users for comparison purposes, as demonstrated later.

2.3 The Updated Risk Map Tool – New Features

2.3.1 General Risk Maps

2.3.1.1 Site Class Considerations

The focus of this research project has been to advance the capabilities of the original web tool with particular emphasis on the risk involved with non-ductile concrete structures. The first issue with the web tool that was addressed was the limitation of using hazard curves specific to the site class on the B/C boundary. This issue was resolved by using the site-adjusted and site-specific hazard curves previously described, in place of the original hazard data, to generate new risk maps. The updated tool enables the user to create a risk map for any particular site class covering the continental US, or estimated site classes at each location of the map. There are advantages to both of these updated risk maps. Building codes declare that site class D is to be assumed if the actual site class at a location is unknown. The updated web tool enables users to generate a risk map that adheres to this requirement by assuming site class D covers the continental US. Figure 6 is similar to Figure 5 in that it is a general risk map for high-rise concrete shear wall structures (C2H) designed at pre-code levels experiencing complete damage, but different in that it for site class D, not the B/C boundary.

Figure 6: Risk Map specific to Site Class D

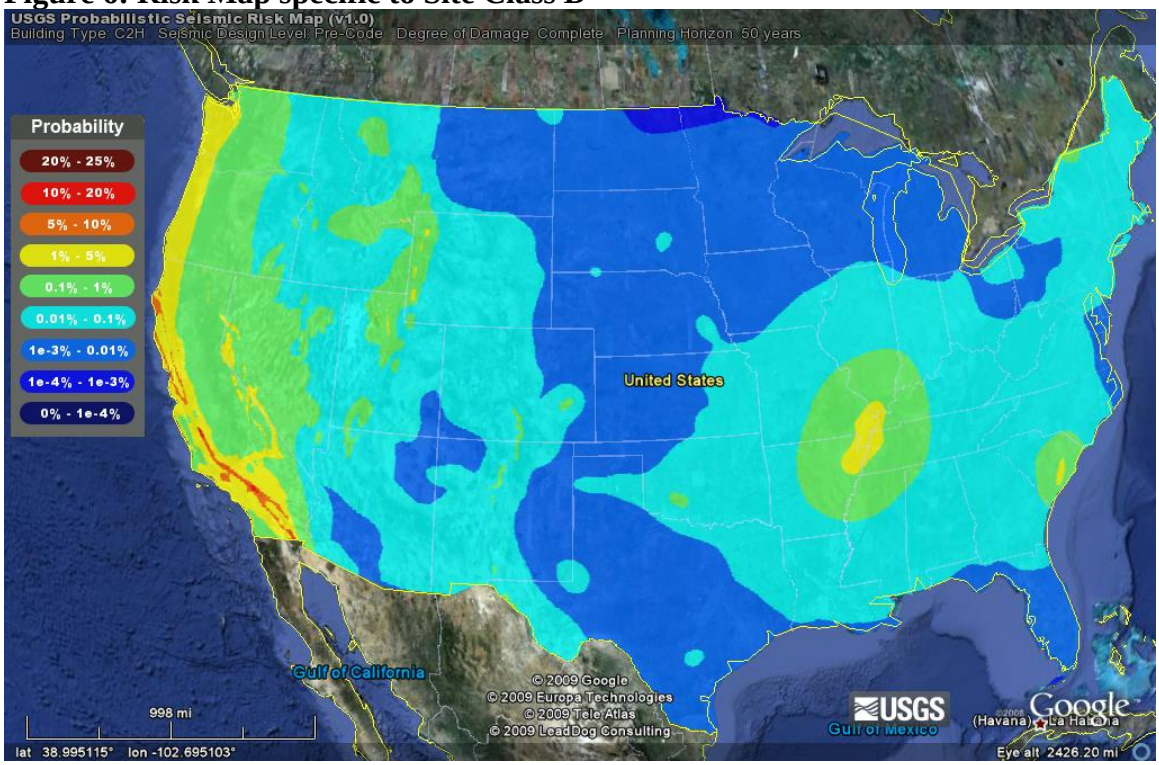

Since the USGS has an approximate site class distribution for the continental US based on topography, it is possible to make a so-called site-specific risk map, based on hazard curves consistent with the site class for each particular location. For example, Figure 7 is a risk map for the same user-specified parameters as Figures 5 and 6, but using site-specific hazard curves. It is evident from the map that incorporation of site class effects into the risk analysis results in an increase in the spatial variability of risk across the map.

Figure 7: Site-Specific Risk Map

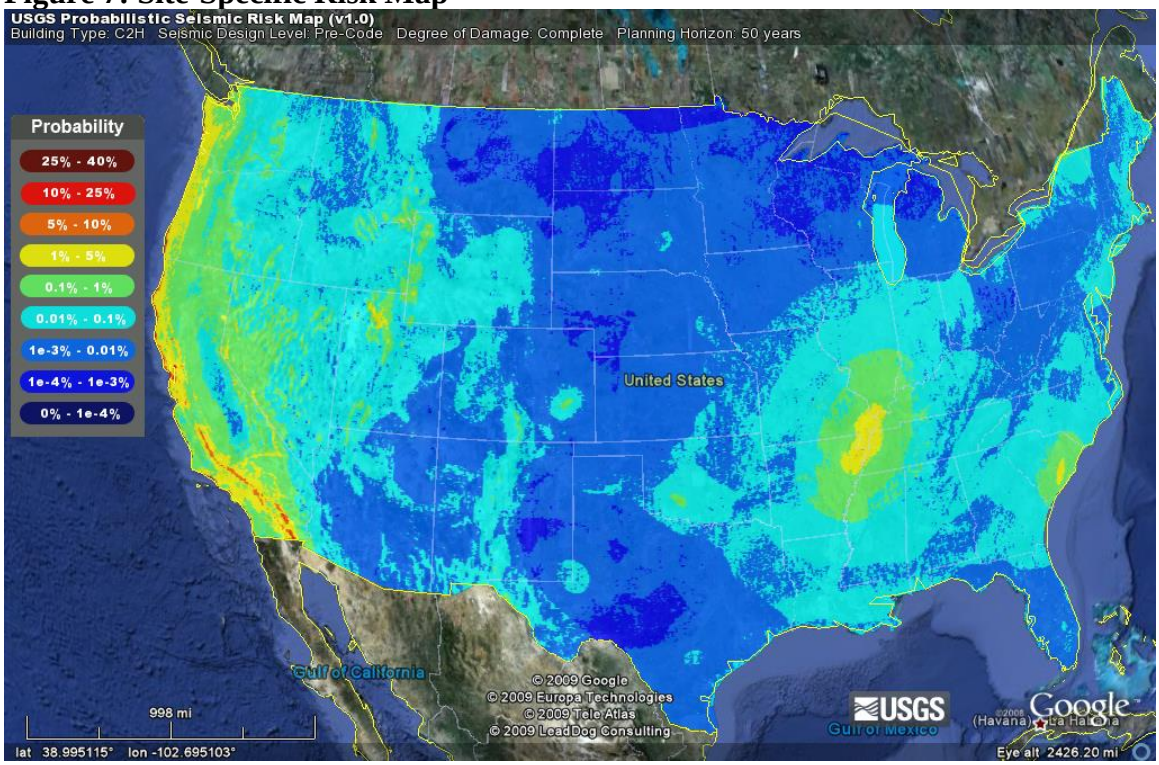

2.3.1.2 "On-the-Fly" Computations

As previously mentioned, another issue that this project aimed to alleviate is the limitation to pre-computed risk maps. A new, efficient MATLAB code was generated to perform risk computations upon selection of parameters. This supports a wider array of user-specified parameter combinations and eliminates the necessity of a large database of risk maps files. An example of the increased freedom for the user that results from this update is specification of a planning horizon of interest. The original web tool provided 1 year, 30 years, and 50 years as the only possible time interval options, but by performing calculations "on-the-fly," the user can specify any positive, finite planning horizon. More importantly, "on-the-fly" computations provide the possibility of using user-specified fragility or vulnerability functions, as opposed to the generic USGS data. The issue of risk map restrictions due to fragility/vulnerability curves will be addressed next.

2.3.1.3 Fragility/Vulnerability Options

Two simultaneous approaches are being used to alleviate the restrictions placed on the risk maps by limiting to the generic USGS fragility curves. The first approach is to derive another set of fragility curves based on more accurate pushover curves and consistent damage state thresholds. The current USGS fragility curves were derived using curvilinear pushover/capacity curves from HAZUS. Ryu et. al. is developing fragility curves based on multilinear pushover curves that are derived for each HAZUS building type. This is an attempt to create fragility functions that are more accurate in the sense that their underlying pushover curves are more realistic and consistent with the other main input to the fragility development: damage state thresholds. Figures A55 and A56 present the curvilinear and multilinear pushover curves for all HAZUS concrete building types. The other method of increasing the flexibility of the risk map tool is to allow users to specify their own fragility or vulnerability curves. Accordingly, the web tool has been updated to read user-inputted fragilities or vulnerabilities instead of the generic USGS curves.

2.3.2 Inventory-Specific Risk Map

2.3.2.1 Overview

The advancement of the USGS risk map web tool was taken a step further by extending its capabilities to developing a risk map for a user-specified inventory instead of a single generic building over the entire continental US. The inventory must contain the following information for each building: location (longitude/latitude) and specification of a fragility/vulnerability. If the USGS generic fragility/vulnerability curves are to be used, a HAZUS structural type, height, code level, and occupancy type (for vulnerability-based risk) must be specified. The inventory may also include the site

class that exists at the location of each building. If this information is specified, the updated tool will use the pre-calculated USGS hazard information corresponding to the given site class at the location of each building; otherwise it will use the so-called site-specific USGS hazard data. This option will improve the accuracy of the risk maps since the USGS site class distribution is based on topography and therefore contains accuracy limitations.

To generate an inventory-specific risk map, the updated web tool first accesses the appropriate fragility or vulnerability for each building in the inventory and the associated hazard curve for each of their locations. If the user includes their own fragility/vulnerability for each building in their inventory, the web tool will read that information and bypass the USGS data. Next, the web tool combines the fragility/vulnerability and hazard curves using the appropriate risk summation (Equation 1 if fragility is used, Equation 2 if vulnerability is used) to determine either: 1) the risk of each building exceeding a particular damage state (specified by user) in 1 year or 2) the expected annual loss ratio. Finally, if fragility information is used, Equation 3 is used to extend the time period from 1 year to a planning horizon specified by the user.

To graphically represent the level of risk for a particular building, a colored box (indicating the level of risk) is placed at the location of each building. The size of the box is dependent on the precision of the latitude and longitude values provided by the user. Very precise latitude and longitudes produce a small box directly on the building, while less precision results in large boxes that may encompass several buildings or even several miles. Scaling of boxes in such a manner is due to the fact that to accurately pinpoint a building, the location needs to be known to at least a hundred thousandth of a

latitudinal/longitudinal unit. Confidentiality issues are also a factor in determining the scaling of the boxes, as will be discussed next.

2.3.2.2 Privacy Issues

Privacy issues can result from mapping the risk for a specific inventory as opposed to a single building across the continental US. Although the ability to pinpoint a specific building is desirable for determining which buildings need to be given priority when it comes to retrofit, it could be undesirable for the owners of high-risk buildings. People might be less likely to visit such buildings, which could be detrimental to the business or practice that exists there. A feature of the updated web tool designed to address this issue is the scaling of the colored boxes depicting risk based on latitude and longitude precision. It was mentioned in the preceding section that limited precision of latitude/longitude values results in boxes that encompass large areas, which may include several buildings. This makes it difficult to determine the building responsible for the risk in the associated area, resulting in increased anonymity. To force the risk map tool to create these large boxes, users can simply round the latitude and longitude values in their inventory. However, since the updated version of the risk map tool is not on the web at this point, privacy issues may not have been fully addressed. Additional privacy protection implementations may include password-protecting the KML files generated by the web tool and setting a lower bound on the size of the boxes.

2.3.3 Loss Ratio Maps

Another improvement on the original version of the USGS risk map web tool is the capability of combining vulnerability, instead of fragility, curves with hazard curves to quantify monetary loss instead of physical damage. The resulting maps, referred to as

loss ratio maps, can be generated for both inventory-specific and general risk maps. In contrast to the fragility-based risk maps, loss ratio maps are expressed as decimals, not percentages. These maps portray the expected annual loss ratio distribution for the continental US or an inventory.

2.3.4 Difference Maps

The final renovation to the USGS risk map web tool is the option to make difference maps. A difference map illustrates the difference in risk between the results for two similar, yet distinct sets of input parameters. Several options and sub-options have been added for difference maps:

1.) The difference in fragility-based risk between two code levels for a given structural type (height included), damage state, planning horizon, and site class distribution (called *code difference maps*):

a.) General difference maps

b.) Inventory-specific difference maps

2.) The difference in fragility-based risk between two site class distribution for a given structural type, damage state, code level, and planning horizon (called *site difference maps*):

a.) General difference maps

b.) Inventory-specific difference maps

3.) The difference in vulnerability-based risk between two code levels for a given structural type, occupancy type, and site class distribution (called *loss ratio difference maps):*

a.) General difference maps

b.) Inventory-specific difference maps

Code and loss ratio difference maps are useful in determining the effect of retrofitting. For example, if a particular concrete structure is originally at pre-code level, but retrofit elevates its level of seismic design to high-code, a large difference in risk will show that the retrofit was effective and worthwhile. The difference maps do not provide any information about absolute risk, but rather they offer a way of quantifying the effectiveness of retrofit. Figure 8 is a code difference map between pre- and high-code for the following parameters: high-rise concrete shear walls (C2H), complete damage, 50 year planning horizon. Figure 9 is a loss ratio difference map for the same parameters as Figure 8, with COM4 (offices) occupancy type. Code and loss ratio difference maps provide a direct comparison between ductile and non-ductile concrete risk and quantify the impact of retrofit.

Figure 8: Damage State Exceedance Probability Difference between Ductile and Non-Ductile Concrete Structures

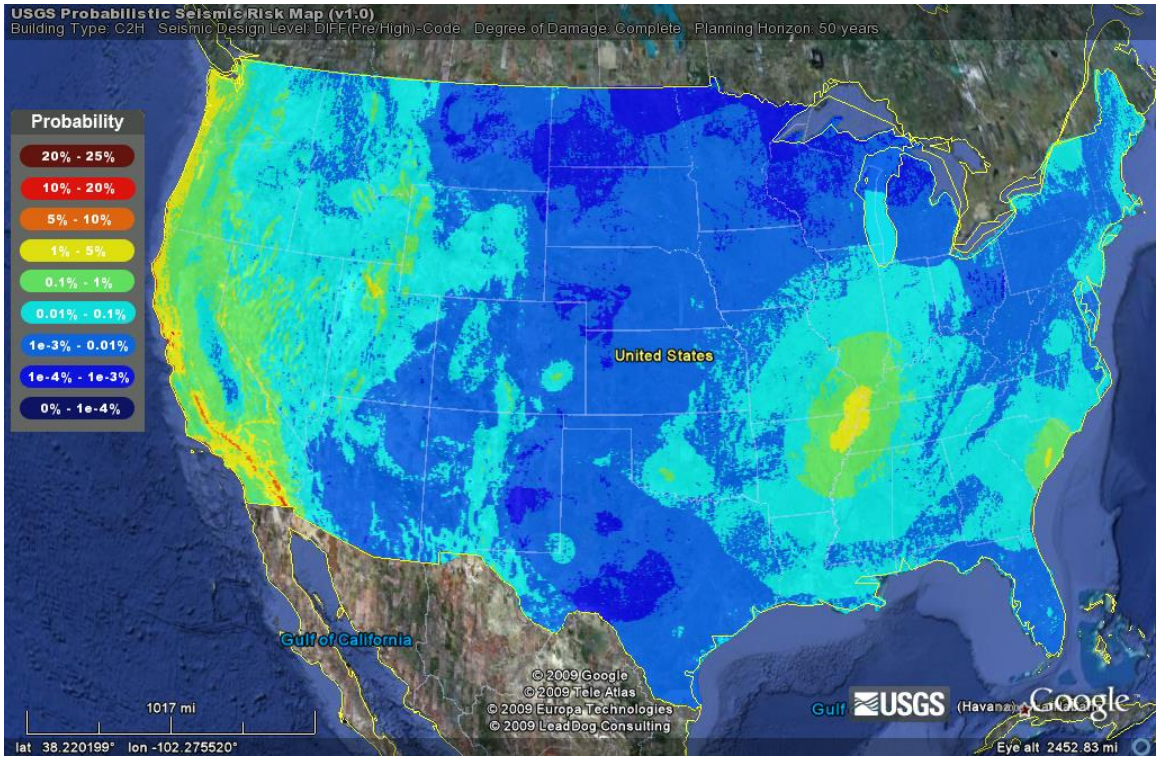

Figure 9: Expected Annual Loss Ratio Difference between Ductile and Non-Ductile Concrete Structures

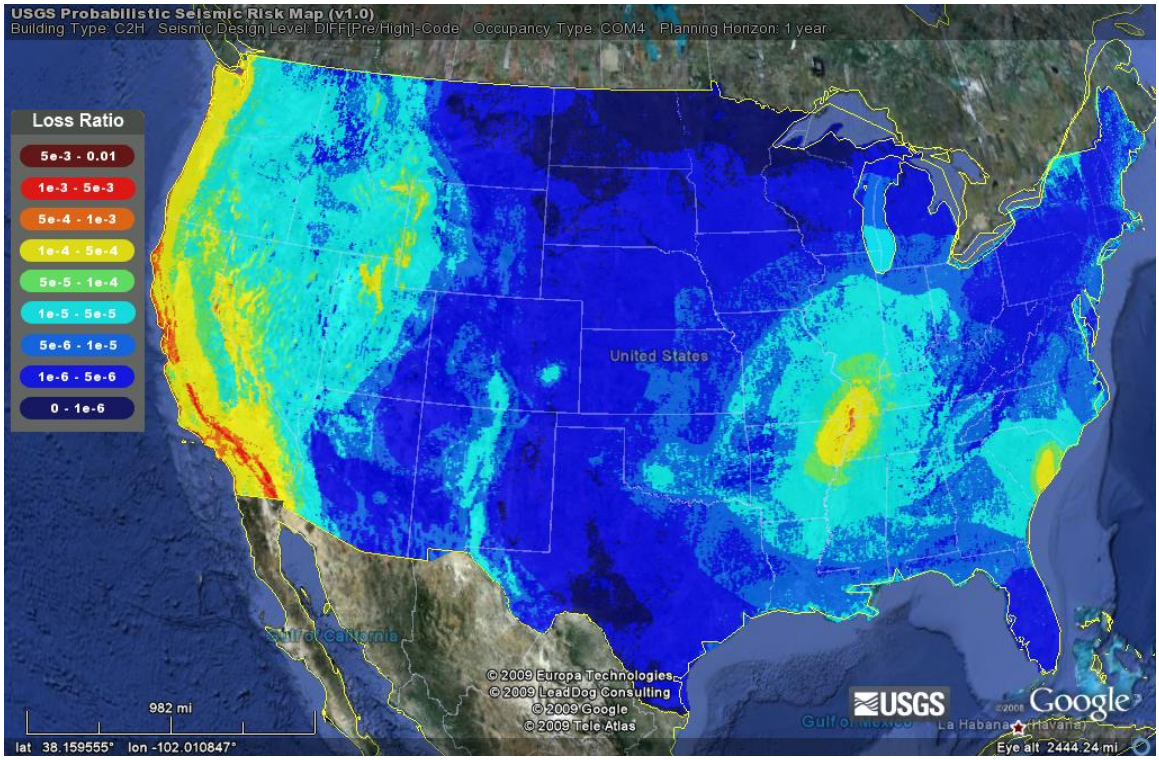

Site difference maps directly demonstrate the effect that site class distribution has on risk. Figures 10 and 11 are site difference maps for the same input parameters used in Figures 5 through 9. Figure 10 portrays the difference between a uniform site class distribution at the B/C boundary and a uniform distribution of site class D (i.e., the difference between Figure 5 and Figure 6), while Figure 11 illustrates the difference between a uniform distribution of site class D and the USGS approximate US site class distribution based on topography (i.e., the difference between Figure 6 and Figure 7).

Figure 10: Difference between Risk Maps for Site Class D and Site Class on B/C Boundary

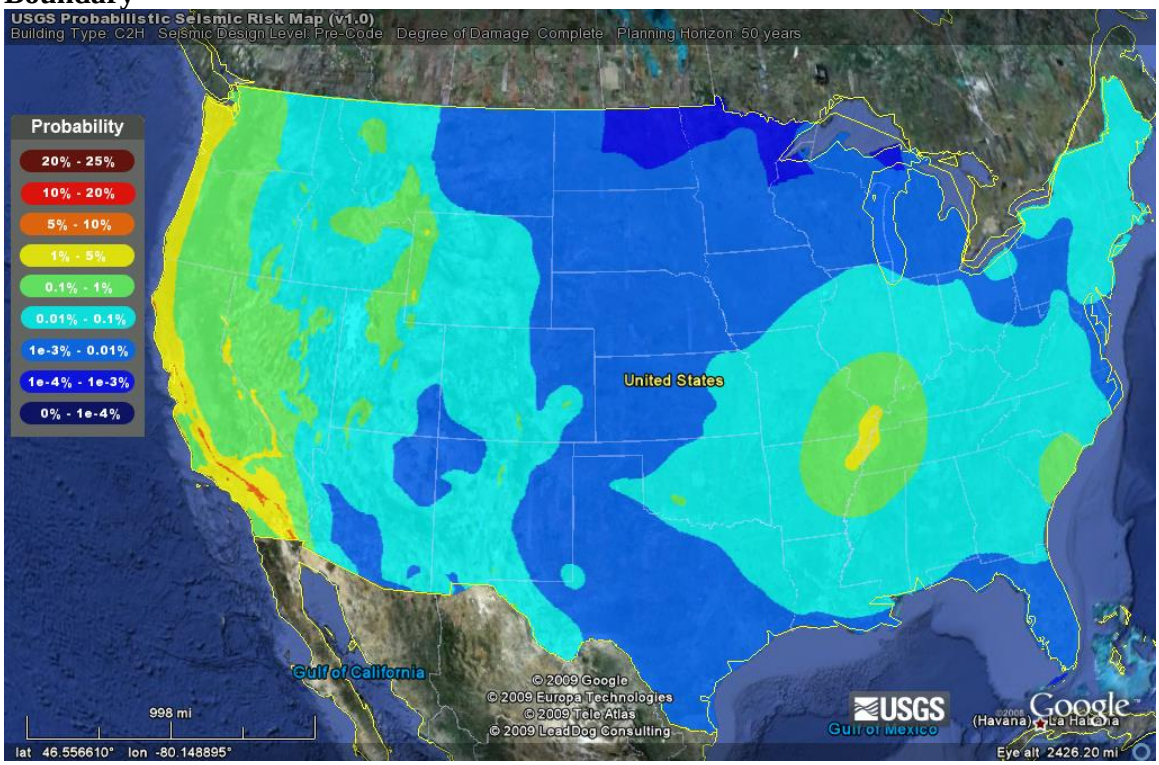

Figure 11: Difference between Risk Maps for Site-Specific Site Class Distribution and Site Class D

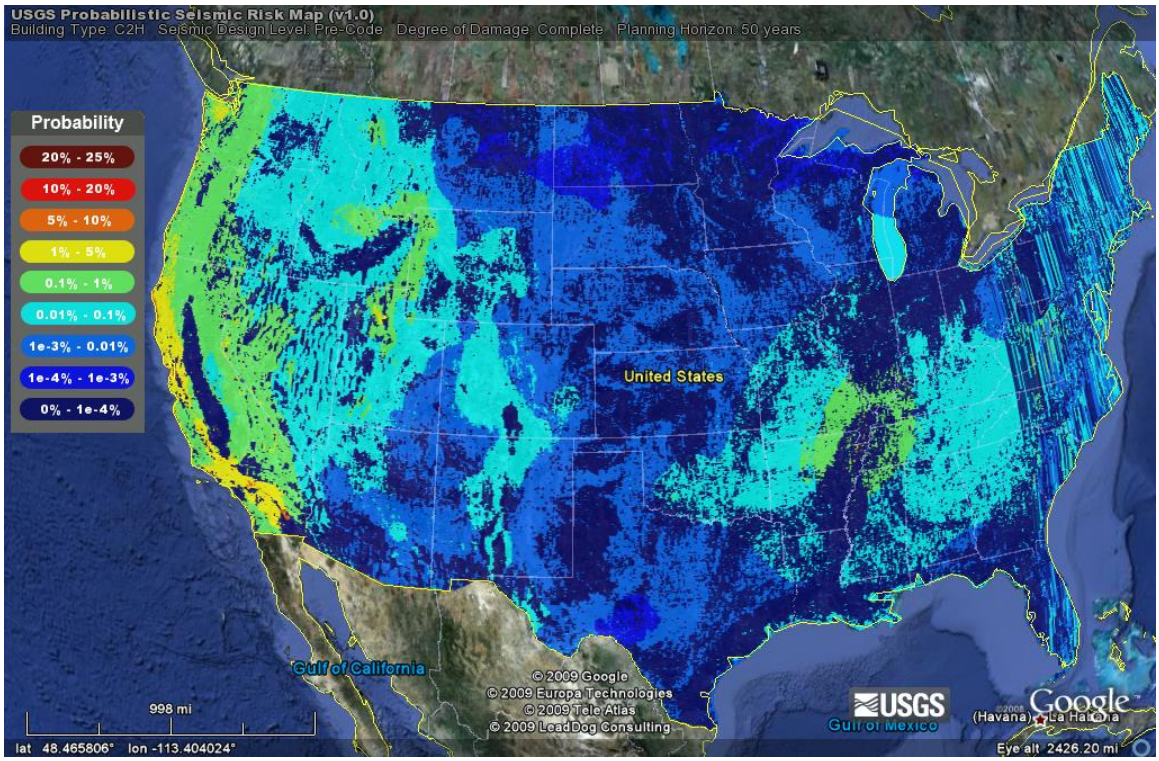

Note that Figure 11 uses absolute values of differences instead of pure differences. The only areas where these two differ are at the locations where site class E exists in Figure 2. Due to the scarcity of site class E in Figure 2, the effect on the map is negligible. Also, it is important to keep in mind that the difference maps illustrate the difference in risk between two different levels of seismic design, not ratios of the two. For example, a difference map portraying a difference of ΔX% signifies that risk was reduced from X% to (X- ΔX)%, not to X*(1 - ΔX/100)% (e.g., for a difference of 10%, risk is reduced from 50% to 40%, not from 50% to 45%).

2.3.5 Risk Map Applications

Extending the web tool to incorporate the inventory-specified option was the most daunting task associated with this research project, but also the most crucial because it provides a means to identify the most problematic buildings in a specified inventory. With the updated web tool, locating and prioritizing by risk the non-ductile concrete buildings in need of seismic retrofit is not only possible, but relatively quick and simple. However, a major obstacle that remains is the availability of an inventory for regions of high seismicity, such as the western US. A comprehensive inventory of the non-ductile concrete buildings in the Los Angeles area is currently being developed by Anagnos et. al, which will be the focus of the case studies in the next section.

2.3.6 Additional Information

The user-specified inventory, fragility, and vulnerability options in the updated web tool will require the data files to be in XML format. The prototype for the web tool was developed in MATLAB using MAT data files, but for web application purposes the code will be translated to Java and altered to read XML files. The USGS generic fragilities

and vulnerabilities were thus converted to XML files so that the new tool can do all necessary computations "on-the-fly." The Appendix (after all figures) provides an example of the currently-required format for the inventory, fragility, and vulnerability XML files.

Notice that risk maps indicating monetary loss have not been included in the updated version of the USGS web tool. This is due to the fact that the sample inventory for Los Angeles provided by Anagnos et. al. (used in the next section) did not include the building values needed to convert from loss ratio to absolute loss. When the updated risk map tool is on the web, it will include this capability.

3 RETROFIT INVESTIGATION METHODOLOGY

When approaching the tremendous task of seismic retrofit of non-ductile concrete buildings in the western United States, a specific strategy is required. To properly develop this strategy, we need a methodology to answer the questions posed at the beginning of this paper.

There are millions of buildings in the western US; however, only a fraction of them are at serious risk of collapse in their lifetime. Therefore, the first task of our seismic retrofit approach is to narrow this massive area down to a couple of problematic regions. Once this is accomplished, these regions can be further broken down until the buildings at unacceptable levels of risk are pinpointed. Finally, retrofit might only be worthwhile if it significantly reduces the expected annual loss ratio or risk of collapse in the lifetime of the building. For example, if a costly retrofit only reduces the risk of collapse by 0.1% in the next 50 years, then the resources poured into that retrofit might have been more

efficiently utilized elsewhere. This strategy to retrofit can be summarized as the following two-step process:

1. Find the areas in the western US where non-ductile concrete buildings have the greatest expected annual loss ratio or risk of catastrophic failure in their lifetime.
2. Quantify the extent to which seismic retrofit would reduce this risk.

The updated USGS risk map web tool was designed to assist with both of these tasks and its utility will be demonstrated in the following section.

3.1 Pinpointing High-Risk Areas and Buildings

Recall that HAZUS does not specify a non-ductile concrete structural type, but the HAZUS concrete structures can be considered non-ductile when coupled with a pre-code level of seismic design. Concrete structures at high-code levels are taken as ductile concrete buildings. Low- and moderate-code levels are considered intermediary between ductile and non-ductile behavior and will therefore be de-emphasized.

The web tool option that allows users to generate general (as opposed to inventory-specific) risk maps is useful to narrow the continental US down into several seismically problematic regions. This can be done by specifying any non-ductile concrete building in the risk map tool, along with the planning horizon and damage state of interest. Our interest lies in catastrophic failure, so the complete damage state is used. It is important to note that there are nine different non-ductile concrete structures (pre-code level coupled with 3 structural systems and 3 heights), which each generate a different risk map for complete damage. It is useful to look at all nine risk maps to attain a comprehensive understanding of non-ductile concrete risk, but the variations among these risk maps at the complete damage state are observed to be small. Therefore, using only

one risk map as a guide to narrow down the search for high-risk regions is a valid estimate. Figure 12 presents the risk map for a high-rise concrete shear wall structure, designed at a pre-code level, experiencing complete damage in 50 years. Figure 13 is a loss ratio map for the same parameters specified in Figure 12, except COM4 (office building) occupancy type is additionally specified. From Figure 12 and 13, the highest-risk areas become apparent, along with the actual risk and expected loss ratio values.

Figure 12: Site-Specific Risk Map used to Narrow the Scope of Retrofit

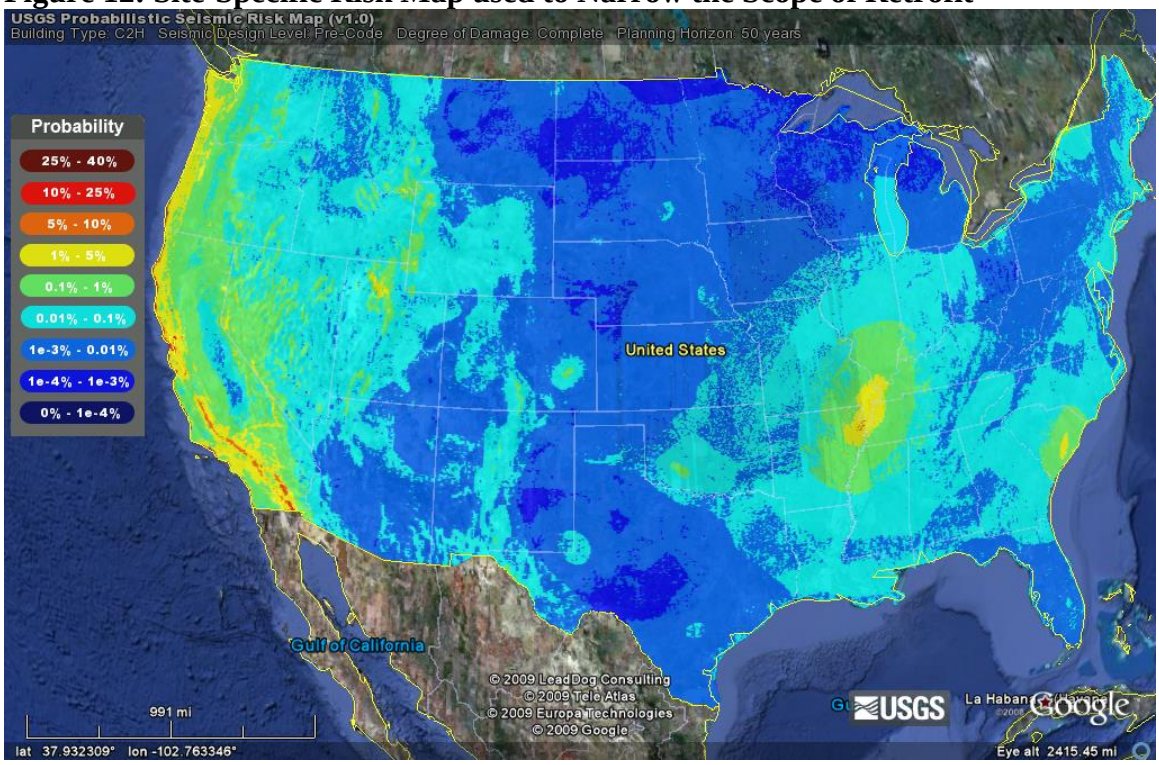

Figure 13: Site-Specific Loss Ratio Map used to Narrow the Scope of Retrofit

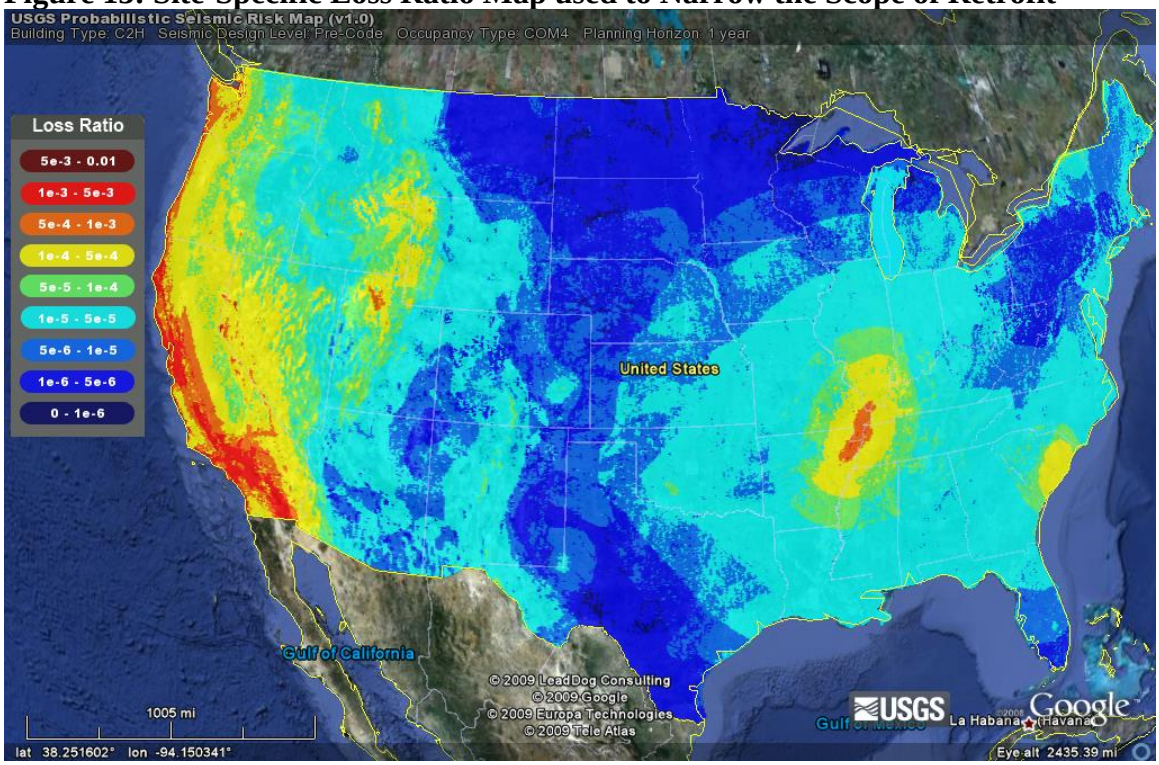

The other non-ductile concrete structure risk maps for complete damage are provided in the Appendix for reference, along with the corresponding risk maps for slight damage for comparison purposes. Also, code difference maps between pre- and high-code levels for all concrete structures are presented in the Appendix to illustrate the risk difference between ductile and non-ductile behavior.

Once the high-priority areas of the western US are sufficiently identified, inventories can be collected and fed into the USGS risk map tool to identify risk on a building-by-building basis. Figure 14 is an inventory-specific risk map for complete damage in a planning horizon of 50 years. Figure 15 is an inventory risk map for slight damage in the next 50 years, provided for comparison purposes. Figure 16 is an expected annual loss ratio, inventory-specific map. Note that different legends are used in Figures 14 through

16, so it is only valid to compare risk levels, not box color. The inventory used for Figures 14 through 16 is a sample inventory of non-ductile concrete buildings in the Los Angeles area provided by Anagnos et. al.

Furthermore, the data underlying the inventory-specific risk maps can be displayed in tabular form and sorted in descending order to prioritize and schedule retrofit. Tables 7 through 9 in the next section provide an example of doing so.

Figure 14: Risk Map of Complete Damage in the next 50 years for LA inventory

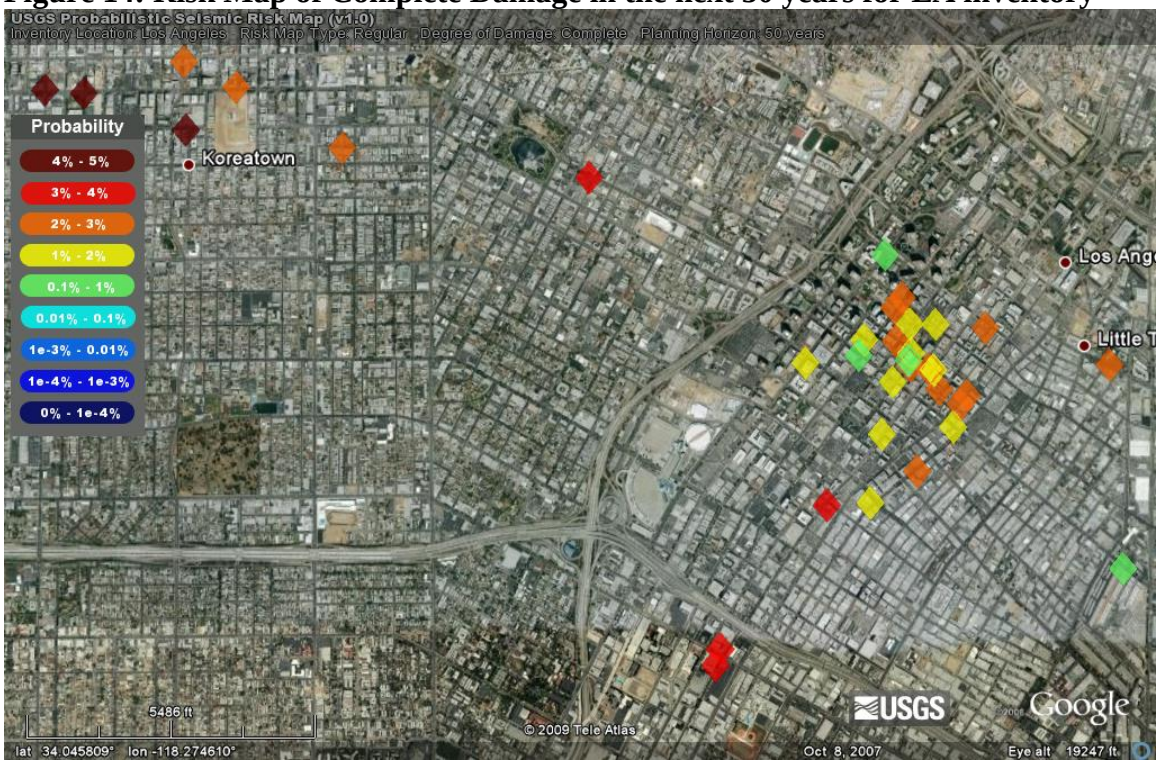

Figure 15: Risk Map of Slight Damage in the next 50 years for LA inventory

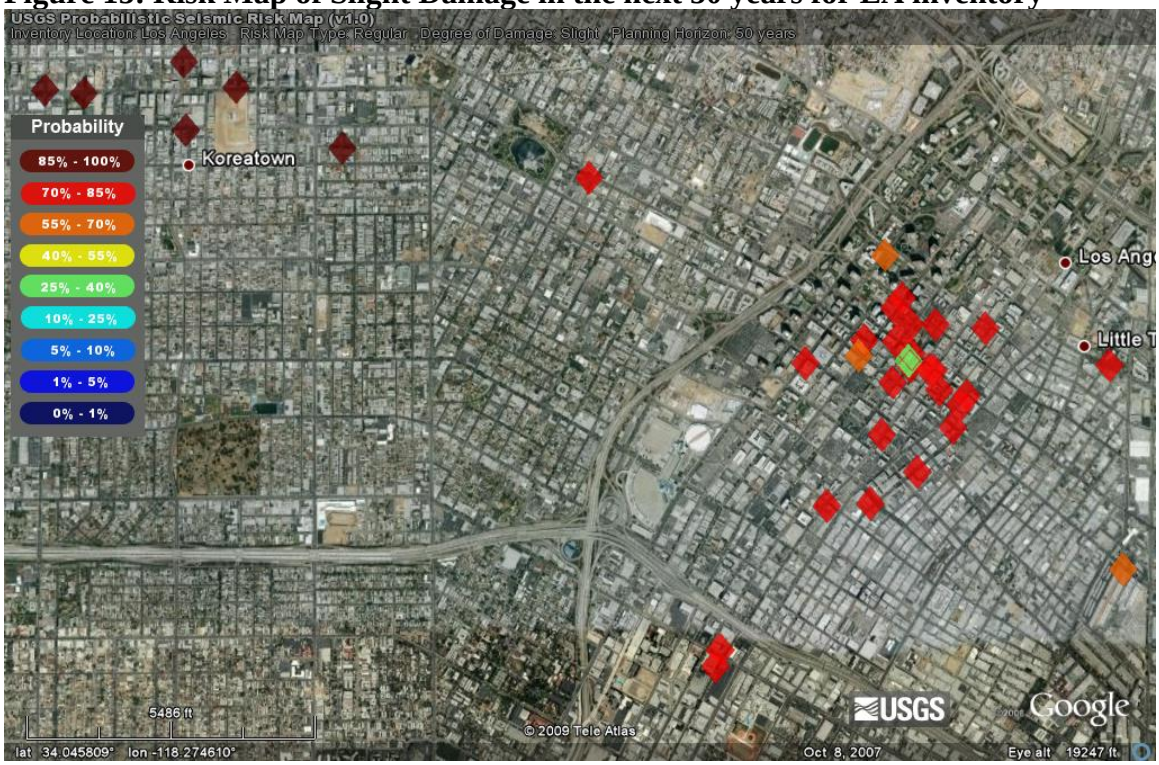

Figure 16: Expected Annual Loss Ratio Map for LA inventory

3.2 Cost-Benefit of Retrofit

Another question to consider before beginning the retrofit process pertains to the utility of retrofit. If the retrofit only reduces the risk of collapse or expected annual loss by a small amount, the resources might be better used elsewhere. The updated USGS web tool offers a method of quantifying the effectiveness of retrofit to a particular building through its difference map capability. By defining an inventory of buildings and selecting the code difference map option, a difference map is generated between the risk associated with the current level of seismic design of each building and the risk associated with the building in its retrofitted state (this retrofitted state is assumed to be high-code level). This difference map will illustrate the decrease in risk that results from retrofitting a particular building. Difference maps may be plotted for any degree of damage, but complete damage is of particular interest due to the focus on mitigation of catastrophic failure of non-ductile concrete structures. Similar to the previous task (pin-pointing high-risk areas and buildings), the data underlying the difference maps can be put in tabular form to rank the buildings in order based on the degree that they will benefit from seismic retrofit. Tables 7 through 9 are examples of how such a table might be organized. Table A1 in the Appendix is the legend for the building numbers in Tables 7 through 9.

Table 7 is of particular interest due to the focus on catastrophic failure of non-ductile concrete structures. Notice that, for the most part, risk correlates very nicely with retrofit benefit (i.e. buildings at a high risk of complete damage will benefit the most from retrofit). Figure 17 is a scatter plot of column 2 of Table 7 vs. column 4 of Table 7, which illustrates the strong positive correlation between risk of complete damage and

benefit (reduced risk) from retrofit. Furthermore, by subtracting the fourth column from the second column by building, it is apparent that retrofit reduces the risk of complete damage for all buildings in this inventory to less than 1% in 50 years after retrofit, the minimum acceptable design standard per recent updates to building codes. This demonstrates the utility of seismic retrofit in terms of reducing risk of complete damage to an acceptable level.

Table 7: Seismic Risk of Complete Damage in 50 years for Non-Ductile Concrete Structures, and the Effect of Retrofit

Building #	Risk of Complete Damage for Pre-Code	Building #	Risk Difference between Pre- and High-Code for Complete Damage
Building 31	4.45%	Building 31	4.19%
Building 51	4.38%	Building 51	4.12%
Building 33	4.37%	Building 33	4.11%
Building 55	4.31%	Building 55	4.05%
Building 56	4.09%	Building 56	3.83%
Building 19	4.08%	Building 57	3.81%
Building 57	4.07%	Building 19	3.77%
Building 44	3.93%	Building 44	3.73%
Building 42	3.77%	Building 42	3.55%
Building 26	3.71%	Building 26	3.52%
Building 5	3.43%	Building 5	3.25%
Building 32	3.41%	Building 32	3.23%
Building 37	3.40%	Building 37	3.13%
Building 30	3.23%	Building 30	2.98%
Building 22	3.22%	Building 22	2.97%
Building 18	3.14%	Building 18	2.97%
Building 45	3.08%	Building 45	2.91%
Building 14	2.91%	Building 14	2.72%
Building 17	2.87%	Building 52	2.68%
Building 52	2.83%	Building 17	2.63%
Building 35	2.71%	Building 54	2.56%
Building 54	2.71%	Building 48	2.55%
Building 48	2.70%	Building 28	2.52%
Building 16	2.66%	Building 16	2.52%
Building 28	2.66%	Building 40	2.51%
Building 40	2.66%	Building 3	2.51%
Building 3	2.66%	Building 35	2.49%
Building 23	2.63%	Building 23	2.48%

Building 50	2.60%	Building 50	2.46%
Building 20	2.57%	Building 20	2.43%
Building 24	2.52%	Building 24	2.36%
Building 34	2.51%	Building 39	2.36%
Building 39	2.50%	Building 34	2.35%
Building 36	2.44%	Building 36	2.29%
Building 27	2.42%	Building 27	2.23%
Building 21	1.98%	Building 21	1.84%
Building 29	1.92%	Building 29	1.78%
Building 1	1.86%	Building 1	1.75%
Building 25	1.83%	Building 25	1.69%
Building 7	1.80%	Building 7	1.69%
Building 15	1.80%	Building 15	1.69%
Building 49	1.71%	Building 49	1.61%
Building 60	1.71%	Building 60	1.61%
Building 9	1.65%	Building 9	1.55%
Building 59	1.61%	Building 59	1.51%
Building 38	1.59%	Building 38	1.50%
Building 53	1.54%	Building 53	1.45%
Building 41	1.54%	Building 41	1.45%
Building 58	1.52%	Building 58	1.43%
Building 46	1.52%	Building 46	1.43%
Building 43	1.48%	Building 43	1.39%
Building 4	0.70%	Building 4	0.68%
Building 2	0.66%	Building 12	0.65%
Building 12	0.65%	Building 2	0.65%
Building 8	0.36%	Building 8	0.36%
Building 47	0.35%	Building 47	0.34%
Building 11	0.34%	Building 11	0.34%
Building 13	0.34%	Building 13	0.33%
Building 6	0.26%	Building 6	0.26%
Building 61	0.21%	Building 61	0.20%
Building 10	0.20%	Building 10	0.20%
Building 62	0.17%	Building 62	0.17%

Figure 17: Scatter Plot of Risk vs. Risk Reduction due to Retrofit for Complete Damage in 50 years

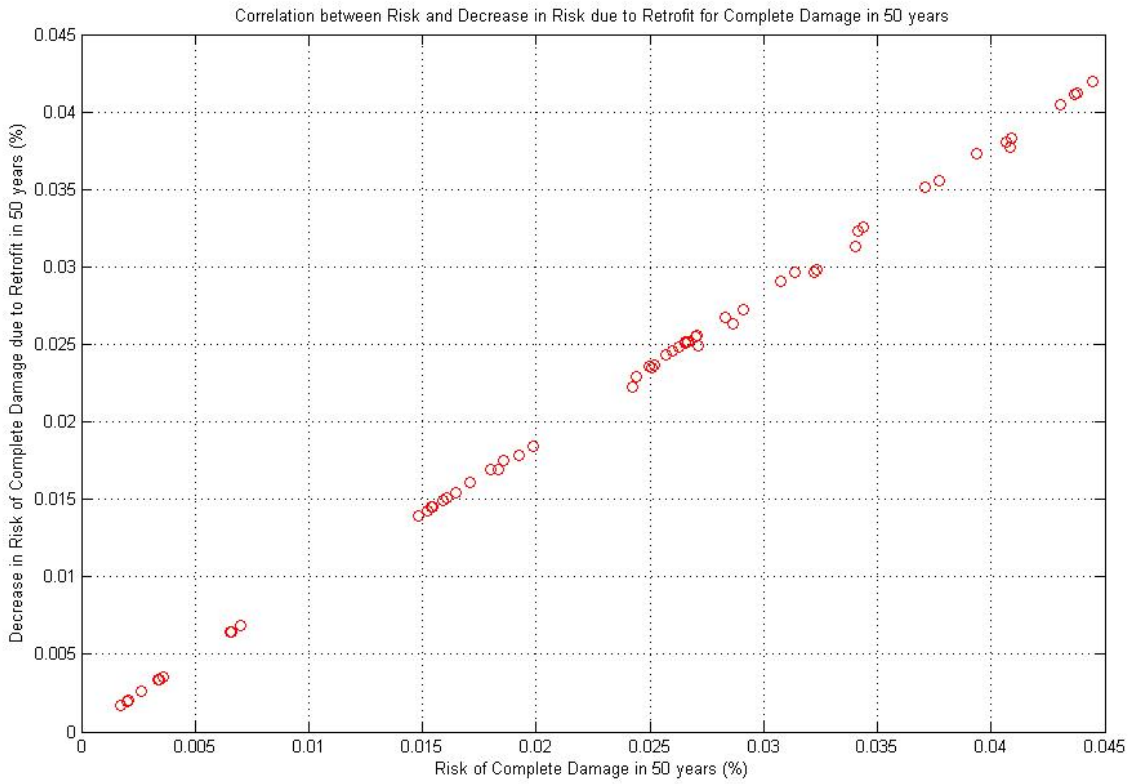

Table 8 is likely of less interest than Table 7, but it presents some very interesting and counter-intuitive results. First, by comparing Tables 7 and 8, it can be seen that the buildings at the highest risk of complete damage are not the same building that are in the highest risk of slight damage. This is due to different ordering of the fragility curves across the buildings in the inventory for complete versus slight damage, as well as different ordering of the hazard curves across the locations for the ground motion levels that cause complete versus slight damage. The different ordering of the fragilities could be caused by buildings being designed specifically to mitigate complete failure with little to no consideration for slight damage. Also, careful examination of Table 8 and, more clearly, Figure 18 shows that there is a negative correlation between risk of slight damage

and retrofit benefit. Notice that the three buildings at the highest risk of slight damage are the exact three building that will benefit least from seismic retrofit. By consulting the legend in Table A1, it can be seen that these three buildings are all high-rise concrete shear wall structures. This result suggests that seismic retrofit is less effective on fragile buildings at mitigating the risk of slight damage, which is counterintuitive. This phenomenon could be due to hazard dominating the risk of slight damage, almost regardless of changes in the fragility like the reduction from retrofit. These are just postulations; further research is required to draw conclusions.

Table 8: Seismic Risk of Slight Damage in 50 years for Non-Ductile Concrete Structures, and the Effect of Retrofit

Building #	Risk of Slight Damage for Pre-Code	Building #	Risk Difference between Pre- and High-Code for Slight Damage
Building 14	89.29%	Building 12	14.18%
Building 24	88.38%	Building 8	13.38%
Building 34	88.33%	Building 61	12.22%
Building 7	88.09%	Building 10	12.02%
Building 15	88.08%	Building 2	11.93%
Building 36	88.04%	Building 4	11.78%
Building 31	86.38%	Building 6	11.09%
Building 44	86.37%	Building 11	10.38%
Building 1	86.12%	Building 13	10.24%
Building 51	86.02%	Building 47	10.15%
Building 33	85.97%	Building 62	9.96%
Building 55	85.88%	Building 27	7.95%
Building 18	85.20%	Building 35	7.77%
Building 56	84.69%	Building 17	7.63%
Building 57	84.62%	Building 39	7.62%
Building 26	84.61%	Building 20	7.53%
Building 60	84.10%	Building 50	7.49%
Building 5	83.71%	Building 16	7.47%
Building 49	83.60%	Building 28	7.46%
Building 32	83.57%	Building 23	7.46%
Building 19	83.48%	Building 3	7.44%
Building 9	83.29%	Building 40	7.43%
Building 42	83.18%	Building 54	7.41%
Building 38	82.59%	Building 48	7.40%
Building 59	82.54%	Building 30	7.35%

Building 41	82.29%	Building 43	7.34%
Building 53	82.00%	Building 22	7.29%
Building 58	81.87%	Building 46	7.26%
Building 29	81.68%	Building 25	7.24%
Building 46	81.67%	Building 58	7.23%
Building 25	81.62%	Building 52	7.23%
Building 21	81.53%	Building 53	7.20%
Building 45	81.30%	Building 21	7.19%
Building 43	81.27%	Building 29	7.18%
Building 37	80.02%	Building 41	7.16%
Building 52	79.75%	Building 37	7.13%
Building 22	79.06%	Building 59	7.09%
Building 48	78.51%	Building 38	7.09%
Building 54	78.44%	Building 45	6.96%
Building 40	78.35%	Building 9	6.95%
Building 3	78.24%	Building 49	6.87%
Building 30	78.24%	Building 60	6.78%
Building 23	78.22%	Building 32	6.56%
Building 28	78.02%	Building 42	6.53%
Building 50	78.00%	Building 5	6.53%
Building 16	77.93%	Building 19	6.50%
Building 20	77.64%	Building 18	6.49%
Building 39	77.03%	Building 1	6.35%
Building 17	76.90%	Building 57	6.29%
Building 35	75.93%	Building 56	6.28%
Building 27	74.68%	Building 26	6.14%
Building 11	68.26%	Building 7	6.02%
Building 2	68.20%	Building 15	6.02%
Building 4	63.03%	Building 55	6.01%
Building 13	60.95%	Building 44	5.97%
Building 47	59.57%	Building 33	5.96%
Building 12	33.23%	Building 51	5.94%
Building 61	30.79%	Building 31	5.86%
Building 10	30.10%	Building 36	5.75%
Building 6	29.02%	Building 34	5.66%
Building 8	28.58%	Building 24	5.65%
Building 62	24.45%	Building 14	5.29%

Figure 18: Scatter Plot of Risk vs. Risk Reduction due to Retrofit for Slight Damage in 50 years

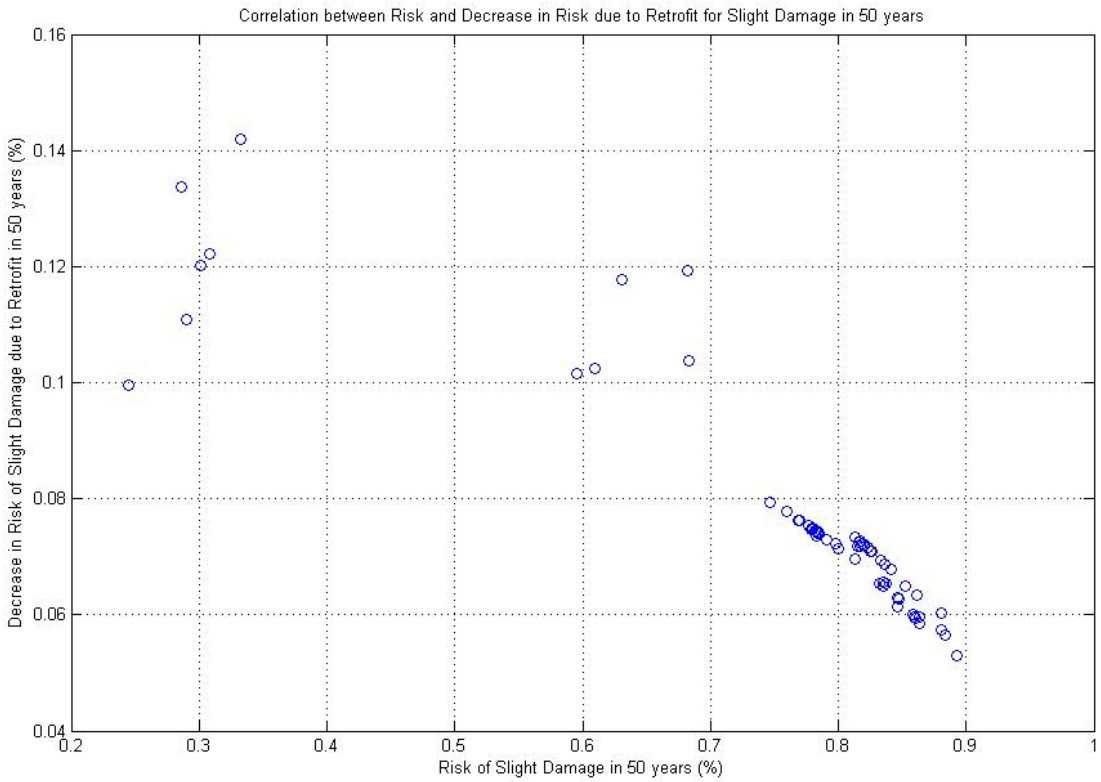

Finally, Table 9 presents the expected annual loss ratios for the sample inventory of non-ductile concrete structures in the Los Angeles area. Similar to Tables 7 and 8, Table 9 includes the decrease in the expected annual loss ratio that buildings would experience after being retrofitted to high-code levels of seismic design. There is a positive correlation between expected annual loss ratio and benefit of retrofit, which can be seen in Figure 19, but it is weaker than that observed for the risk of complete damage.

Table 9: Expected Annual Loss Ratios for Non-Ductile Concrete Structures, and the Effect of Retrofit

Building #	Loss Ratio for Pre-Code	Building #	Loss Ratio Difference between Pre- and High-Code
Building #34	0.001036	Building #51	0.001111
Building #14	0.000955	Building #33	0.001108
Building #24	0.000936	Building #55	0.001092
Building #36	0.000917	Building #31	0.001022
Building #1	0.000904	Building #42	0.000964
Building #11	0.000852	Building #56	0.000931
Building #15	0.000839	Building #57	0.000926
Building #44	0.000811	Building #5	0.000910
Building #51	0.000792	Building #19	0.000906
Building #33	0.000791	Building #32	0.000905
Building #31	0.000789	Building #44	0.000881
Building #55	0.000784	Building #26	0.000881
Building #7	0.000777	Building #48	0.000880
Building #60	0.000734	Building #18	0.000863
Building #56	0.000732	Building #34	0.000861
Building #57	0.000729	Building #45	0.000818
Building #9	0.000715	Building #37	0.000758
Building #13	0.000706	Building #1	0.000754
Building #42	0.000697	Building #54	0.000723
Building #26	0.000697	Building #22	0.000720
Building #47	0.000696	Building #30	0.000720
Building #59	0.000695	Building #40	0.000713
Building #38	0.000694	Building #3	0.000712
Building #49	0.000689	Building #16	0.000710
Building #5	0.000682	Building #52	0.000691
Building #18	0.000679	Building #35	0.000680
Building #32	0.000678	Building #39	0.000672
Building #41	0.000677	Building #24	0.000669
Building #53	0.000676	Building #14	0.000661
Building #58	0.000671	Building #36	0.000652
Building #21	0.000669	Building #17	0.000643
Building #43	0.000655	Building #28	0.000635
Building #19	0.000654	Building #23	0.000629
Building #29	0.000652	Building #50	0.000622
Building #48	0.000648	Building #20	0.000615
Building #25	0.000639	Building #27	0.000554
Building #45	0.000618	Building #15	0.000549
Building #46	0.000618	Building #9	0.000484
Building #37	0.000615	Building #59	0.000472
Building #22	0.000590	Building #38	0.000470
Building #2	0.000584	Building #7	0.000465
Building #61	0.000581	Building #53	0.000458

Building #30	0.000569	Building #21	0.000456
Building #54	0.000553	Building #58	0.000453
Building #40	0.000549	Building #29	0.000448
Building #3	0.000547	Building #60	0.000447
Building #16	0.000544	Building #43	0.000443
Building #50	0.000528	Building #25	0.000431
Building #35	0.000527	Building #49	0.000424
Building #17	0.000526	Building #41	0.000412
Building #39	0.000521	Building #2	0.000405
Building #28	0.000521	Building #46	0.000386
Building #23	0.000521	Building #12	0.000292
Building #4	0.000512	Building #11	0.000282
Building #20	0.000510	Building #13	0.000257
Building #10	0.000500	Building #47	0.000236
Building #27	0.000470	Building #6	0.000222
Building #6	0.000462	Building #4	0.000209
Building #12	0.000451	Building #10	0.000204
Building #52	0.000433	Building #61	0.000202
Building #8	0.000380	Building #8	0.000193
Building #62	0.000319	Building #62	0.000140

Figure 19: Scatter Plot of Expected Annual Loss Ratio vs. Reduction in Expected Annual Loss Ratio due to Retrofit

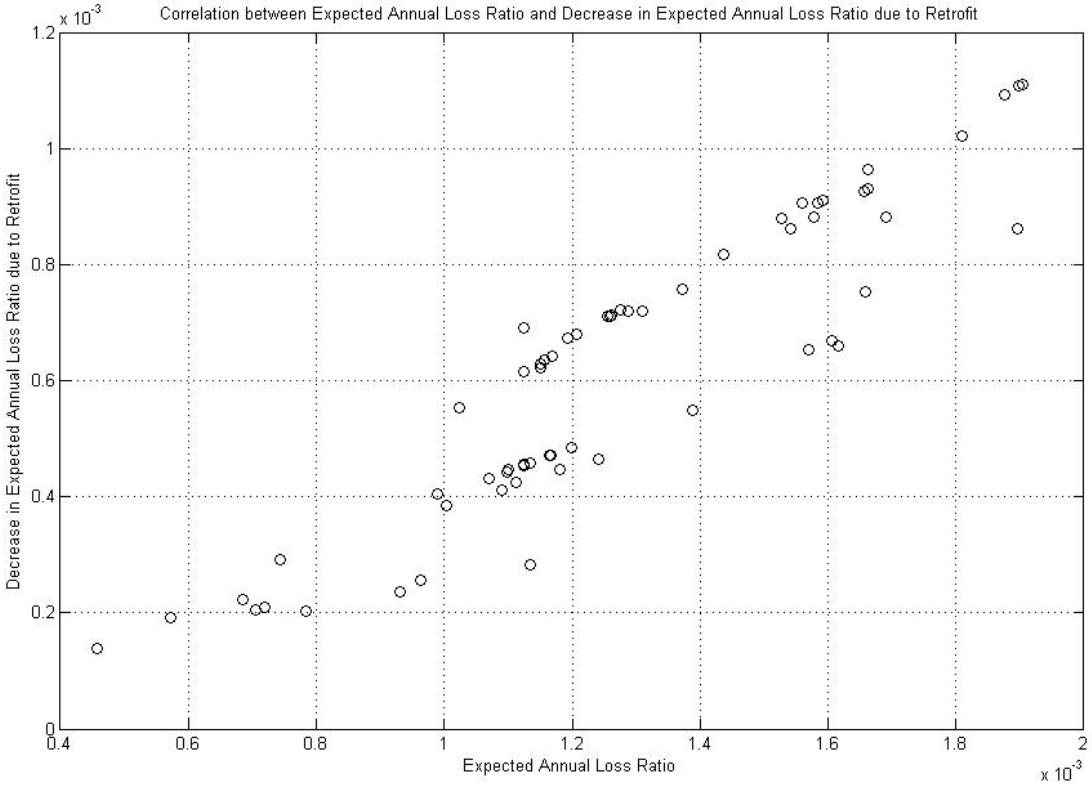

Figures 20 and 21 illustrate the extent to which the risk of slight and complete damage, respectively, in the next 50 years for the sample LA inventory would be reduced if all of the buildings were retrofitted to a high level of seismic design. Analogously, Figure 22 portrays the decrease in expected annual loss ratio that would result from increasing the ductility of all of the buildings in the inventory. Even within this relatively small inventory of 62 buildings, retrofit would have a variable effect in terms risk mitigation, e.g., from 0%-5% reduction of risk for complete damage and 5%-20% for slight damage. Figure 20 provides a means to rapidly identify the buildings that will benefit most from seismic retrofit, in terms of reduction of the risk of complete damage, and those that will only benefit slightly. Figure 21 is included to allow for comparison across damage states, and Figure 22 for comparison with the results for expected annual loss ratio.

Figure 20: Difference Map for Complete Damage in the next 50 years for LA inventory

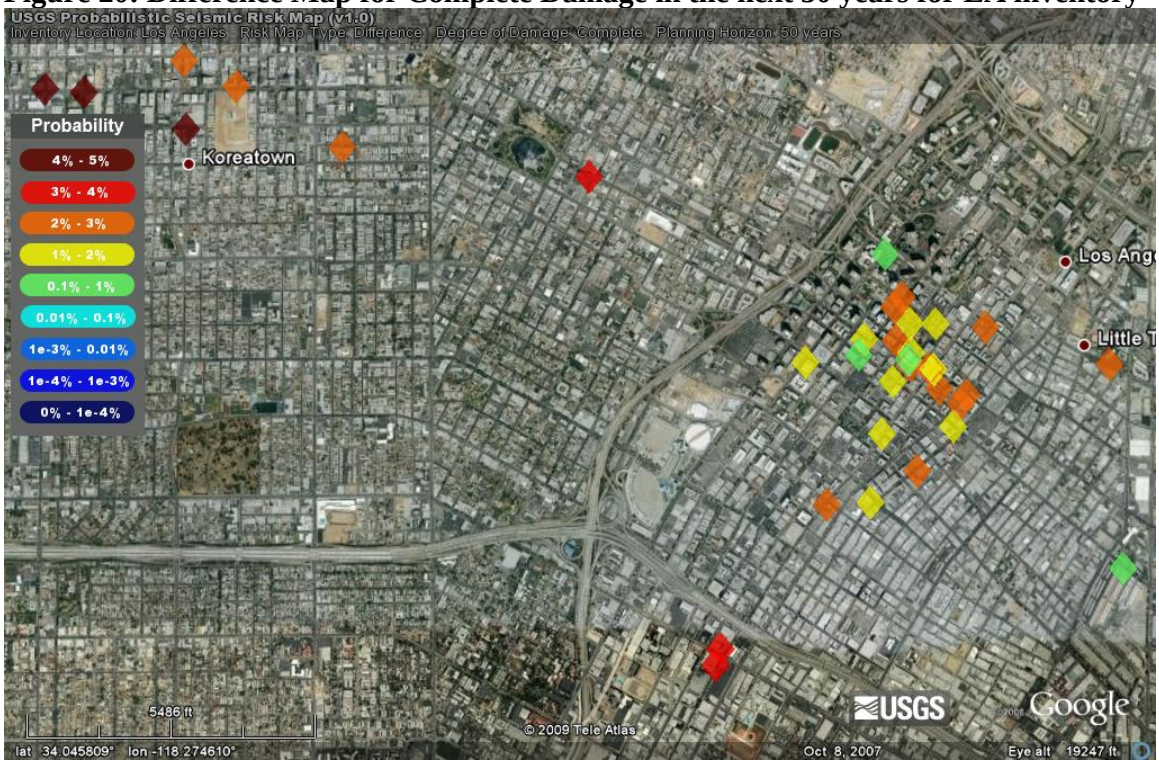

Figure 21: Difference Map for Slight Damage in the next 50 years for LA inventory

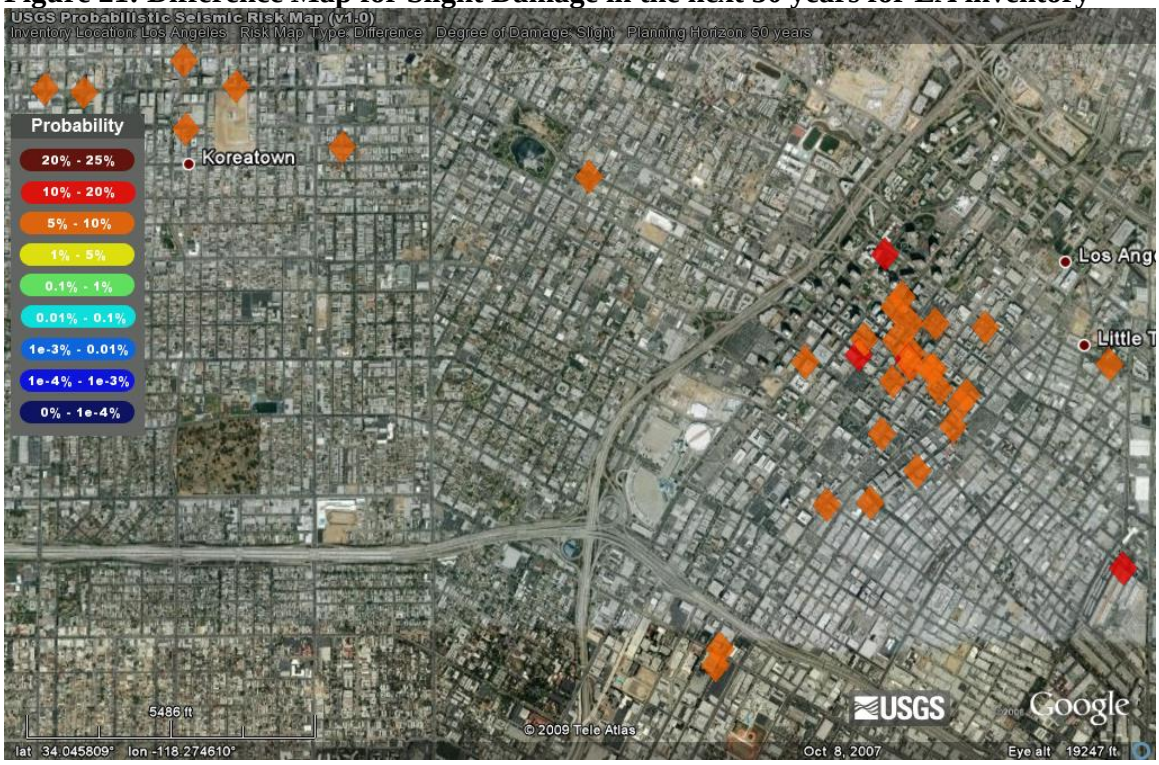

Figure 22: Expected Annual Loss Ratio Difference Map for LA inventory

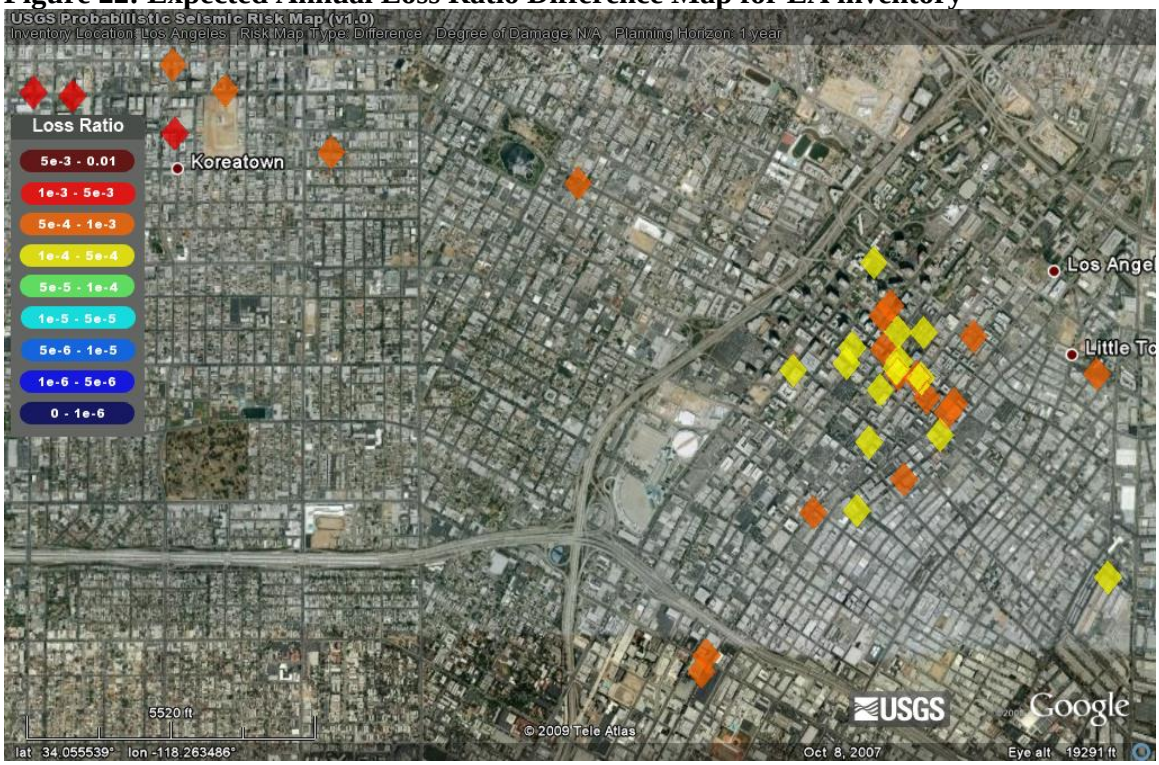

4 CONCLUSION

The updated USGS risk map web tool provides a means for a quick and comprehensive seismic retrofit investigation. It was designed and developed considering the case of non-ductile concrete buildings in imminent threat of catastrophic failure, but is applicable to all structural types specified in HAZUS or by a user. The web tool enables users to quickly narrow the scope of a retrofit project from the entire US to increasingly smaller problematic regions and finally to specific buildings. However, to pinpoint risky buildings, an inventory of an area must be collected and inserted into the web tool.

While the capabilities of the risk map web tool have been greatly extended from its original form, there is still plenty of room for future improvement. Among others, one such improvement could be the incorporation of more accurate site class (or V_S30) data, in the regions where it is available, and/or hazard curves that are more accurate for site classes other than the B/C boundary than those obtained in this report via the NEHRP site coefficients. A default exposure/inventory of buildings based on HAZUS census tract/block-level data might also be incorporated, as could fragility/vulnerability curves that depend not only on the type of building but also on its location, since buildings are designed differently in different regions. Another future capability of the web tool could be the incorporation of building values, in order to extend the expected annual loss ratios to produce maps of the expected annual monetary loss, and retrofit costs, in order to perform more formal benefit-cost analyses as another means to quantify the utility of retrofit. Finally, the interactive capabilities of the web tool can be extended, e.g., to read user-friendly file types such as Excel, and Google Maps in addition to Google Earth.

Appendix

Figure A1: Risk Map for C1L, Pre-Code, Slight Damage, 50 years

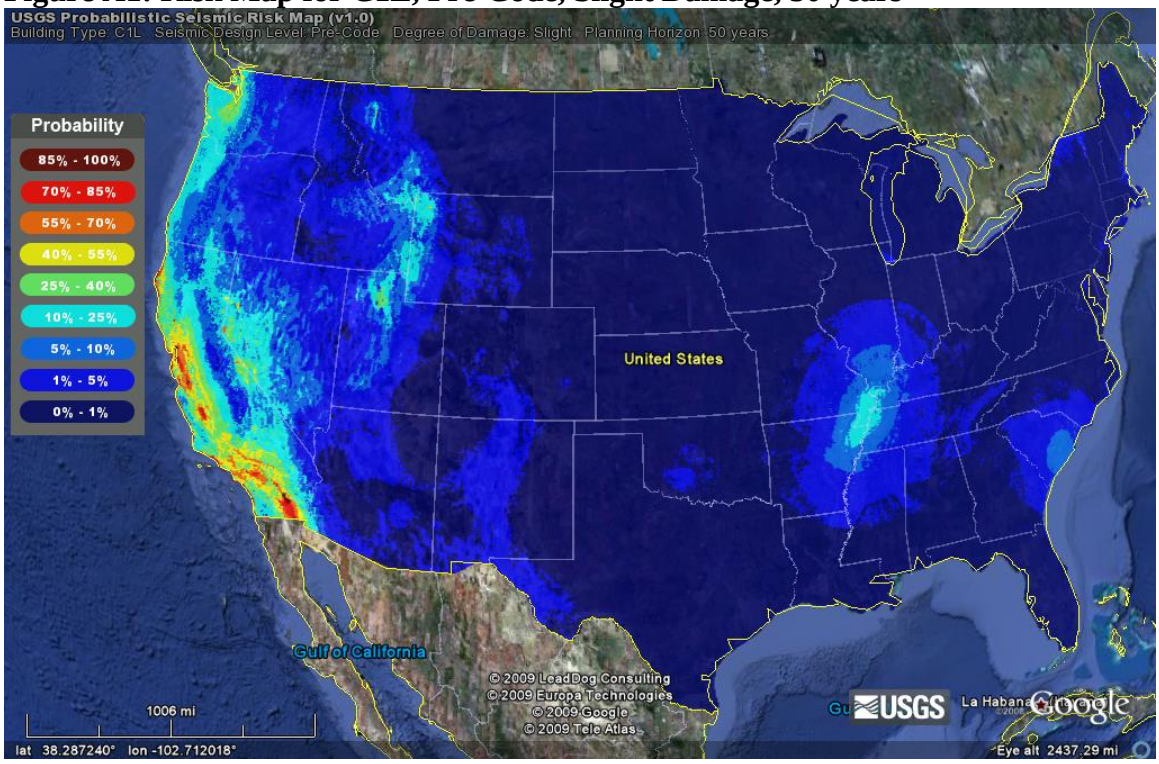

Figure A2: Risk Map for C1L, High-Code, Slight Damage, 50 years

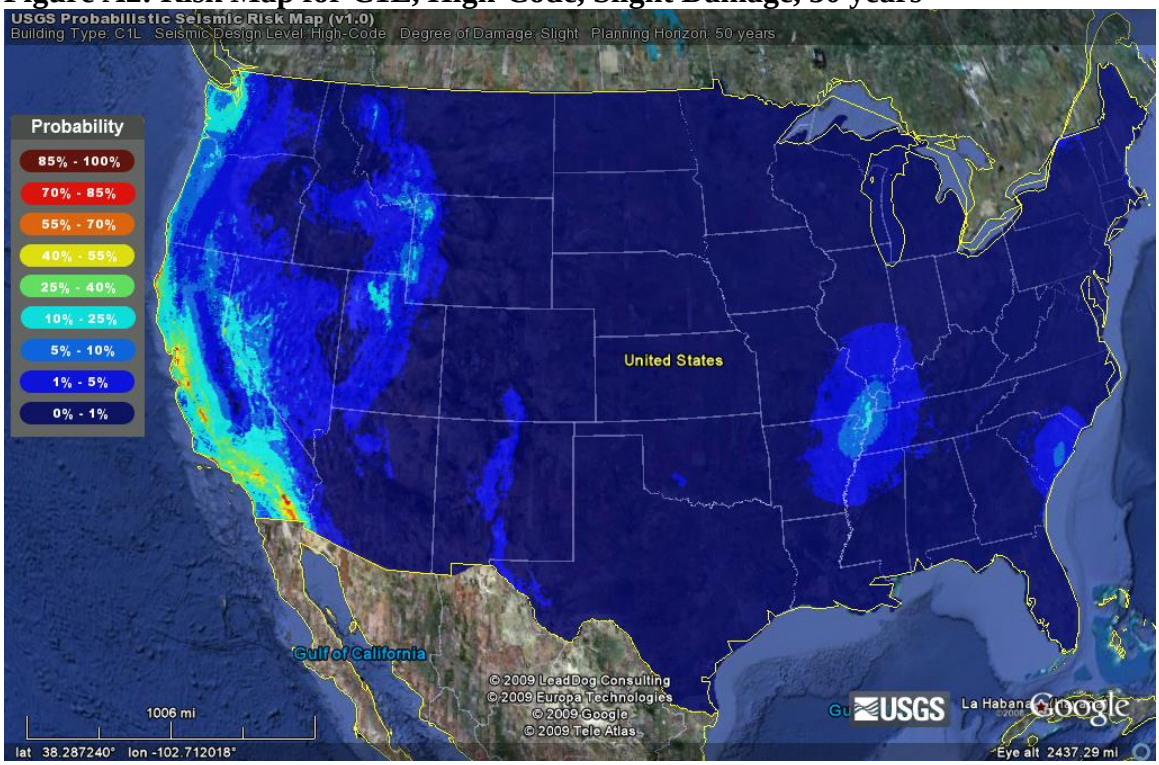

Figure A3: Difference Map for C1L, Pre- vs. High-Code, Slight Damage, 50 years

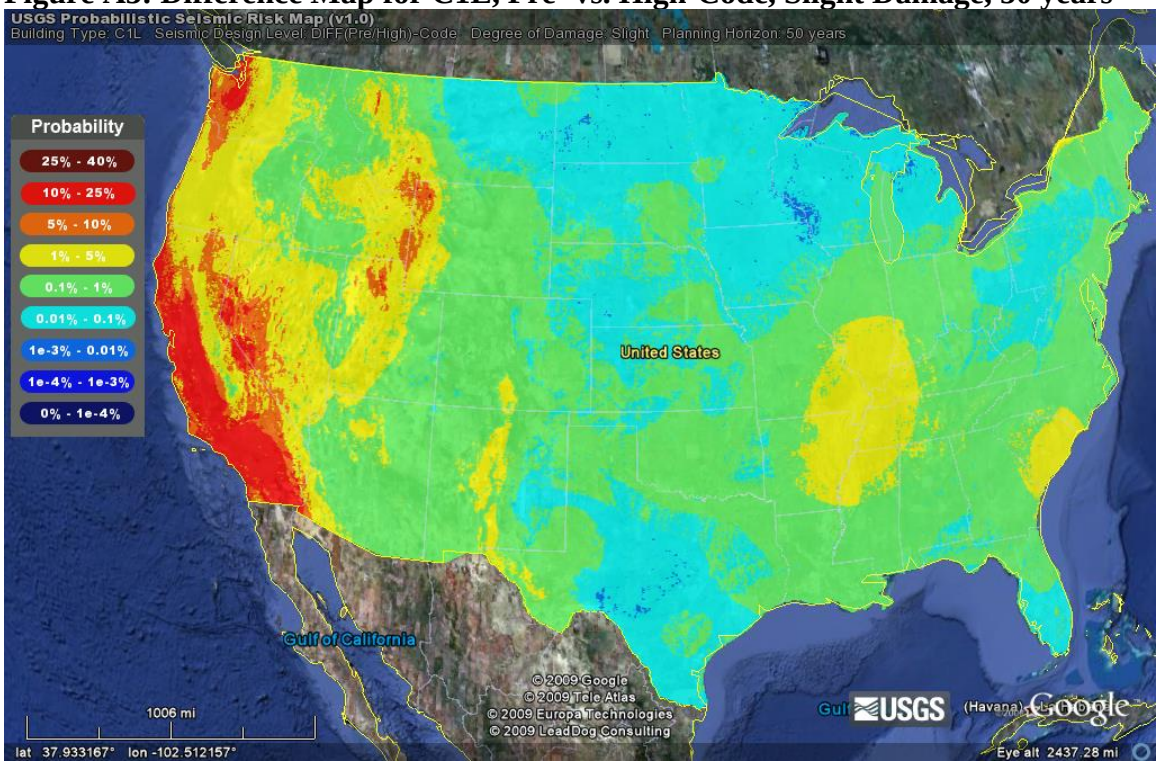

Figure A4: Risk Map for C1L, Pre-Code, Complete Damage, 50 years

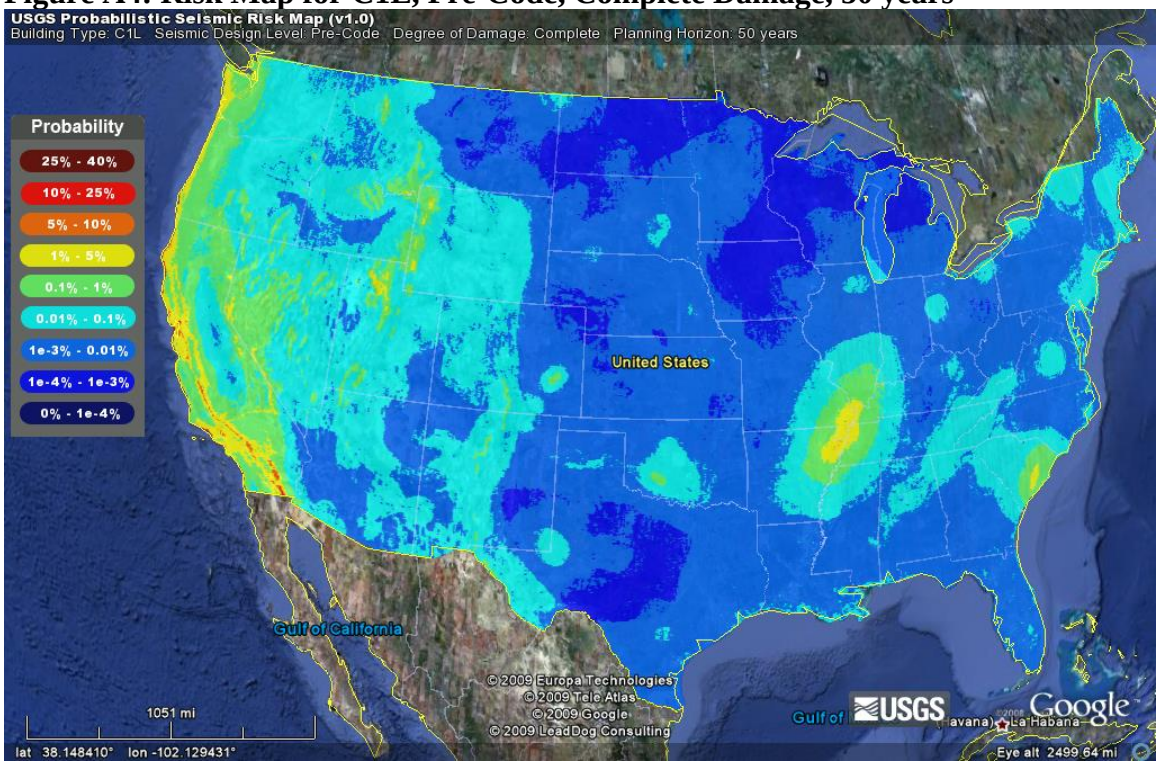

Figure A5: Risk Map for C1L, High-Code, Complete Damage, 50 years

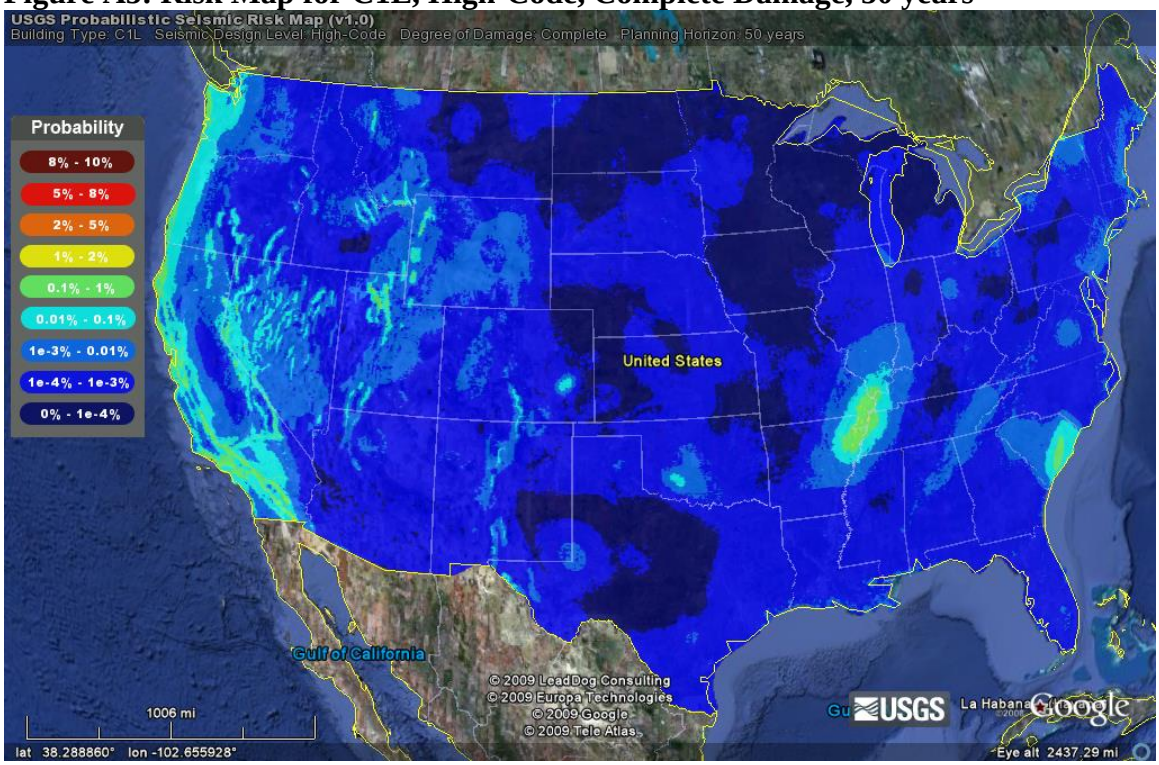

Figure A6: Difference Map for C1L, Pre -vs. High-Code, Complete Damage, 50 years

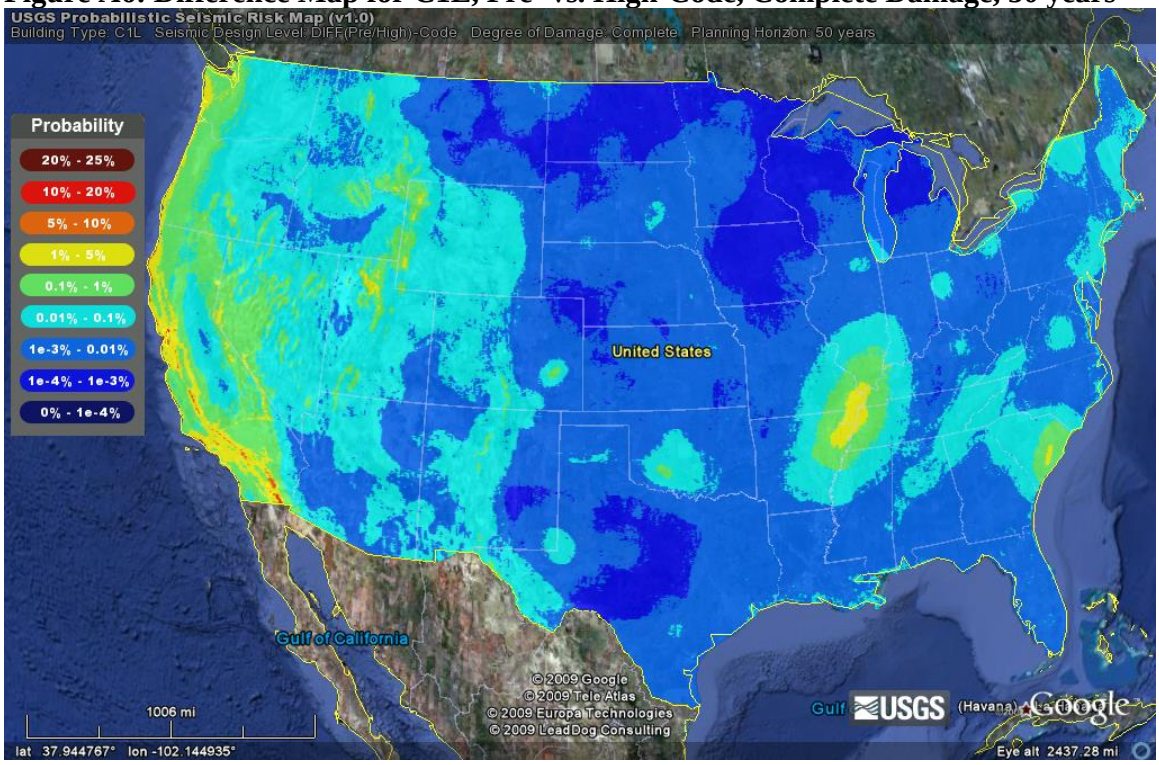

Figure A7: Expected Loss Ratio Map for C1L, Pre-Code, COM4, 1 year

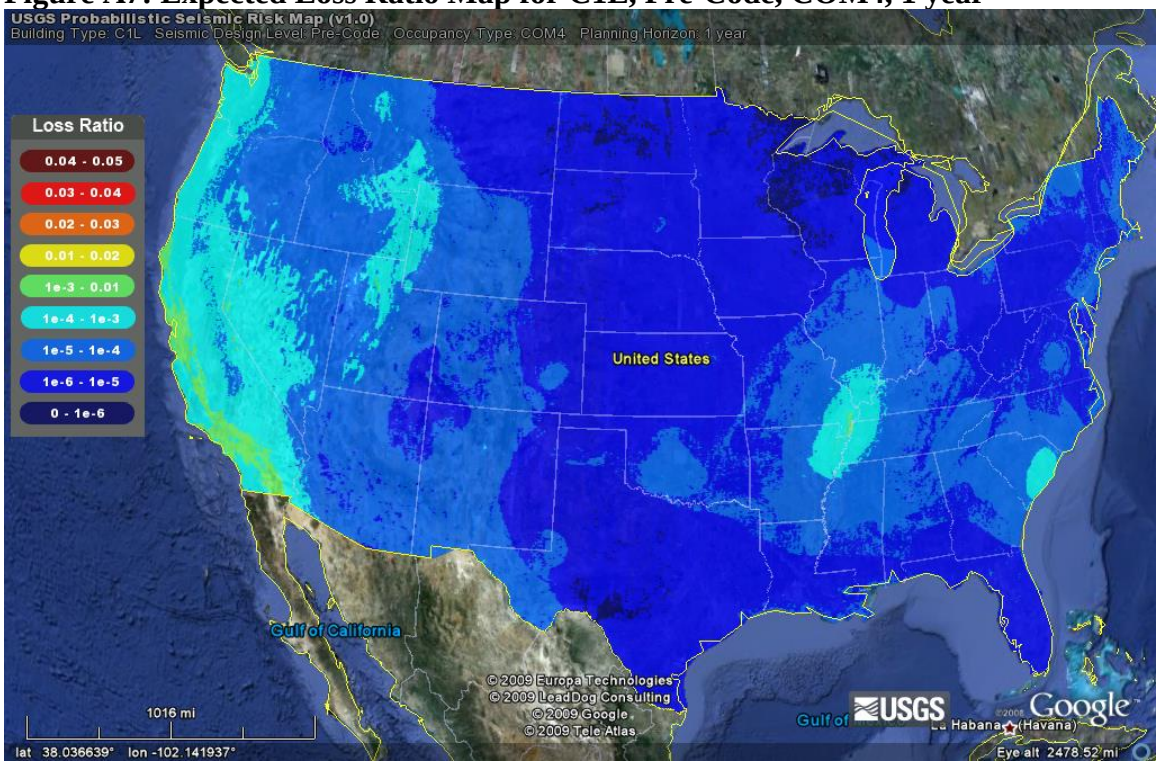

Figure A8: Expected Loss Ratio Map for C1L, High-Code, COM4, 50 years

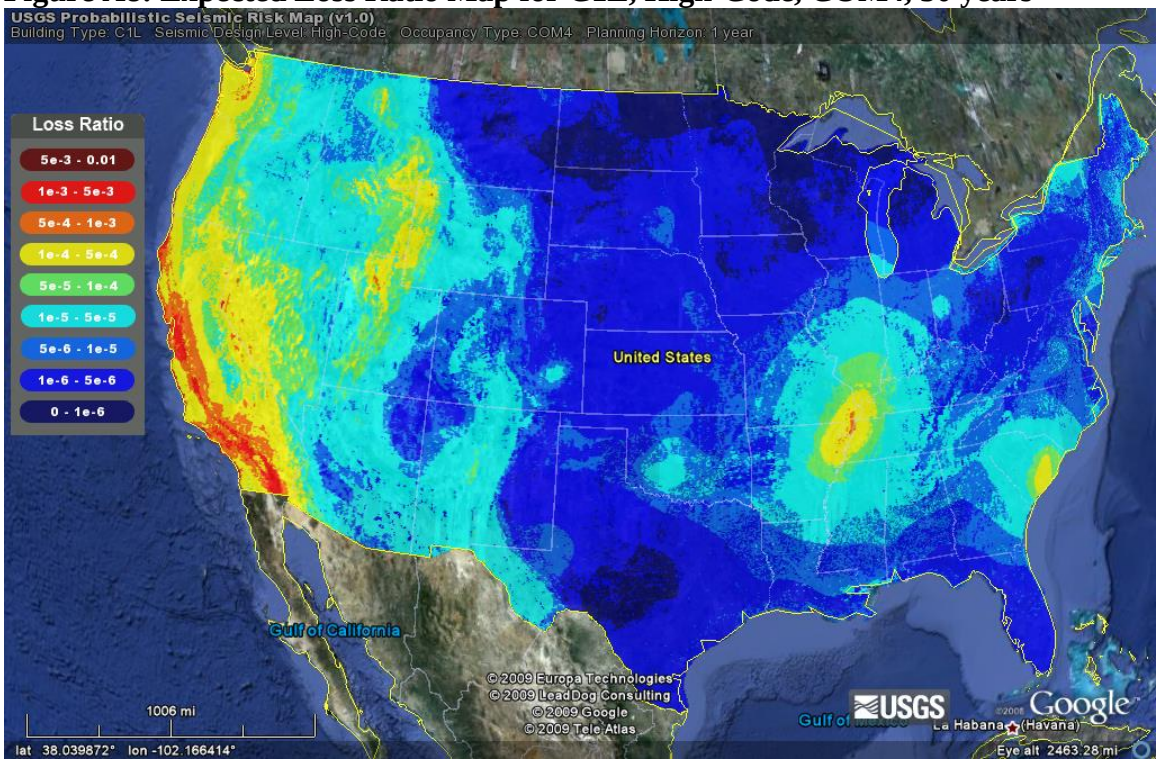

Figure A9: Expected Loss Ratio Difference Map for C1L, Pre-Code, COM4, 1 year

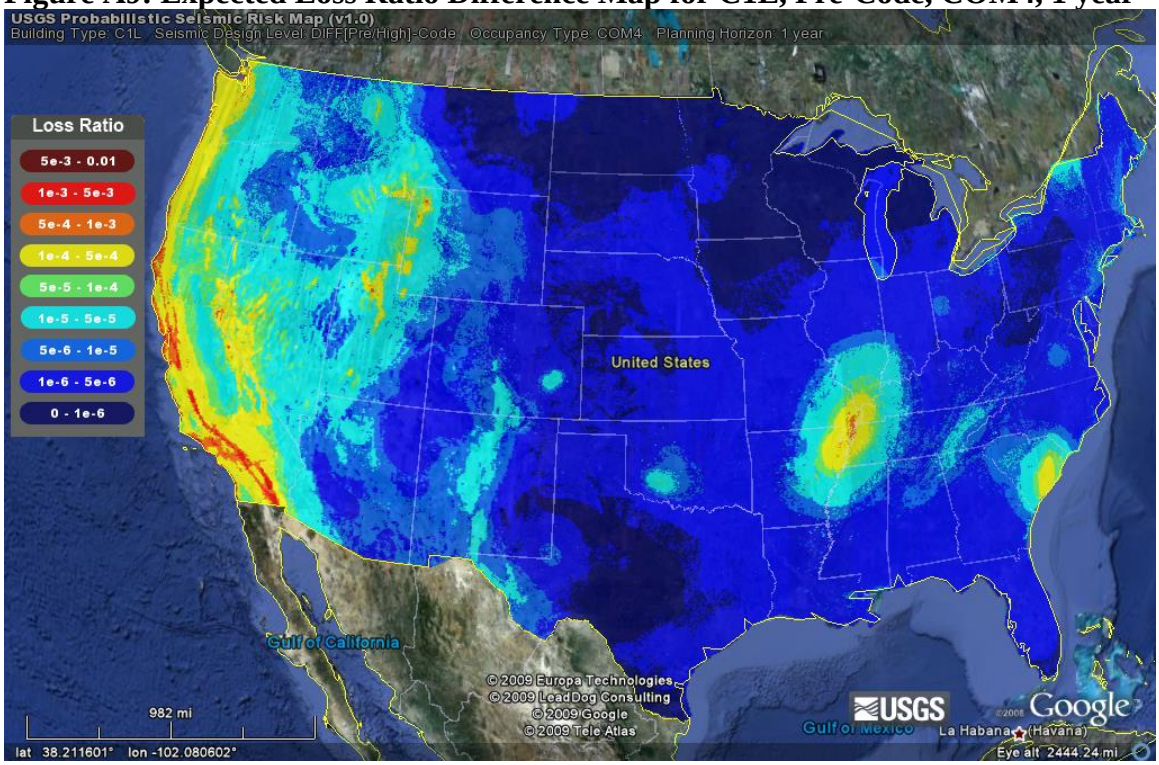

Figure A10: Risk Map for C1M, Pre-Code, Slight Damage, 50 years

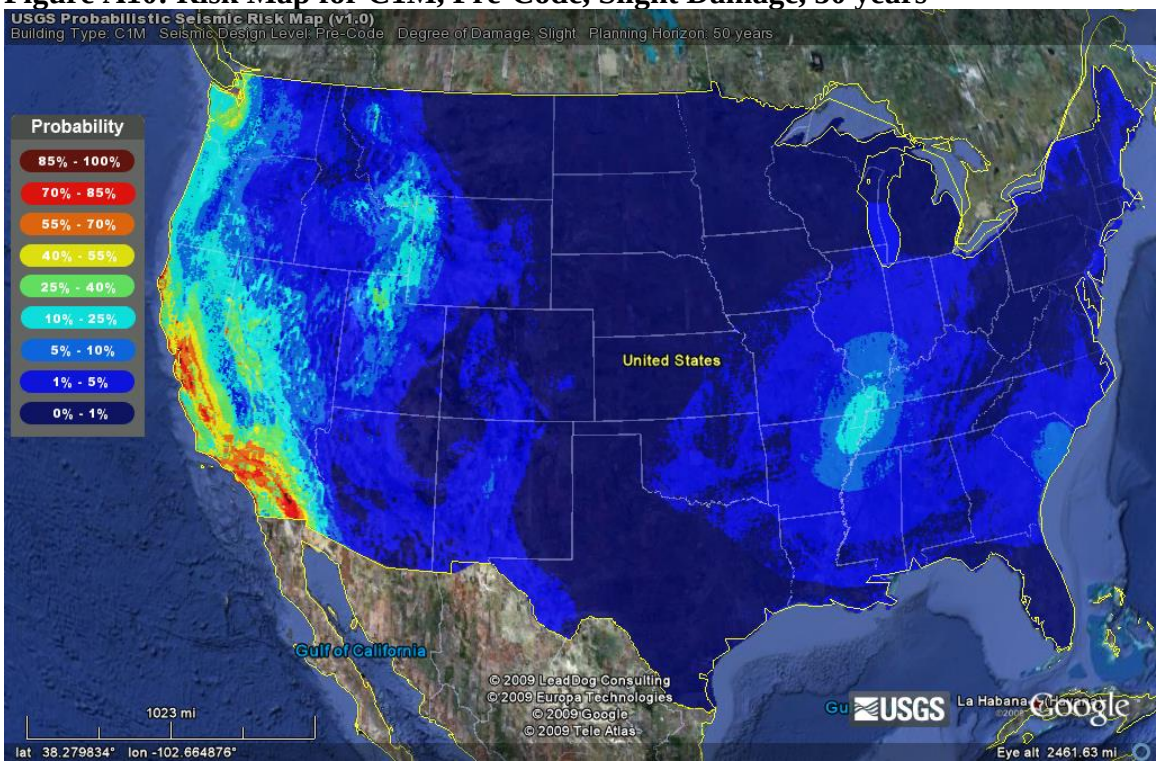

Figure A11: Risk Map for C1M, High-Code, Slight Damage, 50 years

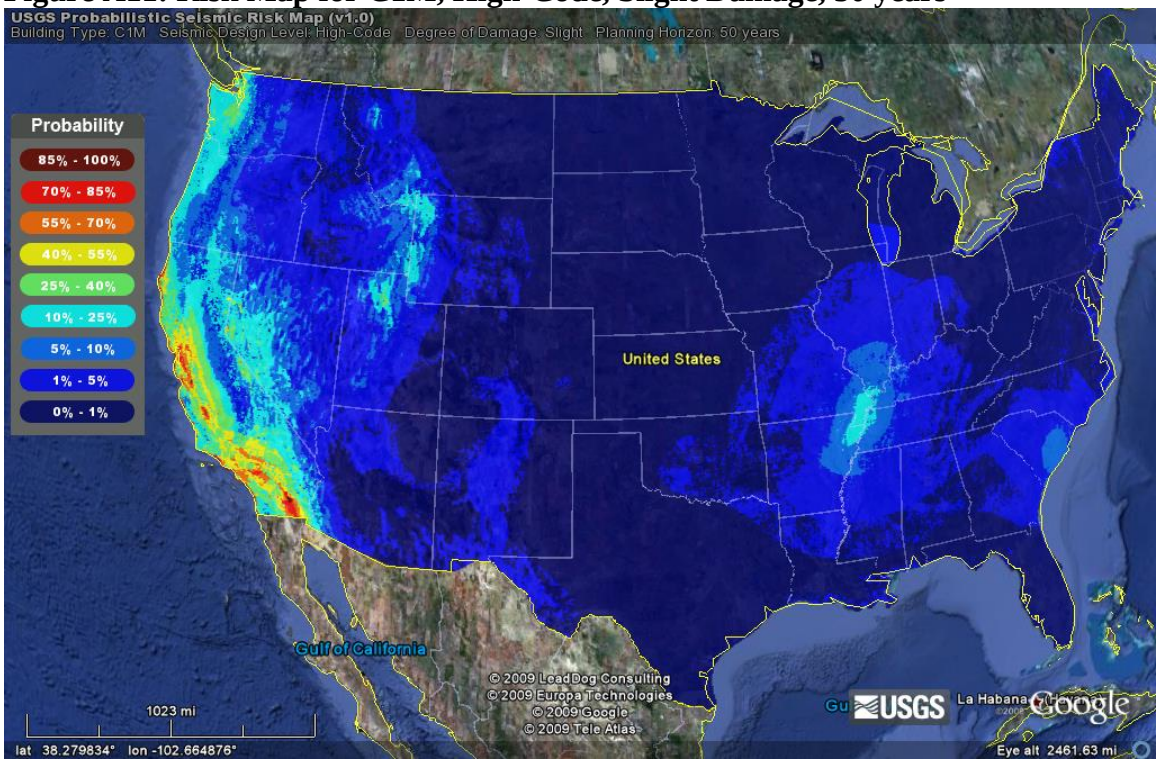

Figure A12: Difference Map for C1M, Pre- vs. High-Code, Slight Damage, 50 years

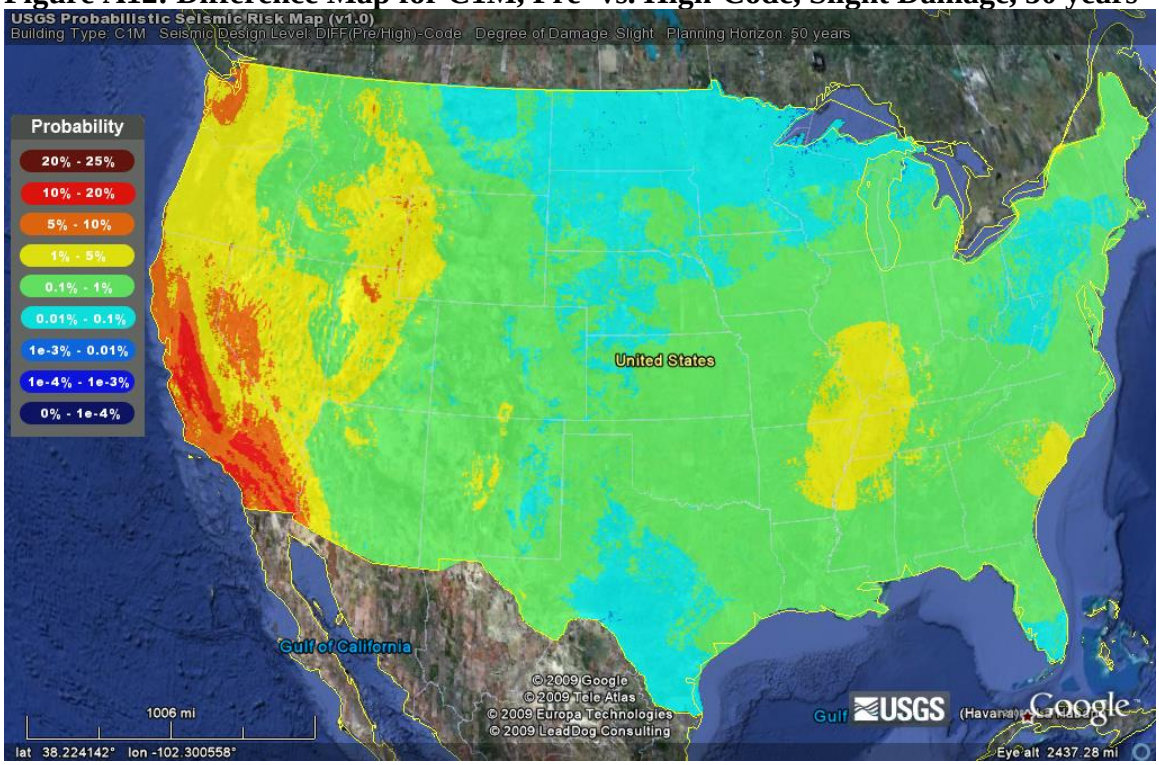

Figure A13: Risk Map for C1M, Pre-Code, Complete Damage, 50 years

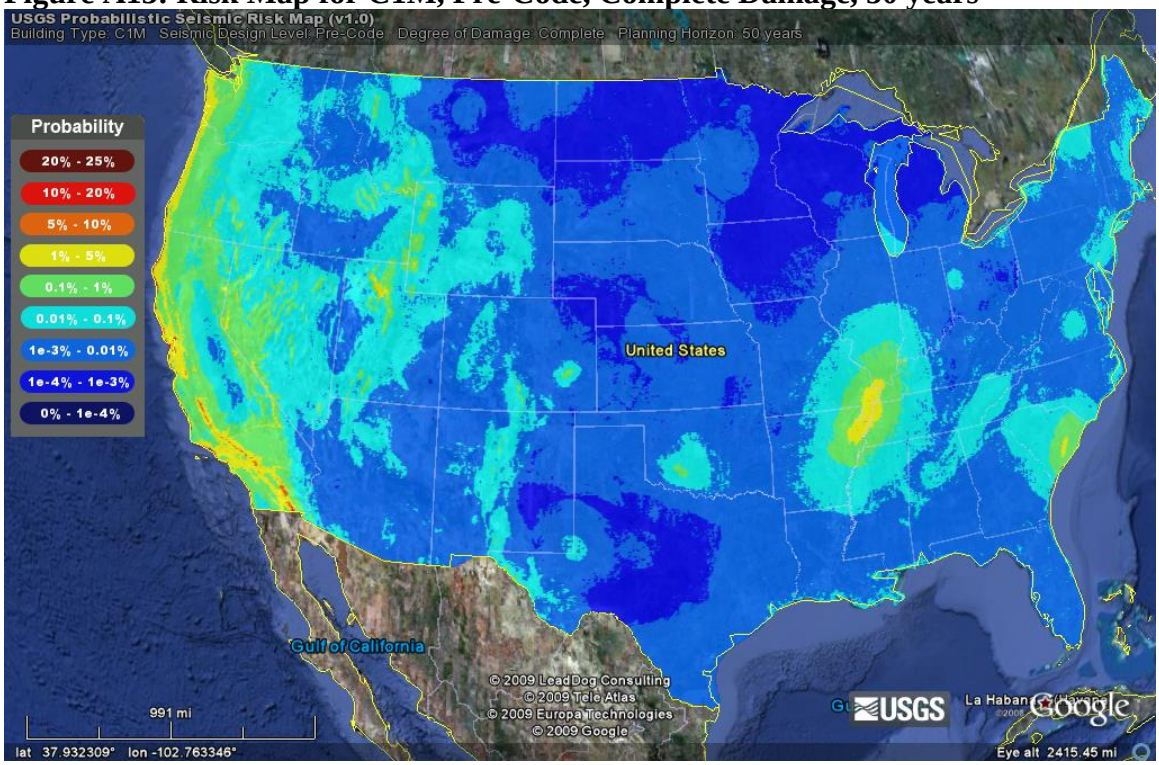

Figure A14: Risk Map for C1M, High-Code, Complete Damage, 50 years

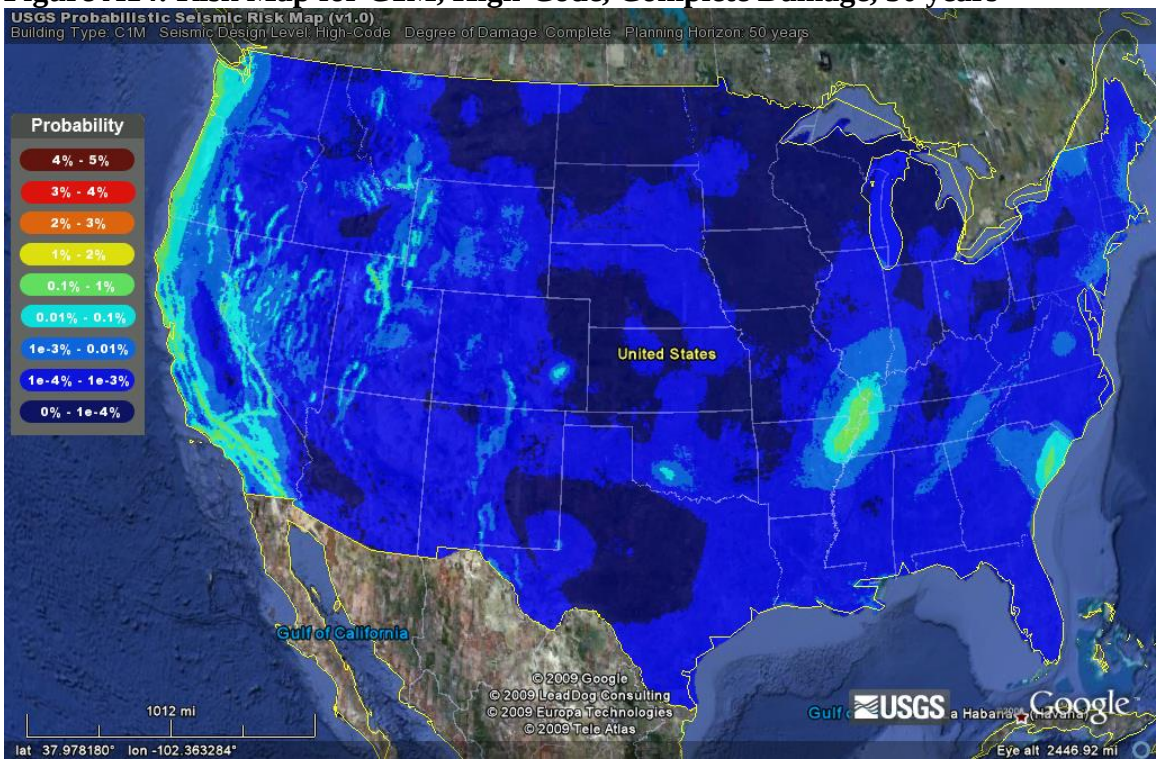

Figure A15: Difference Map for C1M, Pre- vs. High-Code, Complete Damage, 50 years

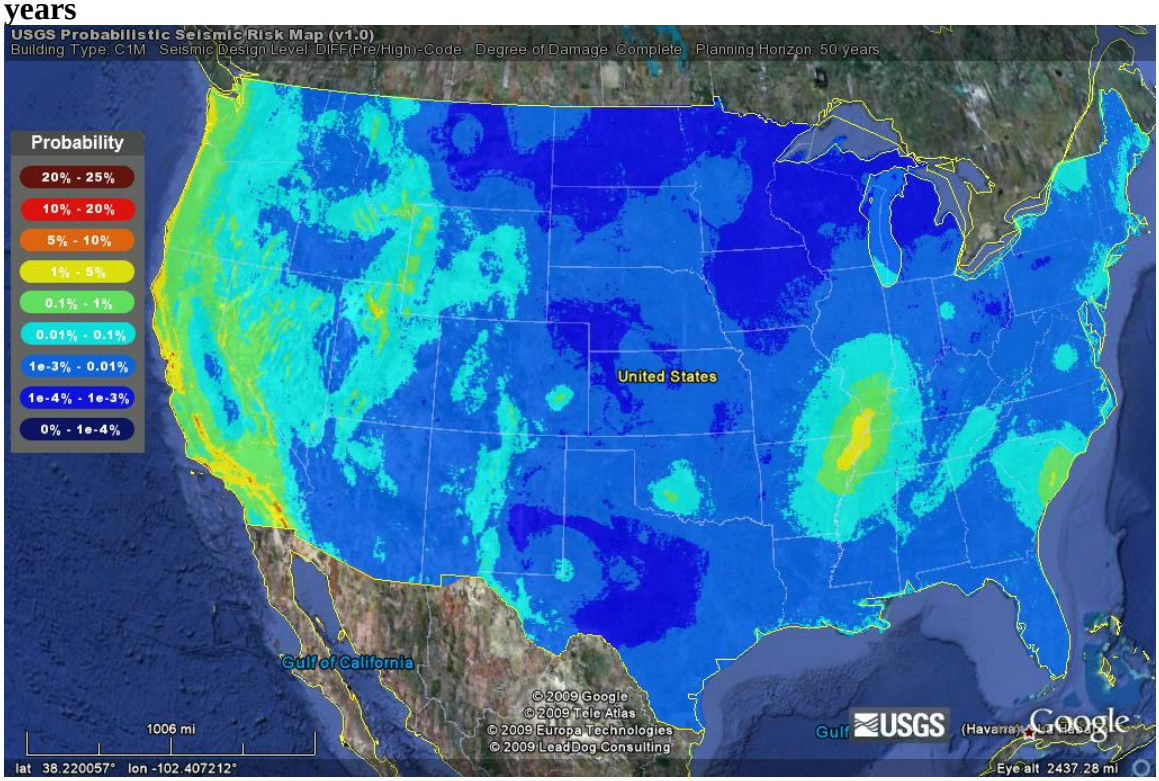

Figure A16: Expected Loss Ratio Map for C1M, Pre-Code, COM4, 1 year

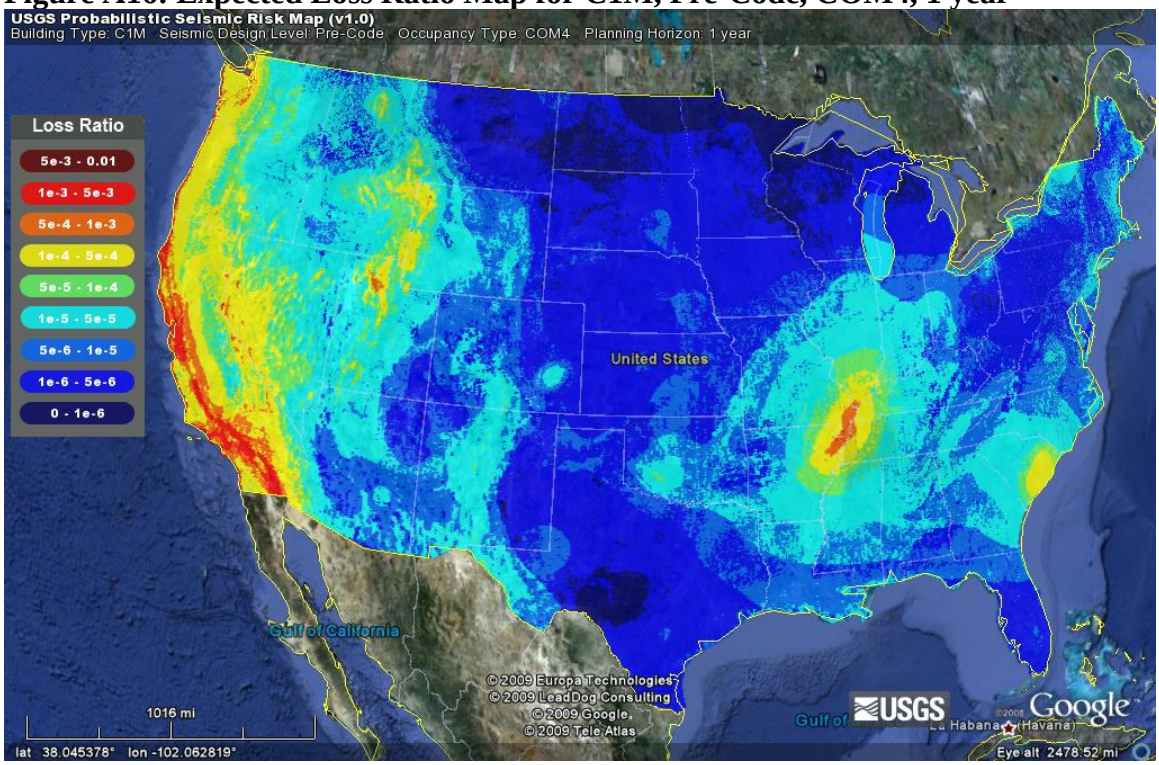

Figure A17: Expected Loss Ratio Map for C1M, High-Code, COM4, 1 year

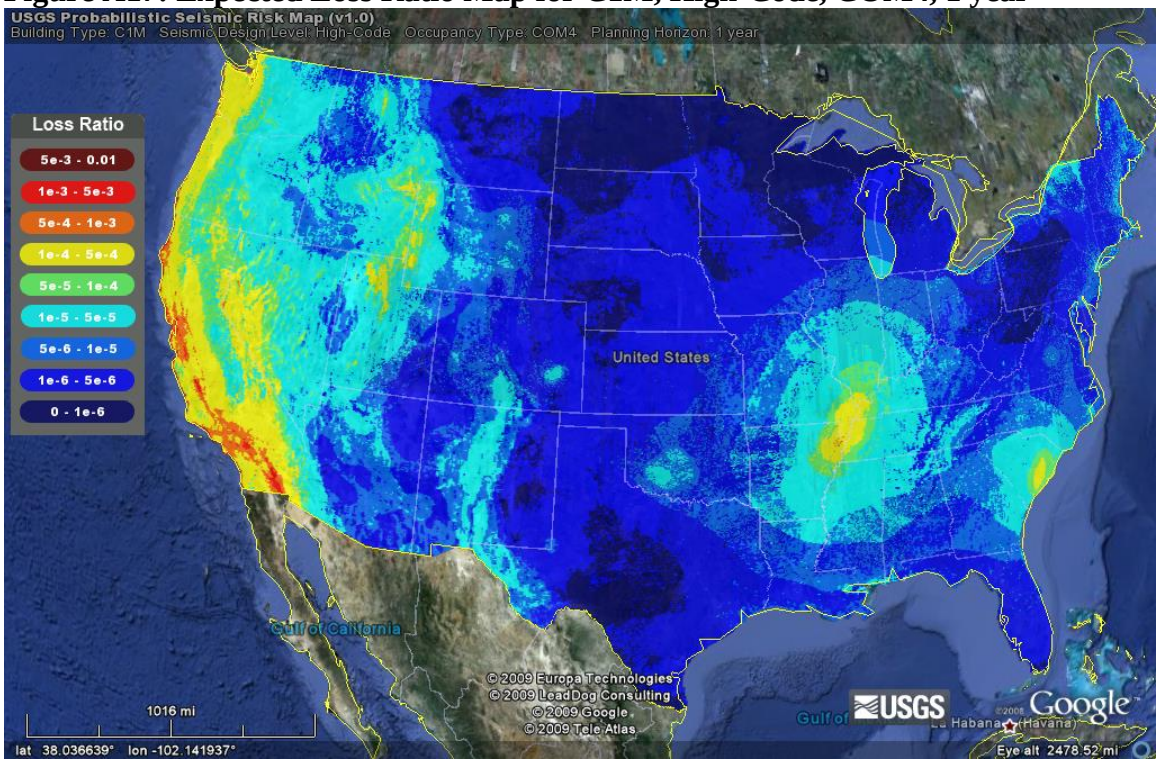

Figure A18: Expected Loss Ratio Difference Map for C1M, Pre- vs. High-Code, COM4, 1 year

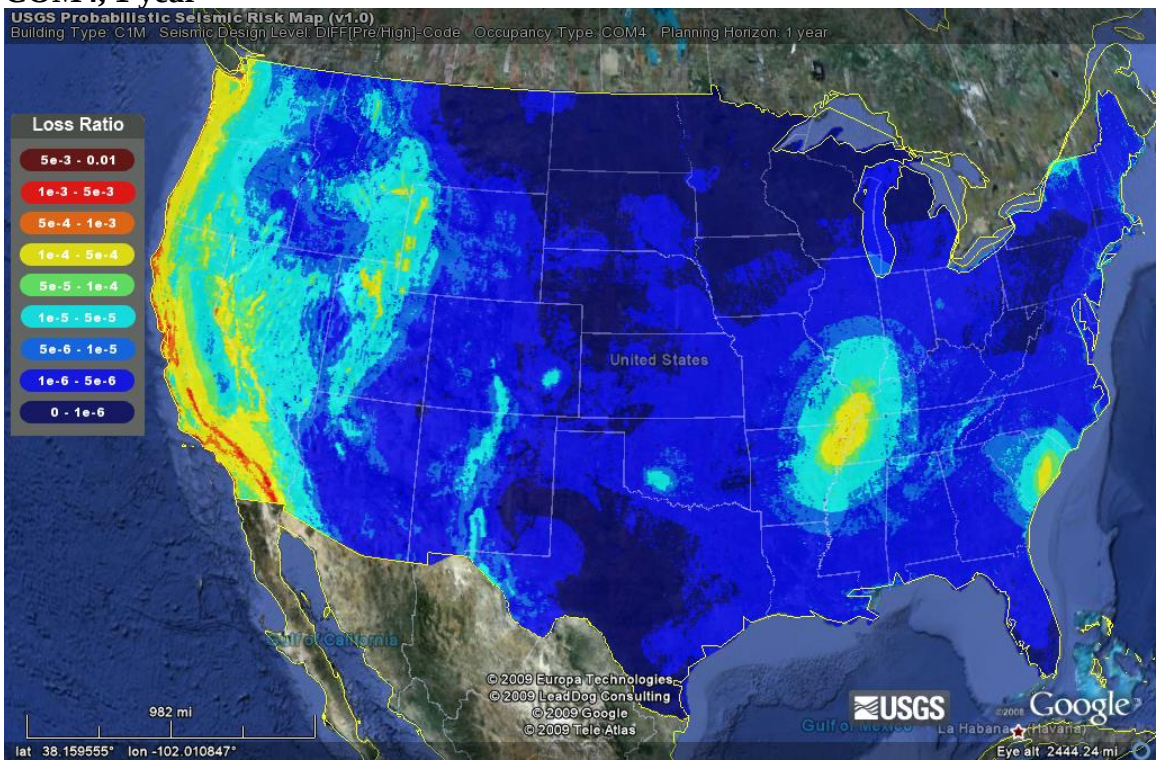

Figure A19: Risk Map for C1H, Pre-Code, Slight Damage, 50 years

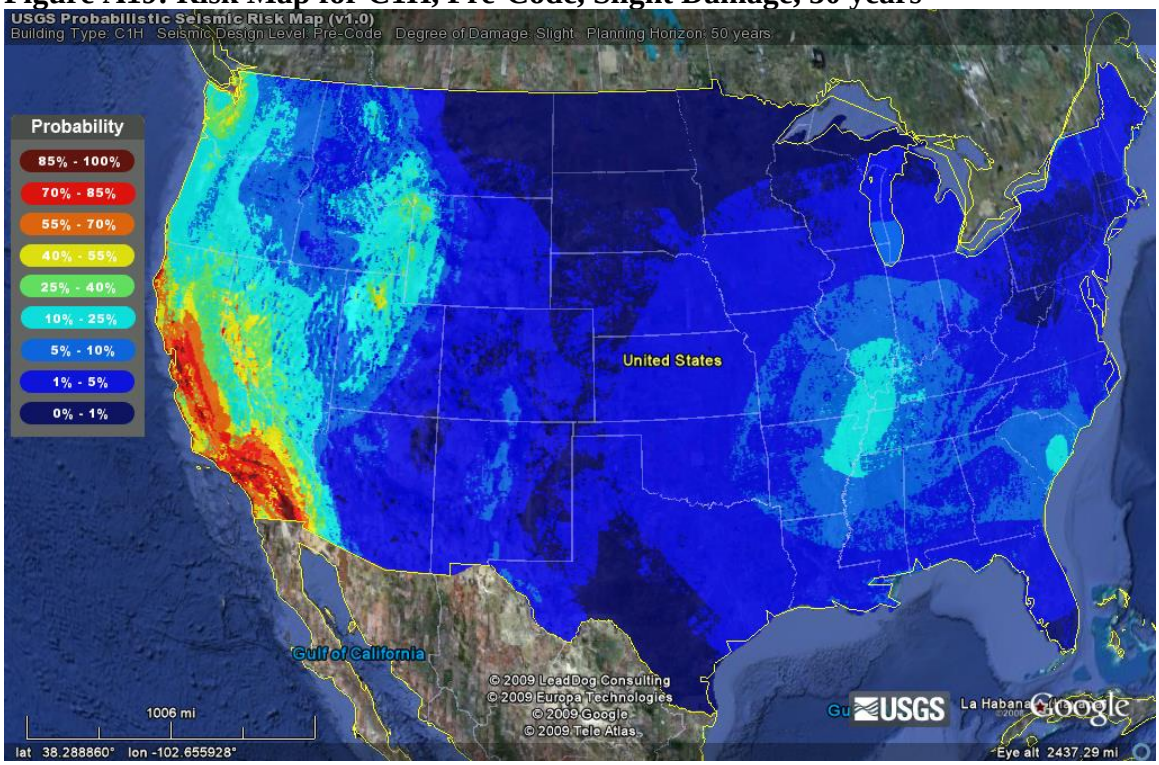

Figure A20: Risk Map for C1H, High-Code, Slight Damage, 50 years

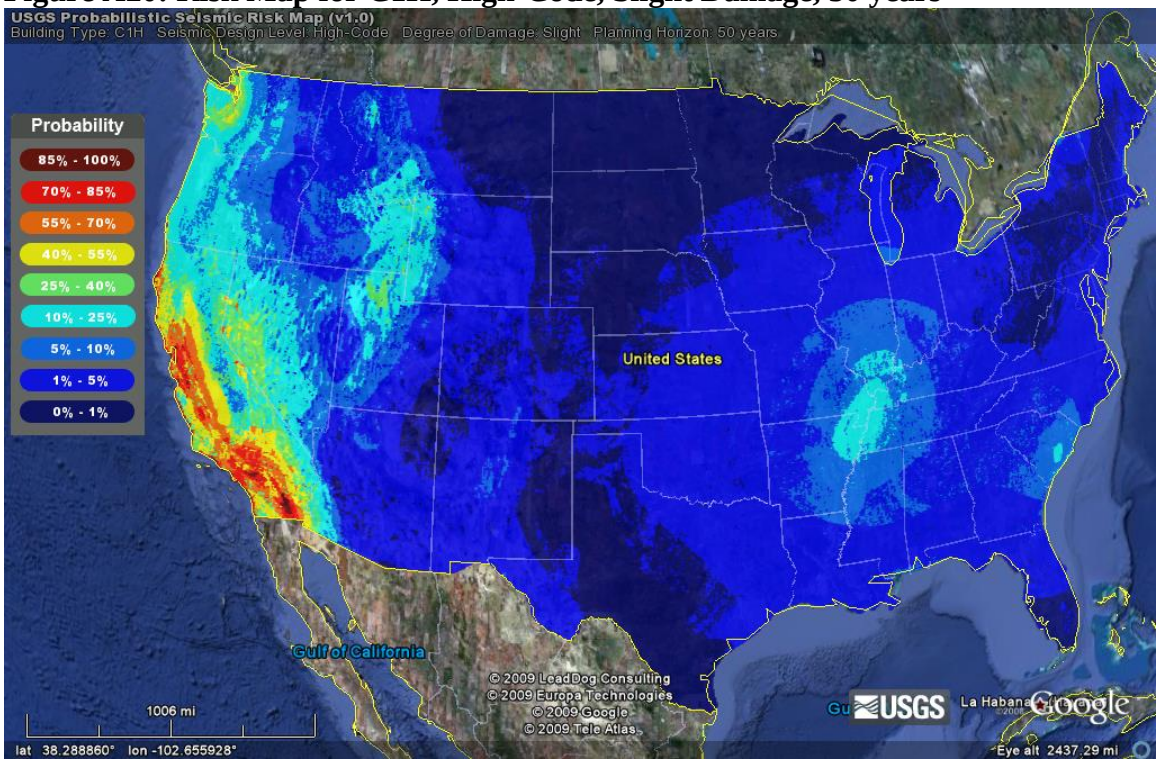

Figure A21: Difference Map for C1H, Pre- vs. High-Code, Slight Damage, 50 years

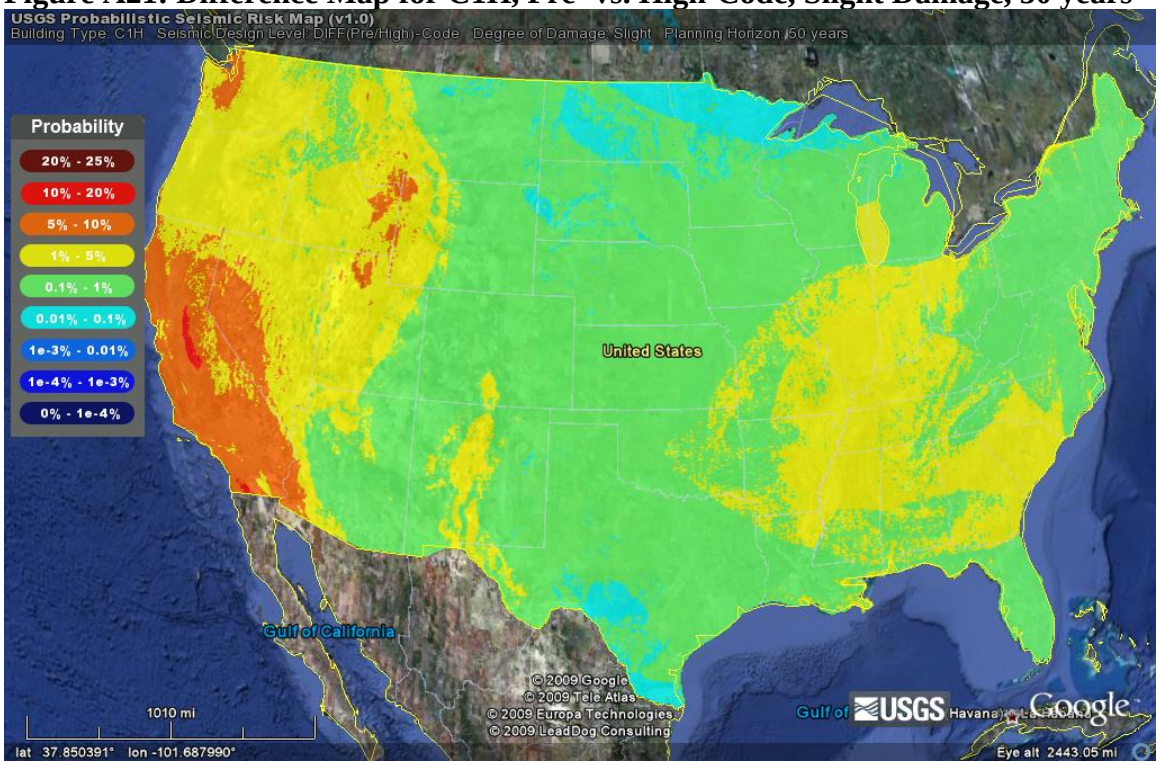

Figure A22: Risk Map for C1H, Pre-Code, Complete Damage, 50 years

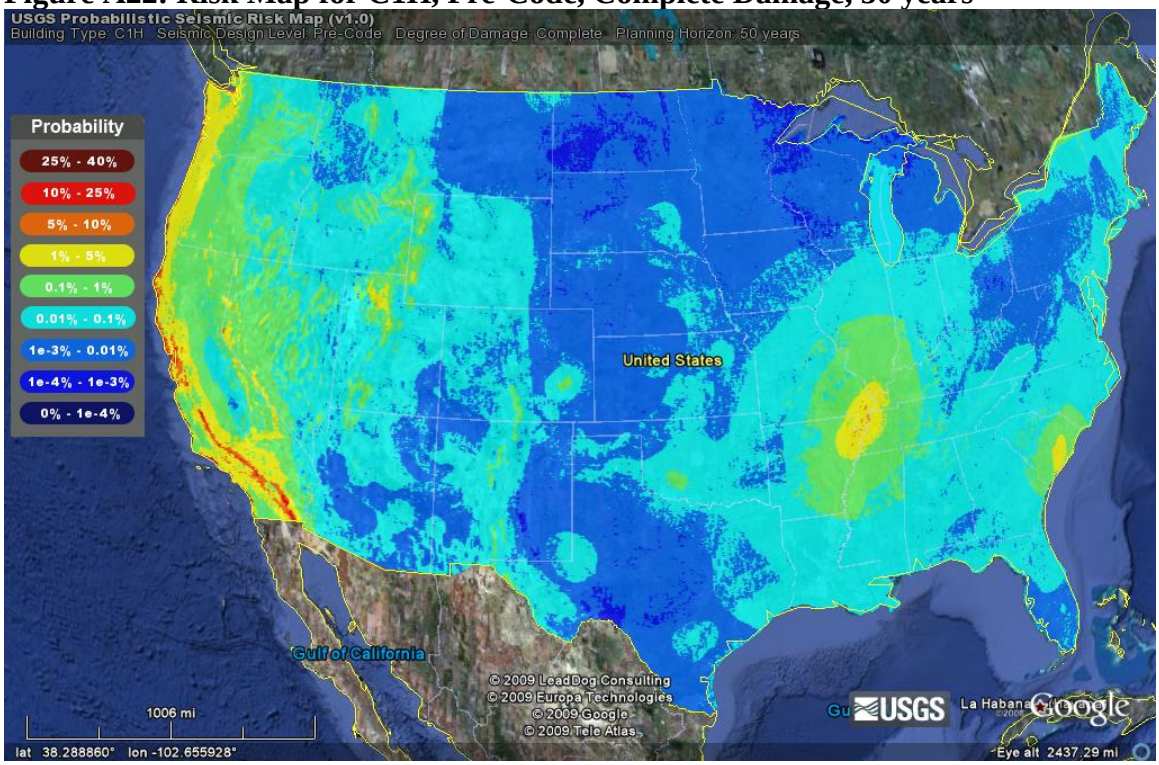

Figure A23: Risk Map for C1H, High-Code, Complete Damage, 50 years

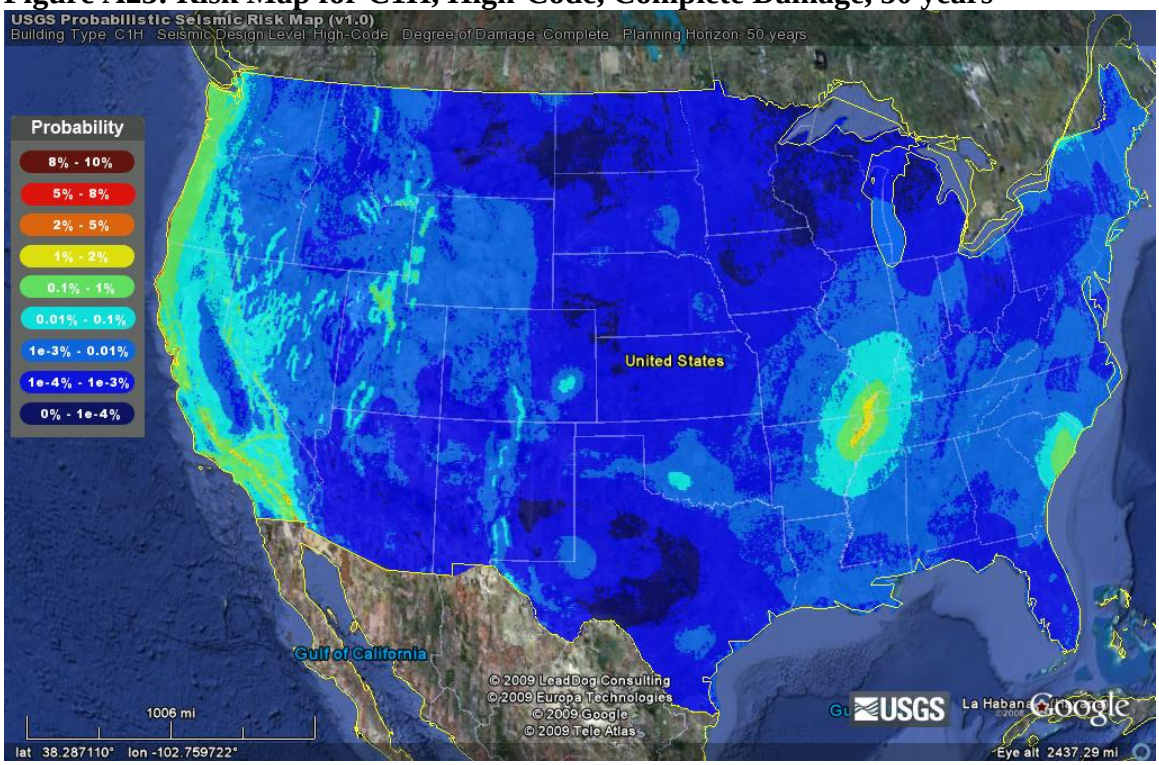

Figure A24: Difference Map for C1H, Pre- vs. High-Code, Complete Damage, 50 years

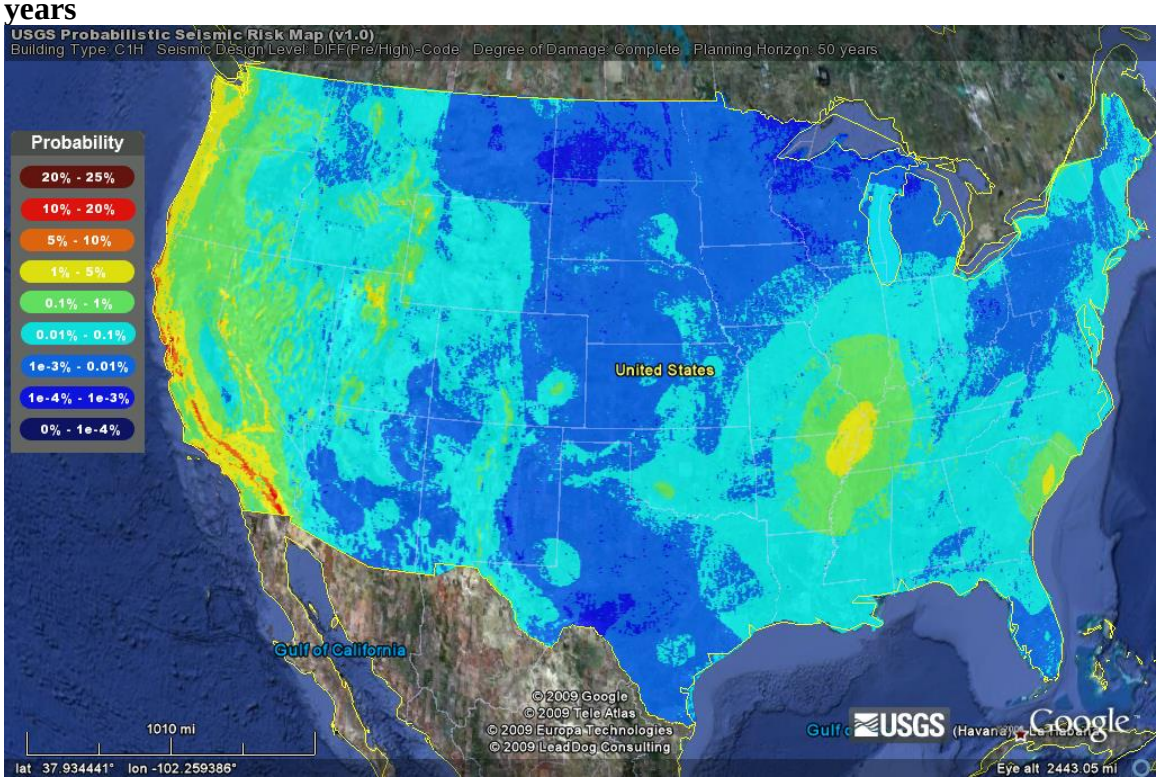

Figure A25: Expected Loss Ratio Map for C1H, Pre-Code, COM4, 1 year

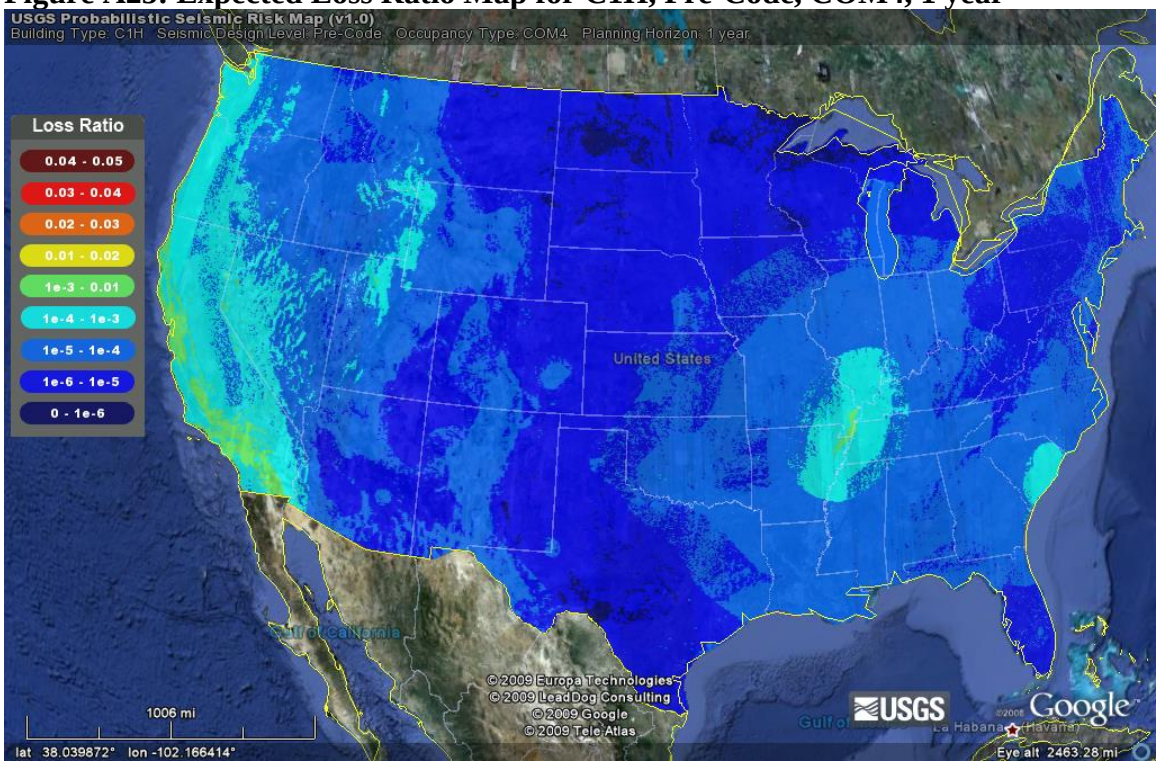

Figure A26: Expected Loss Ratio Map for C1H, High-Code, COM4, 1 year

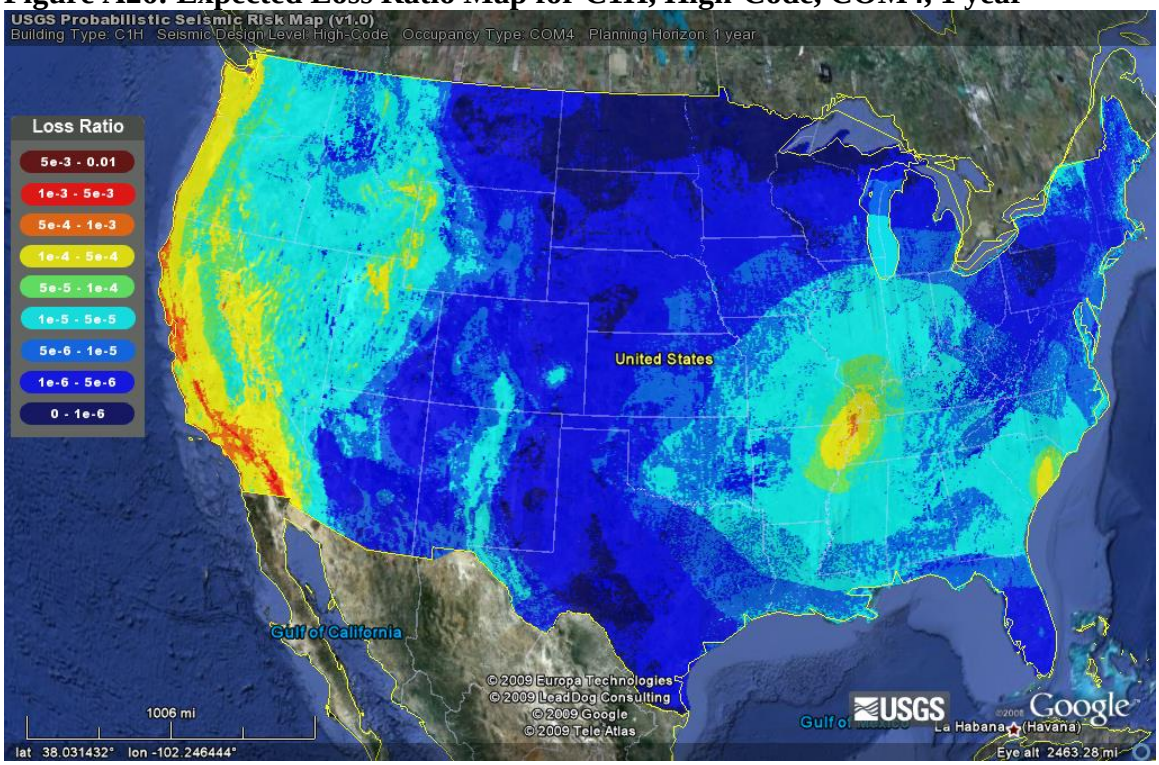

Figure A27: Expected Loss Ratio Difference Map for C1H, Pre- vs. High-Code, COM4, 1 year

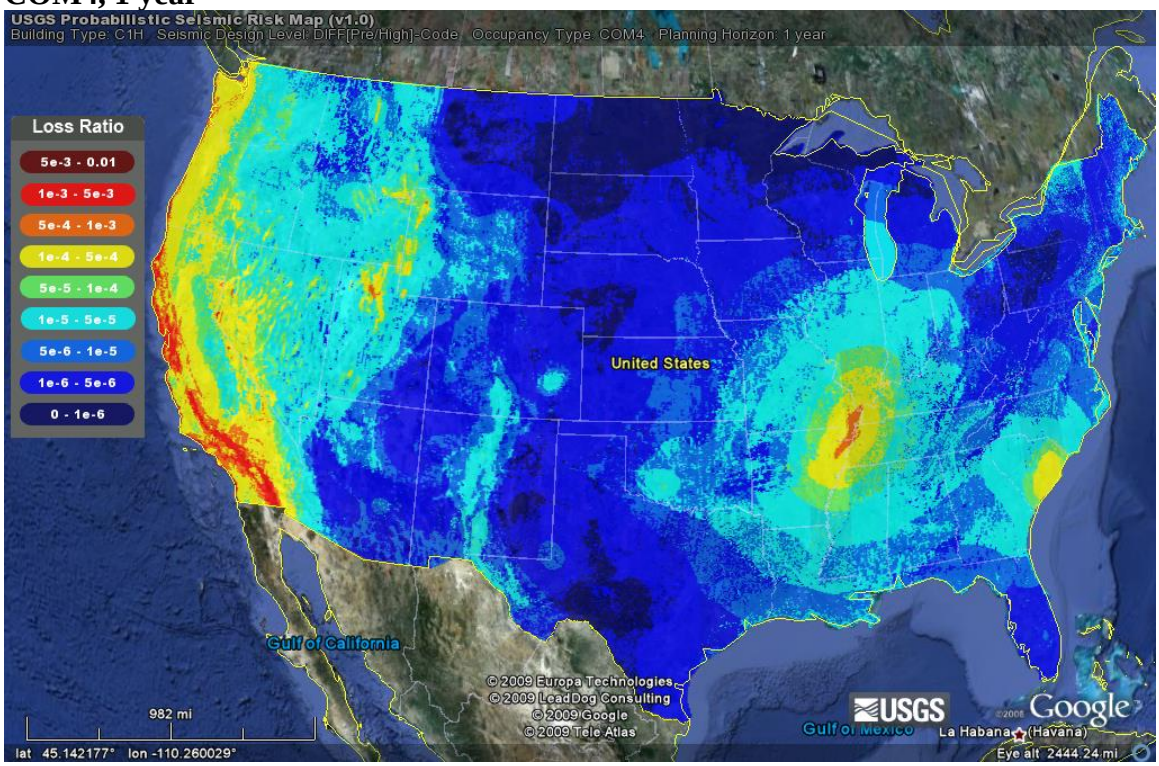

Figure A28: Risk Map for C2L, Pre-Code, Slight Damage, 50 years

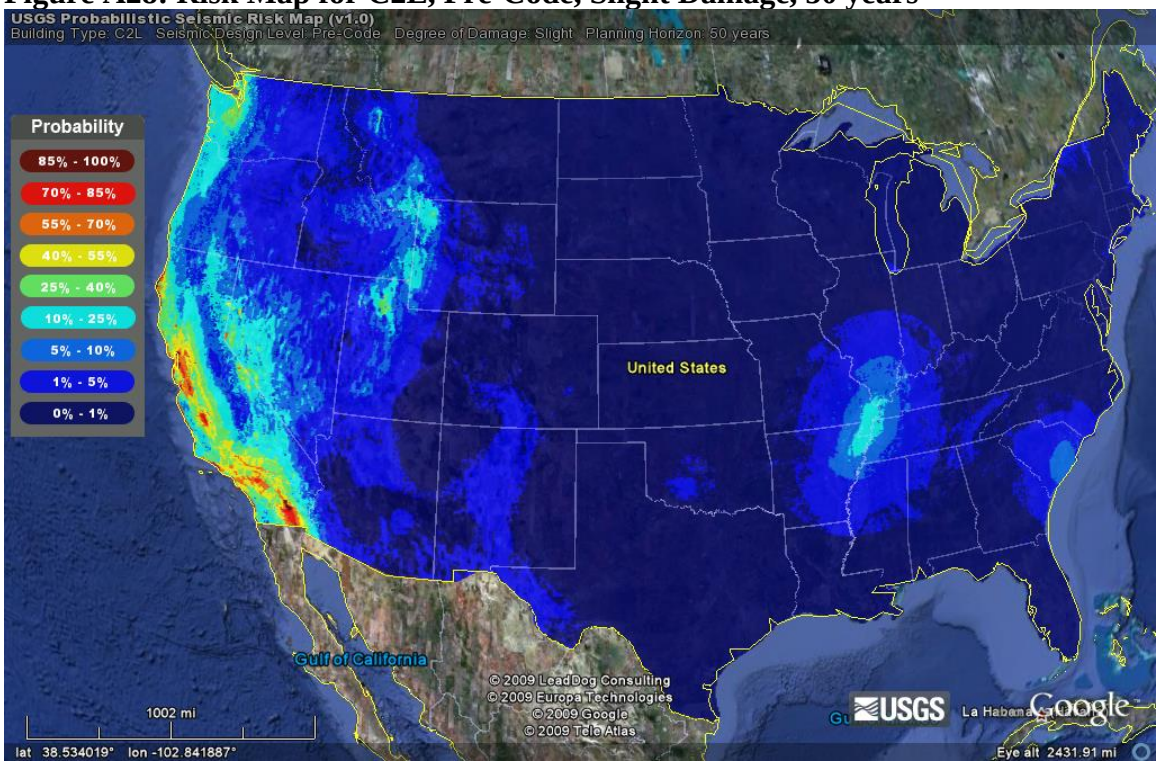

Figure A29: Risk Map for C2L, High-Code, Slight Damage, 50 years

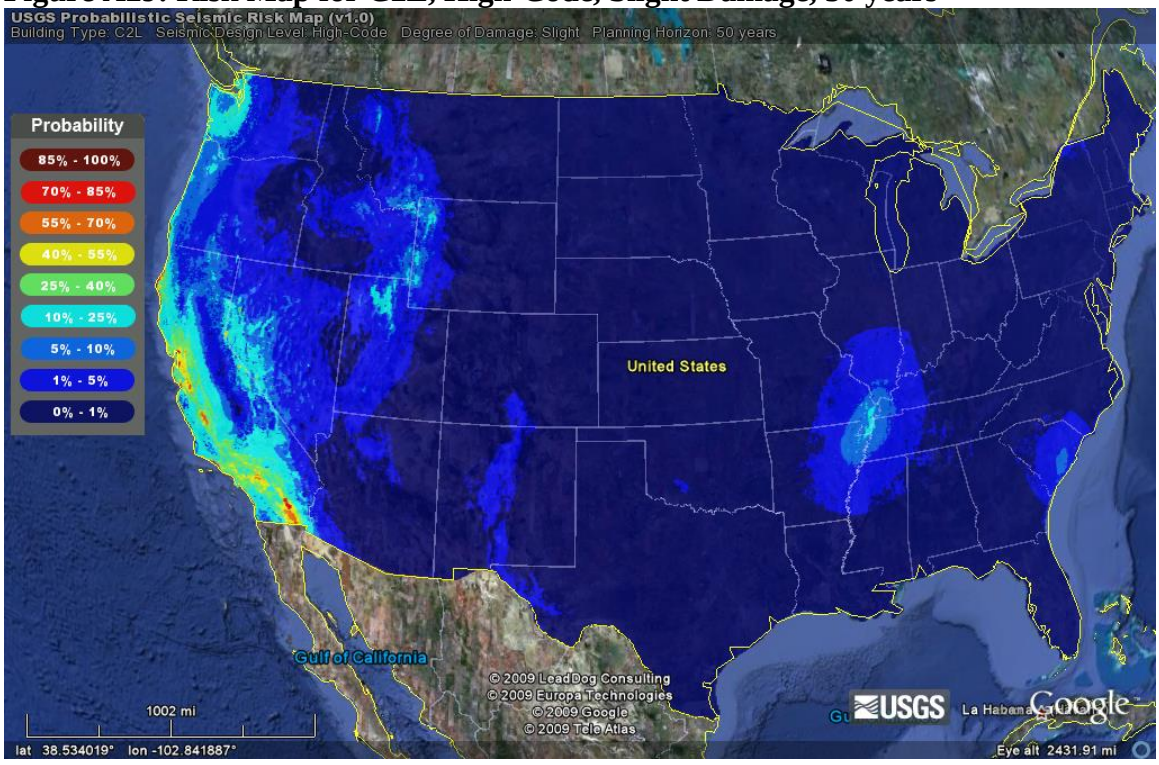

Figure A30: Difference Map for C2L, Pre- vs. High-Code, Slight Damage, 50 years

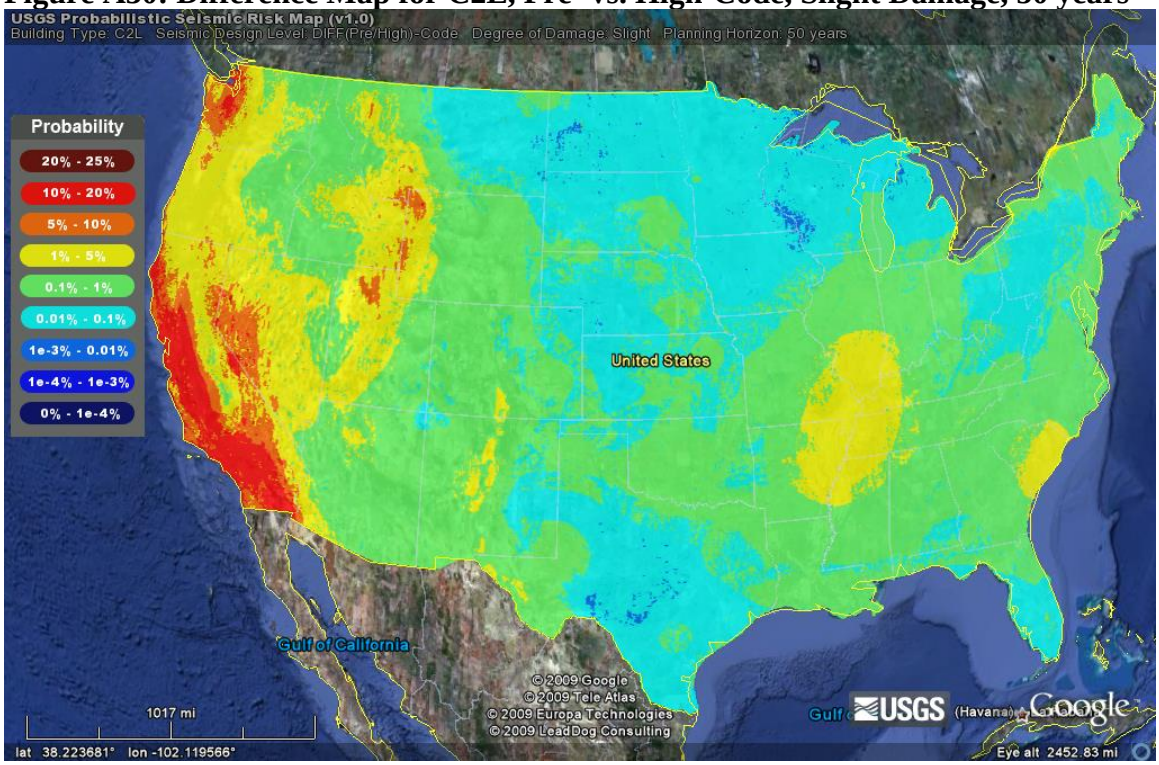

Figure A31: Risk Map for C2L, Pre-Code, Complete Damage, 50 years

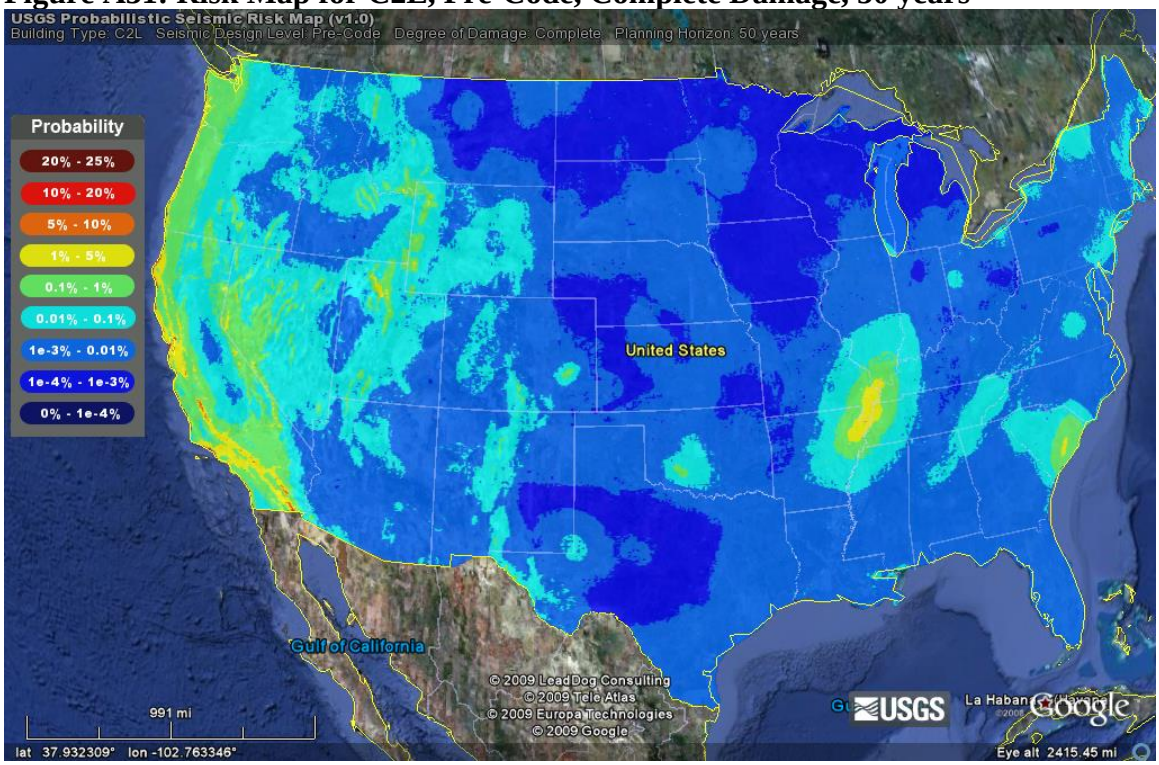

Figure A32: Risk Map for C2L, High-Code, Complete Damage, 50 years

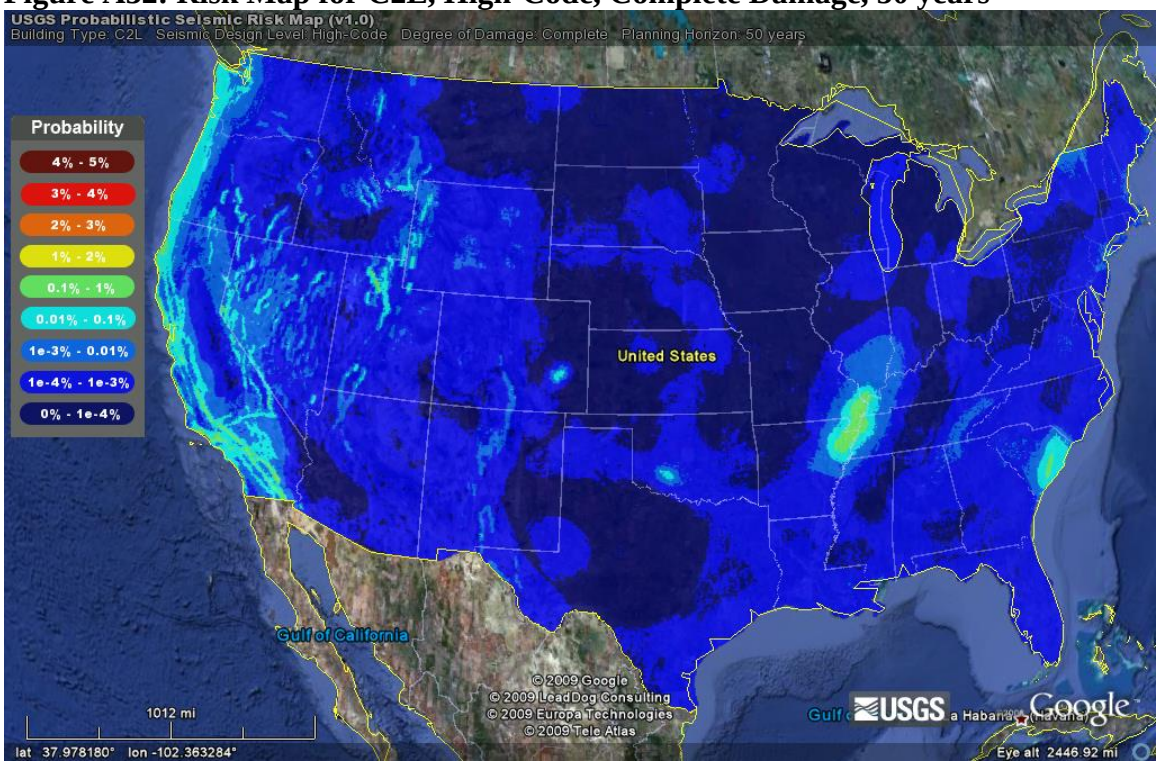

Figure A33: Difference Map for C2L, Pre- vs. High-Code, Complete Damage, 50 years

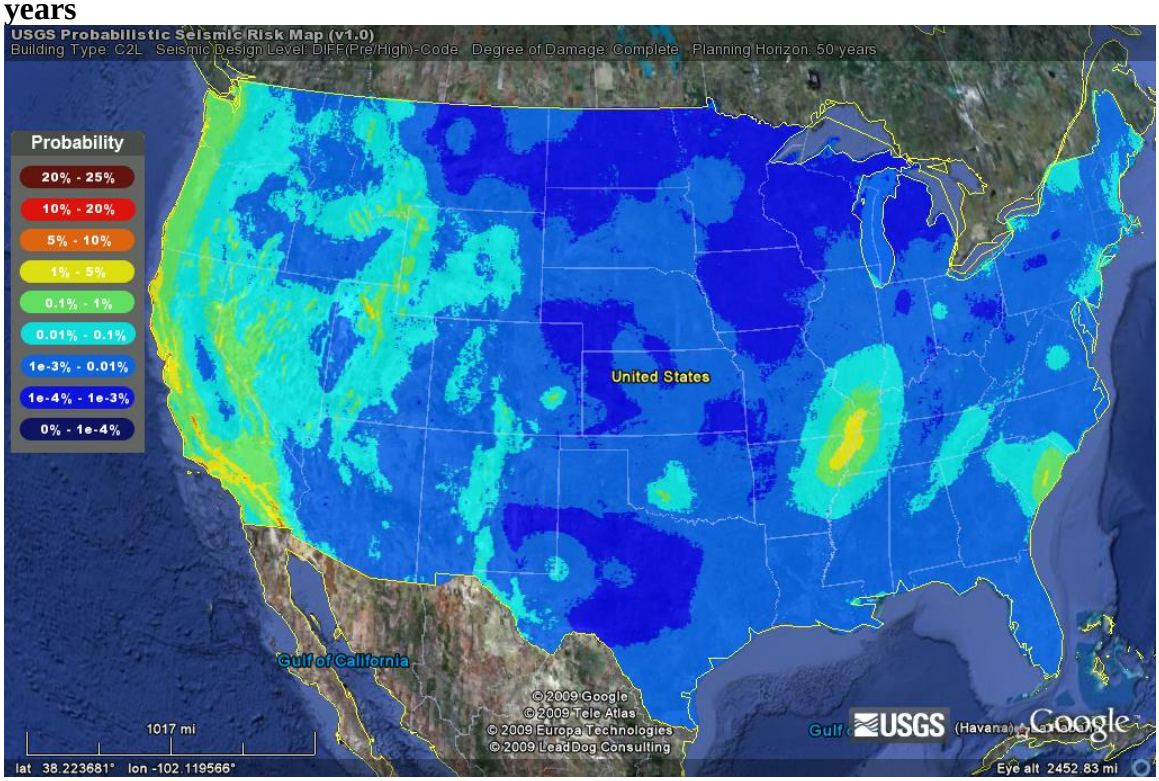

Figure A34: Expected Loss Ratio Map for C2L, Pre-Code, COM4, 1 year

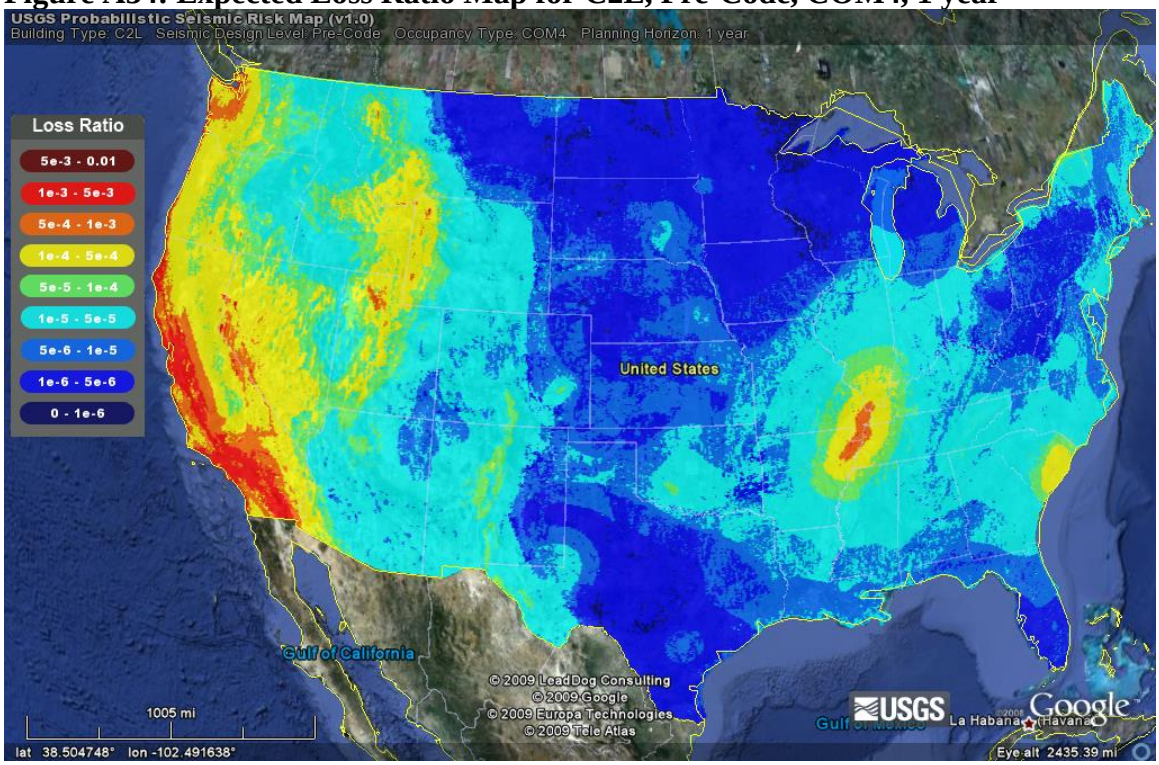

Figure A35: Expected Loss Ratio Map for C2L, High-Code, COM4, 1 year

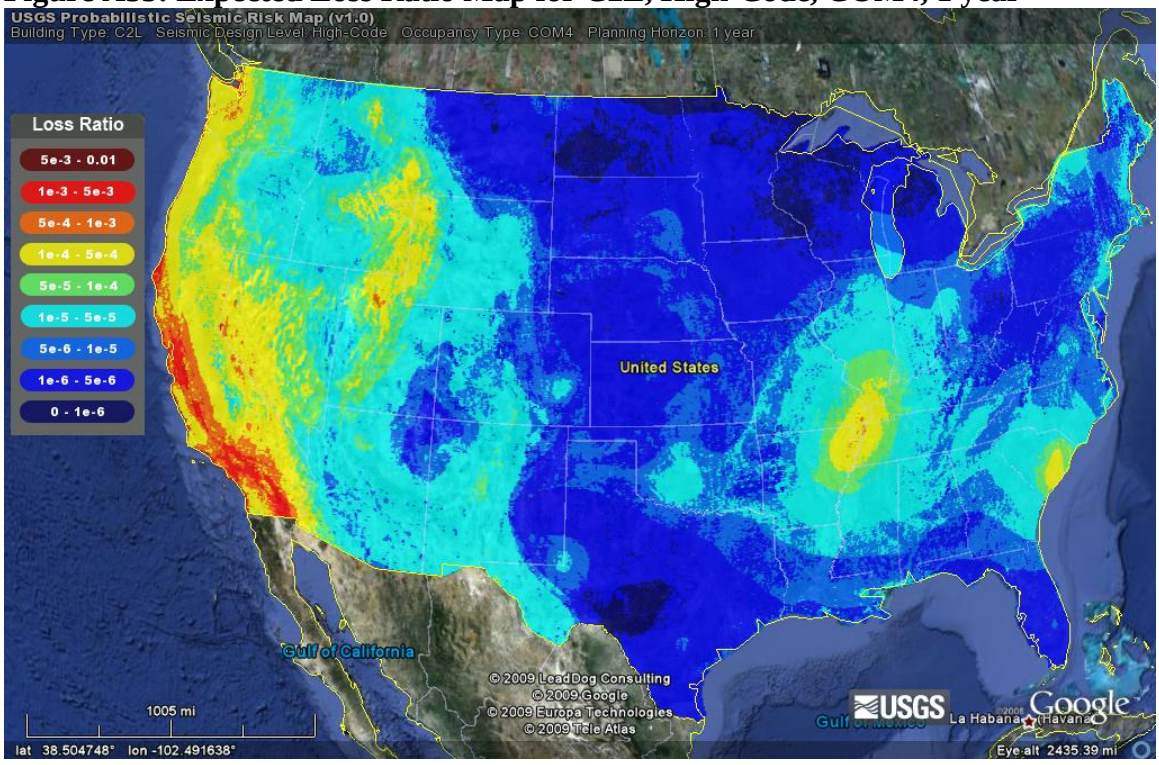

Figure A36: Expected Loss Ratio Difference Map for C2L, Pre- vs. High-Code, COM6, 1 year

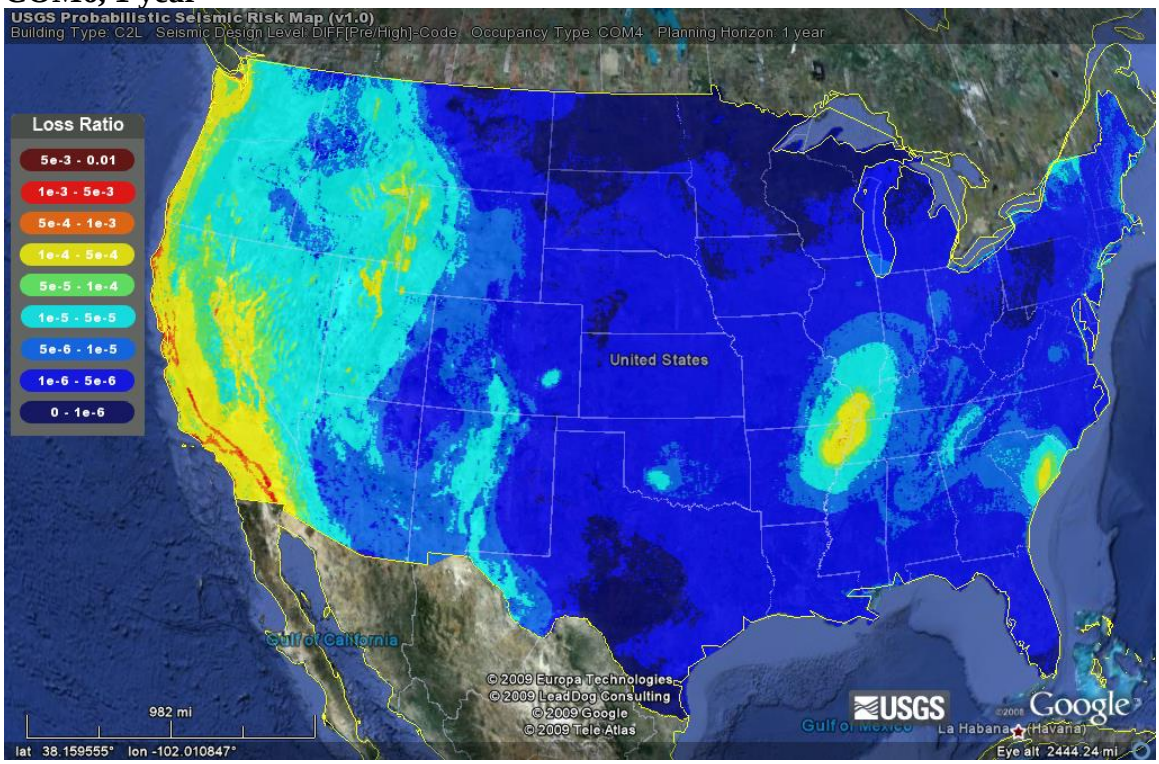

Figure A37: Risk Map for C2M, Pre-Code, Slight Damage, 50 years

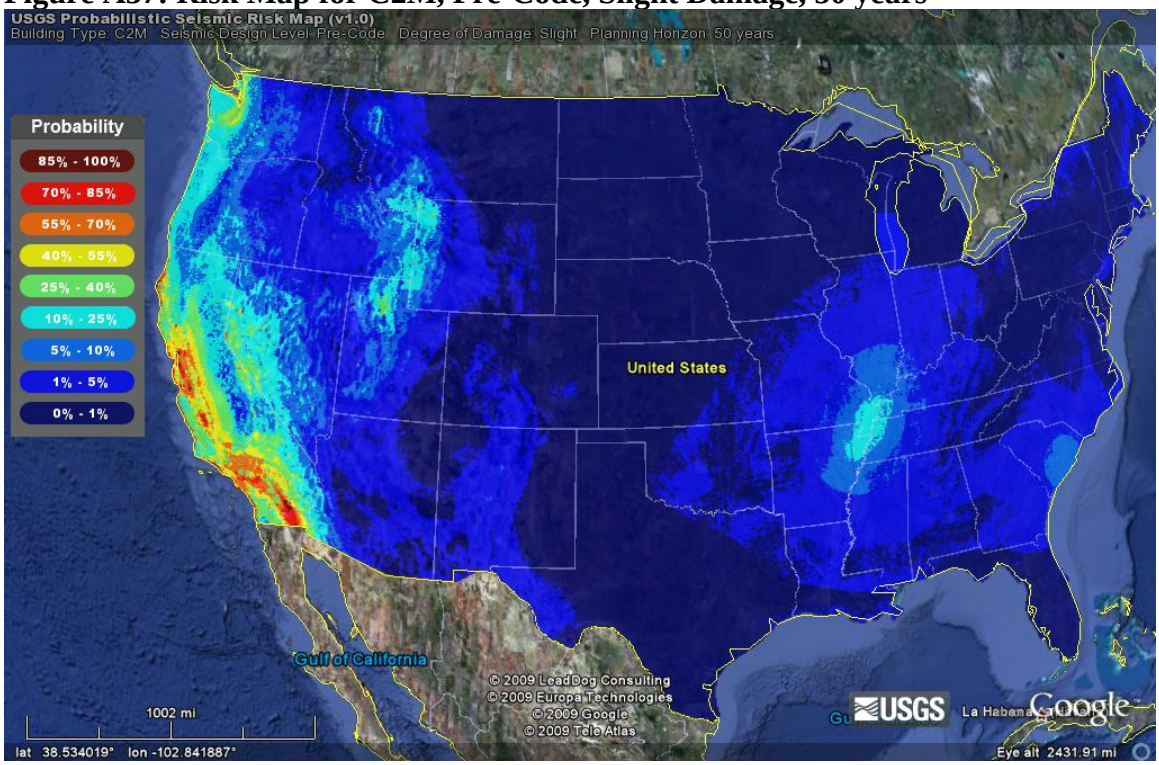

Figure A38: Risk Map for C2M, High-Code, Slight Damage, 50 years

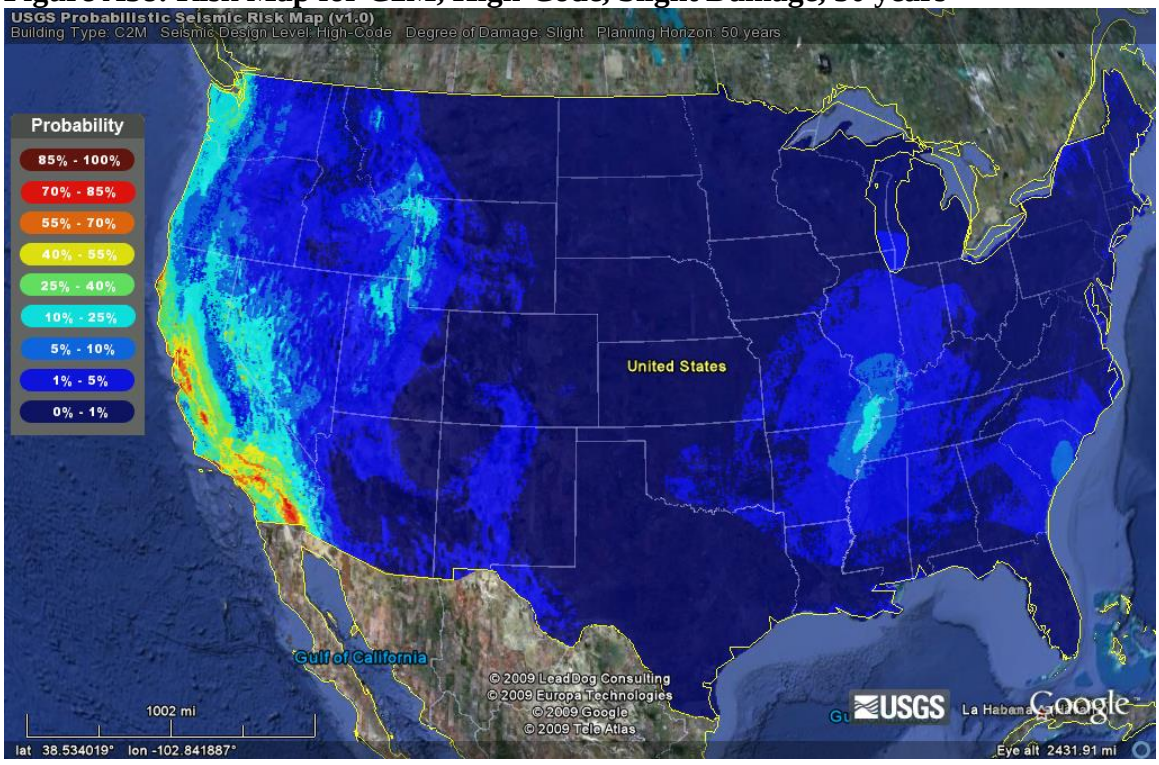

Figure A39: Difference Map for C2M, Pre- vs. High-Code, Slight Damage, 50 years

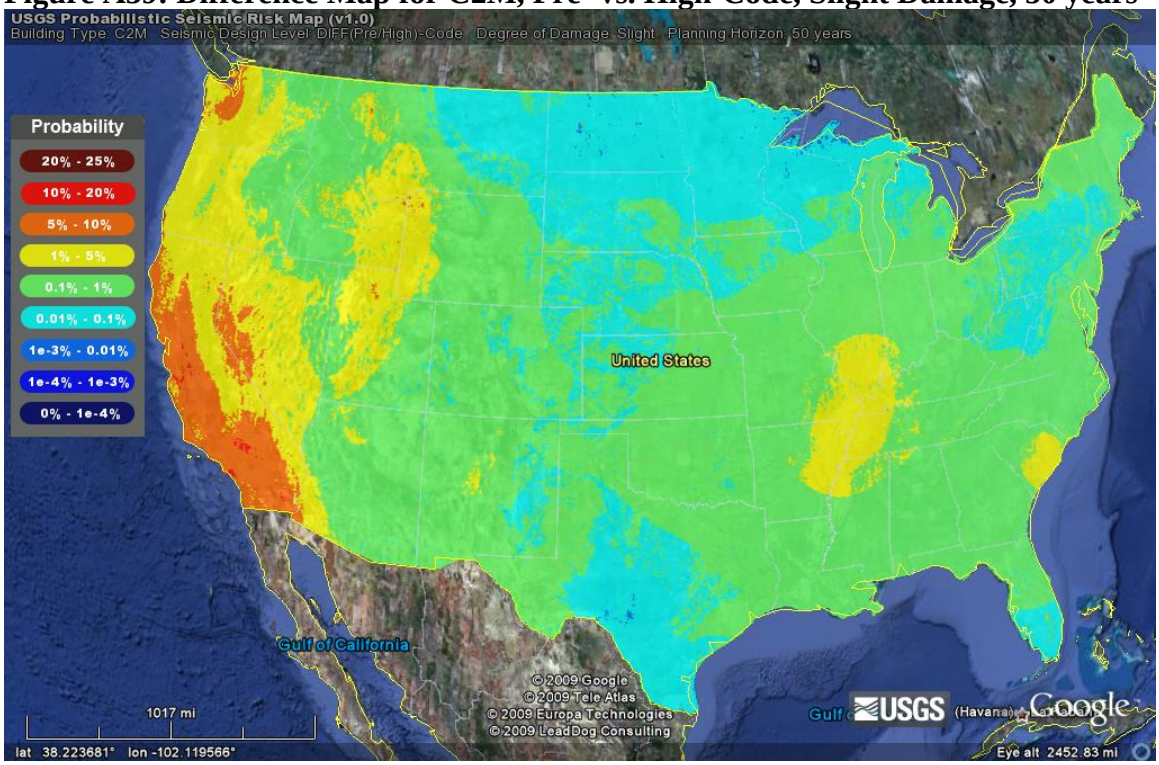

Figure A40: Risk Map for C2M, Pre-Code, Complete Damage, 50 years

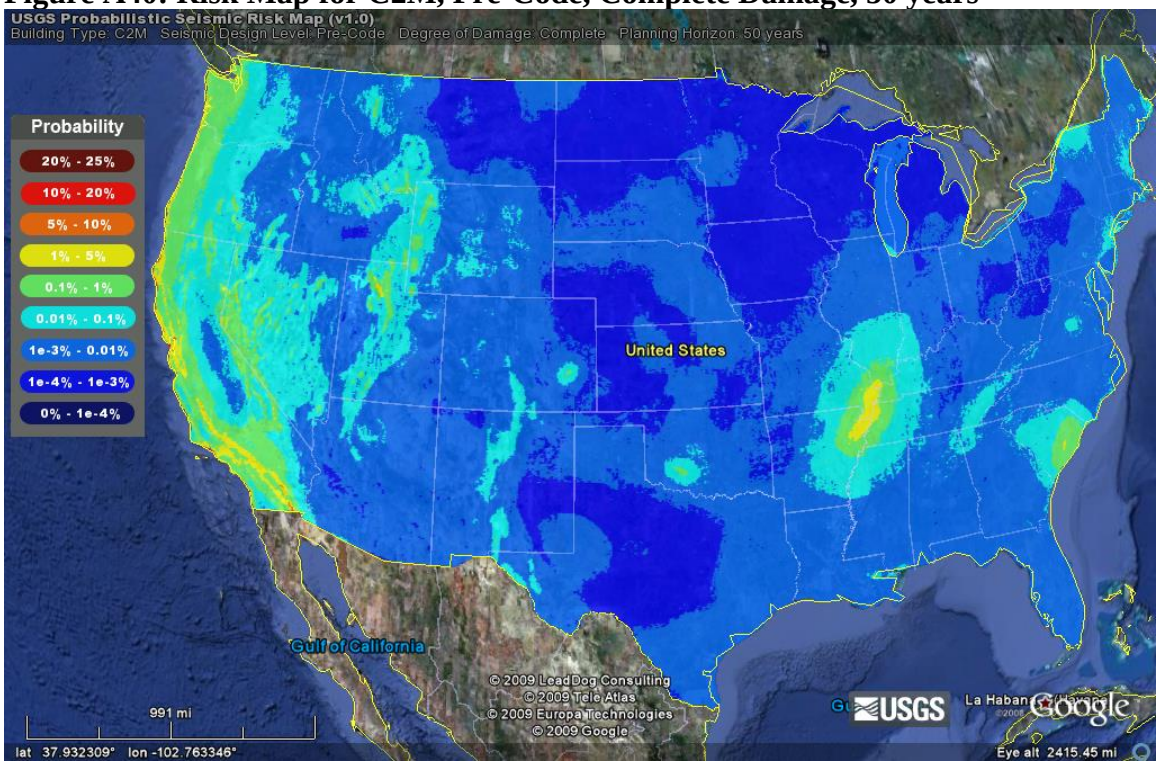

Figure A41: Risk Map for C2M, High-Code, Complete Damage, 50 years

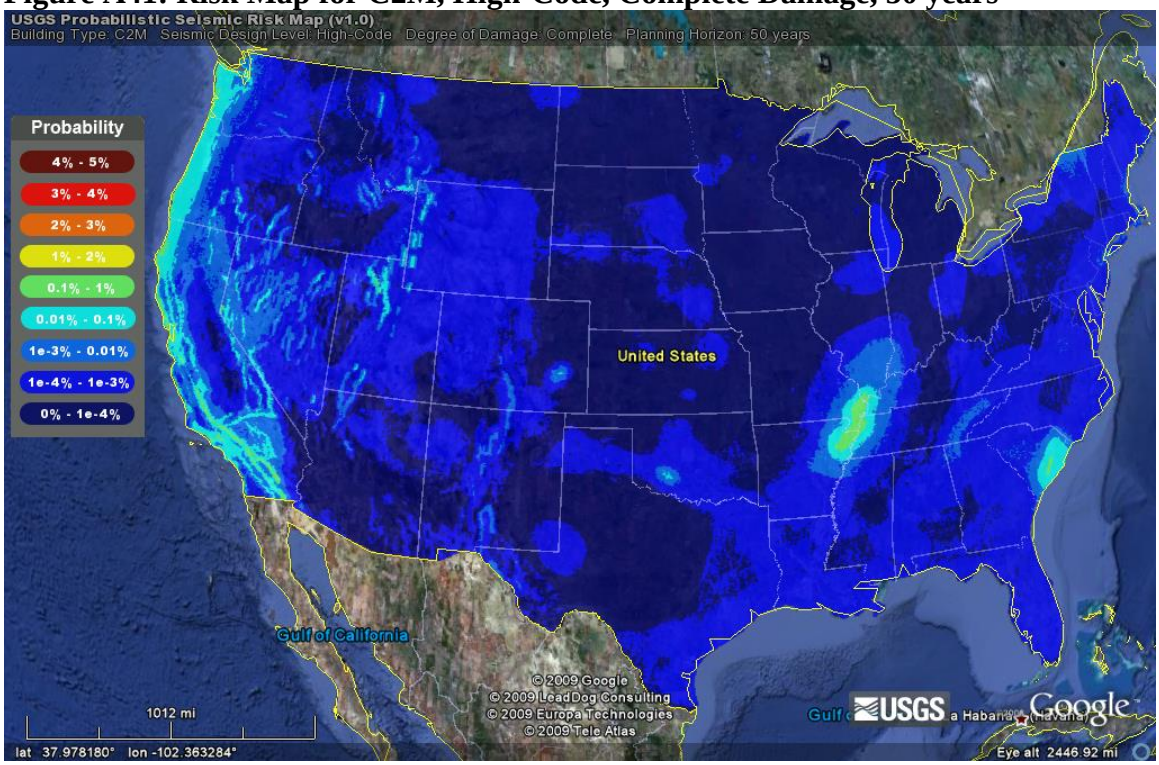

Figure A42: Difference Map for C2M, Pre- vs. High-Code, Complete Damage, 50 years

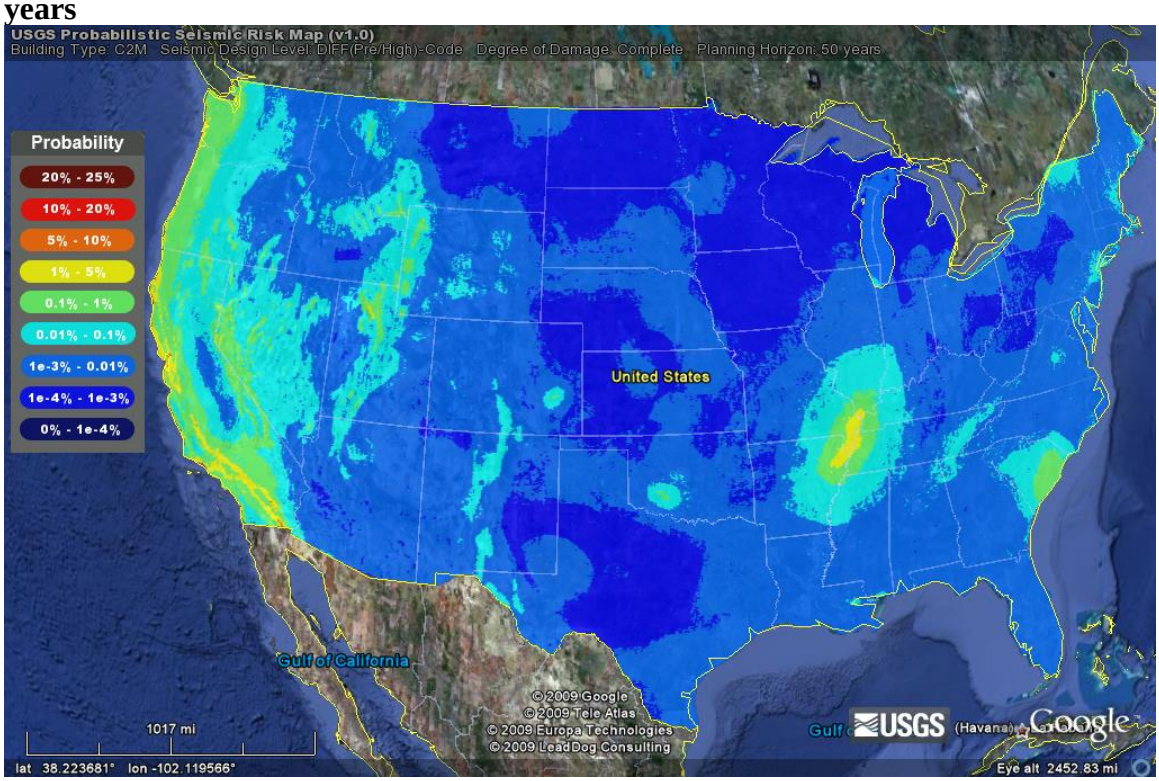

Figure A43: Expected Loss Ratio Map for C2M, Pre-Code, COM4, 1 year

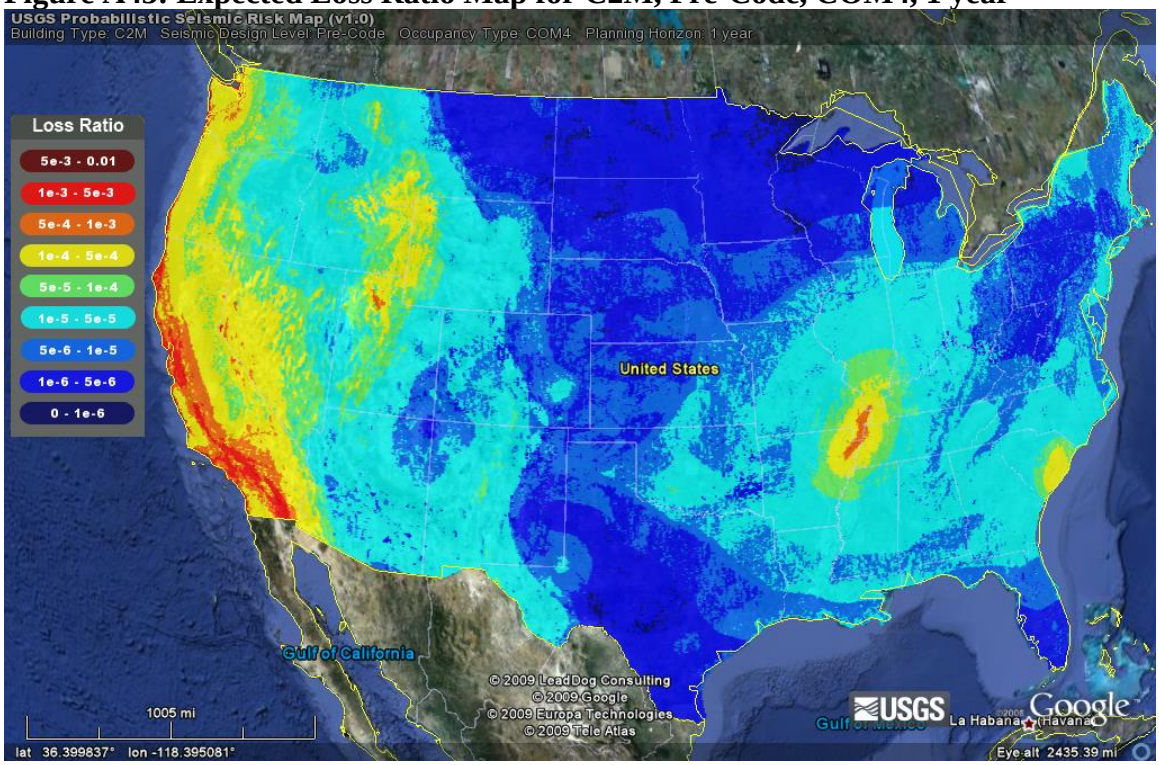

Figure A44: Expected Loss Ratio Map for C2M, High-Code, COM4, 1 year

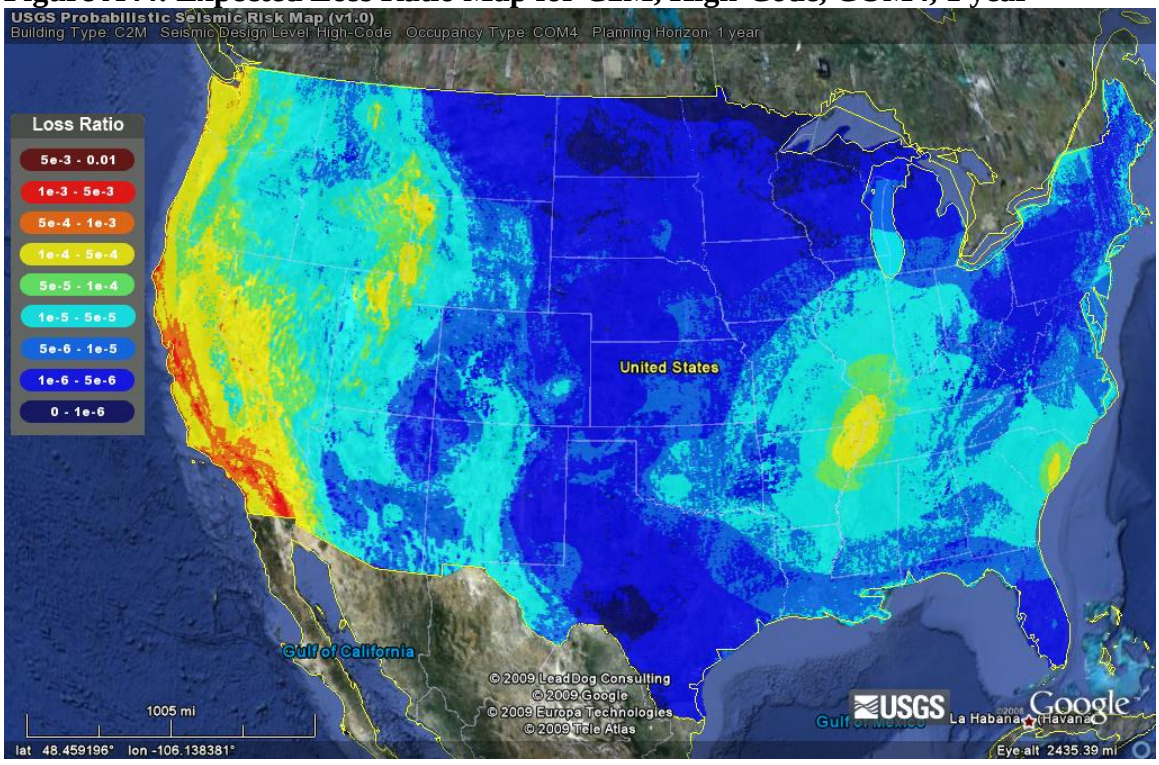

Figure A45: Expected Loss Ratio Difference Map for C2M, Pre- vs. High-Code, COM4, 1 year

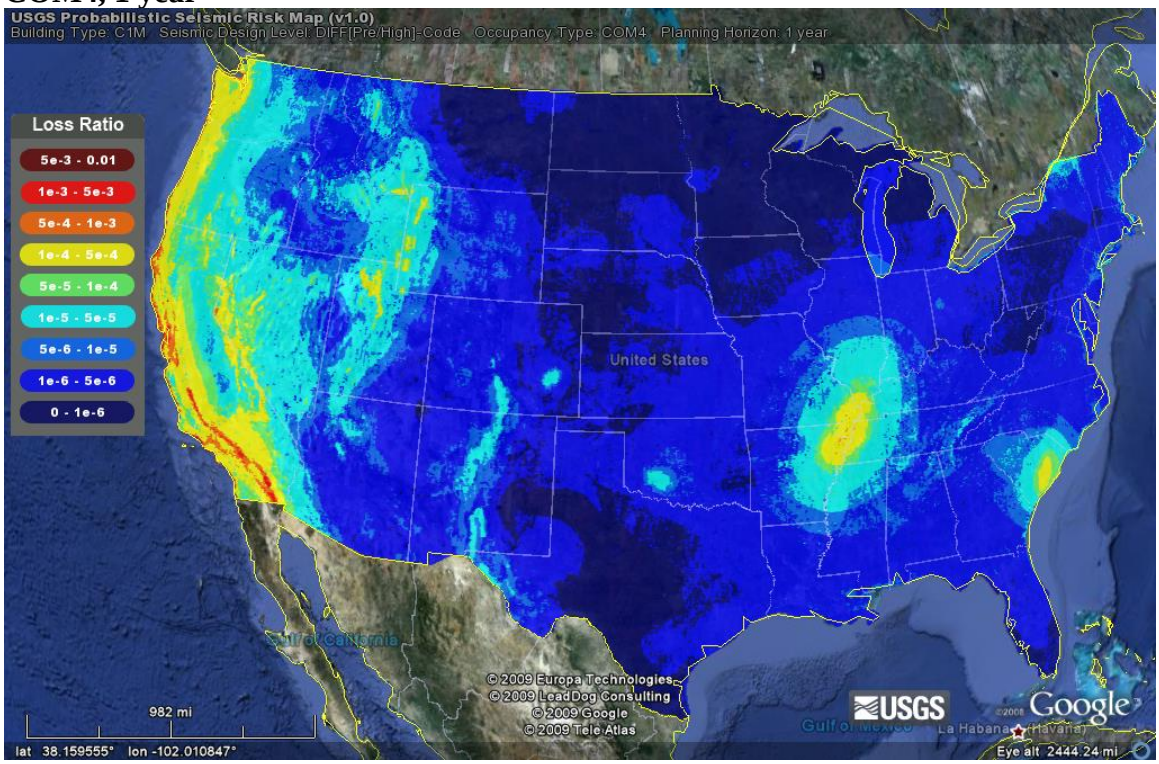

Figure A46: Risk Map for C2H, Pre-Code, Slight Damage, 50 years

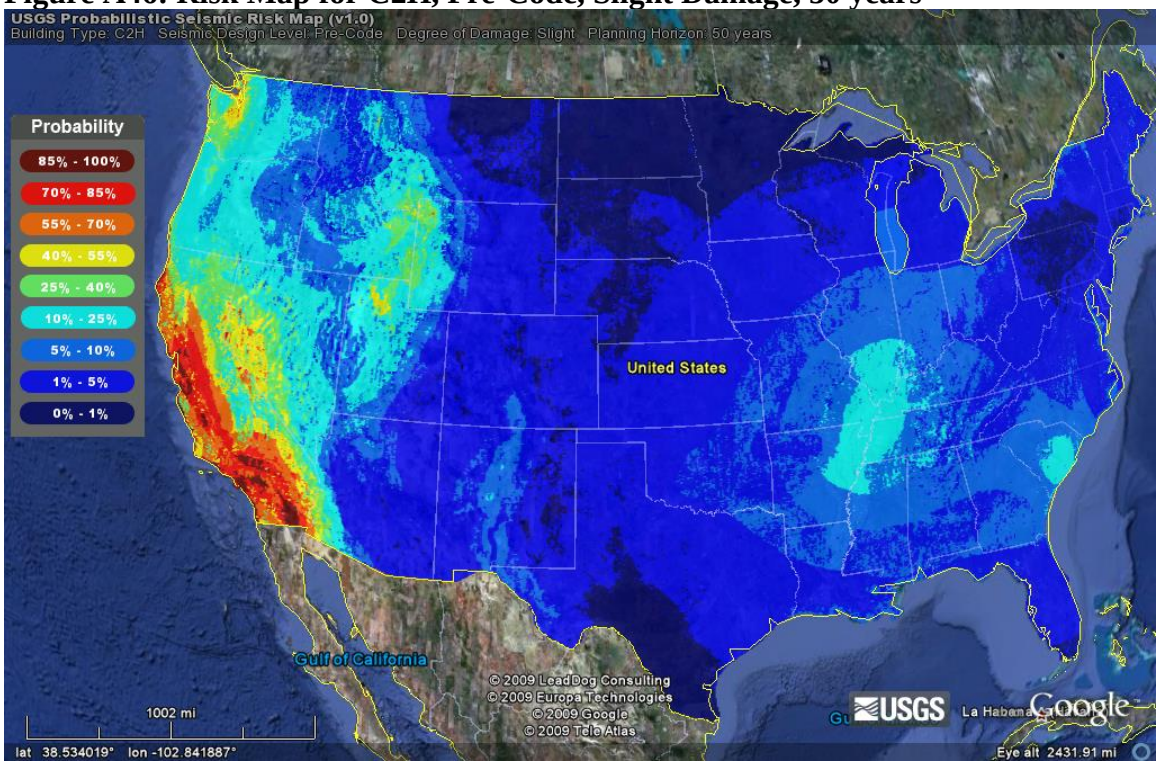

Figure A47: Risk Map for C2H, High-Code, Slight Damage, 50 years

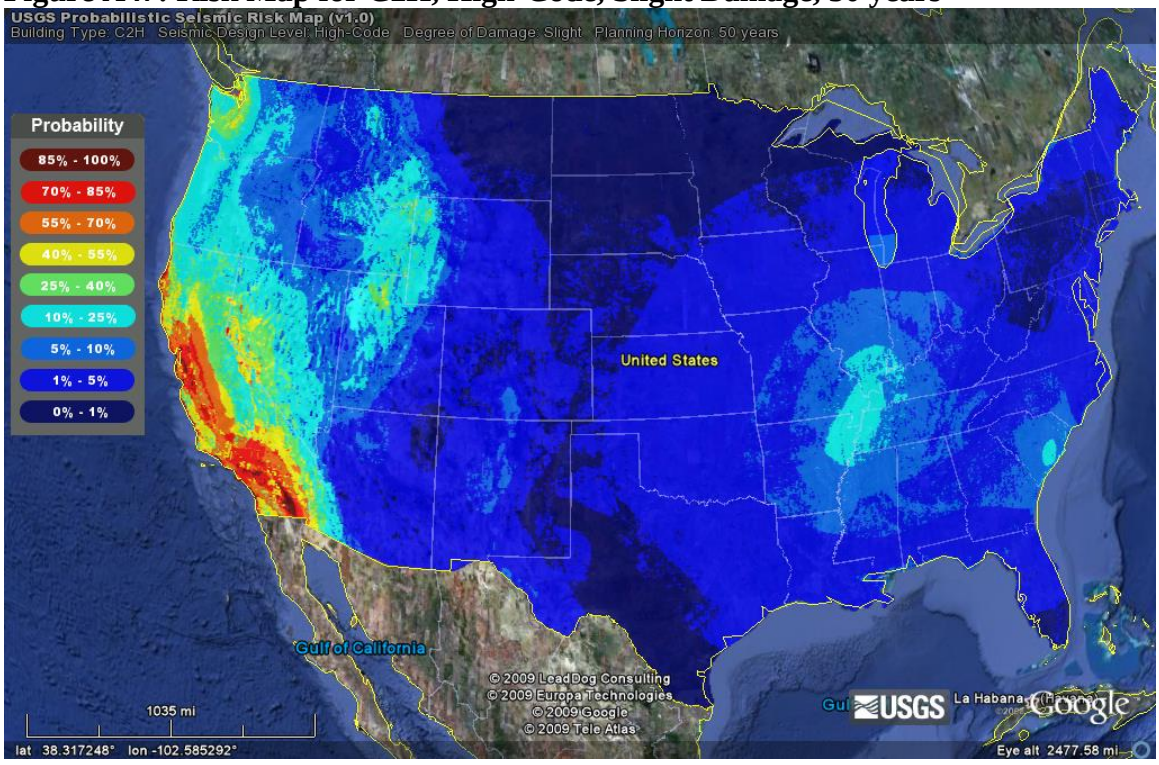

Figure A48: Difference Map for C2H, Pre- vs. High-Code, Slight Damage, 50 years

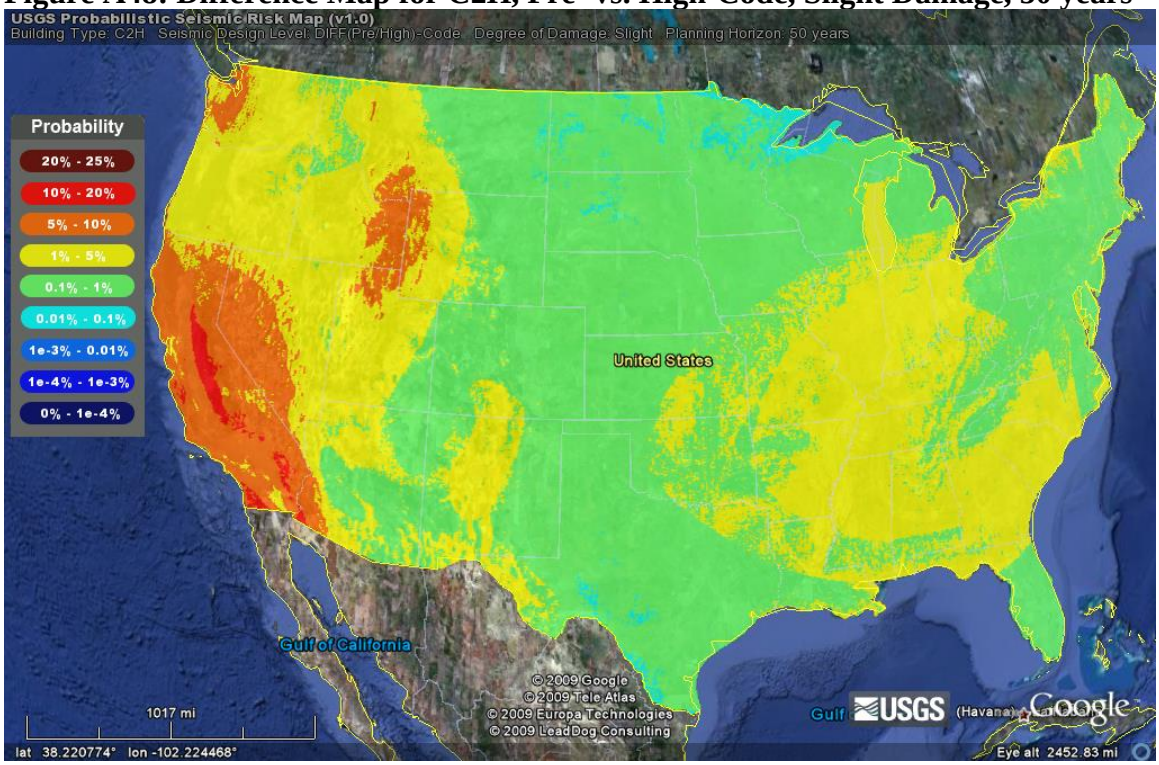

Figure A49: Risk Map for C2H, Pre-Code, Complete Damage, 50 years

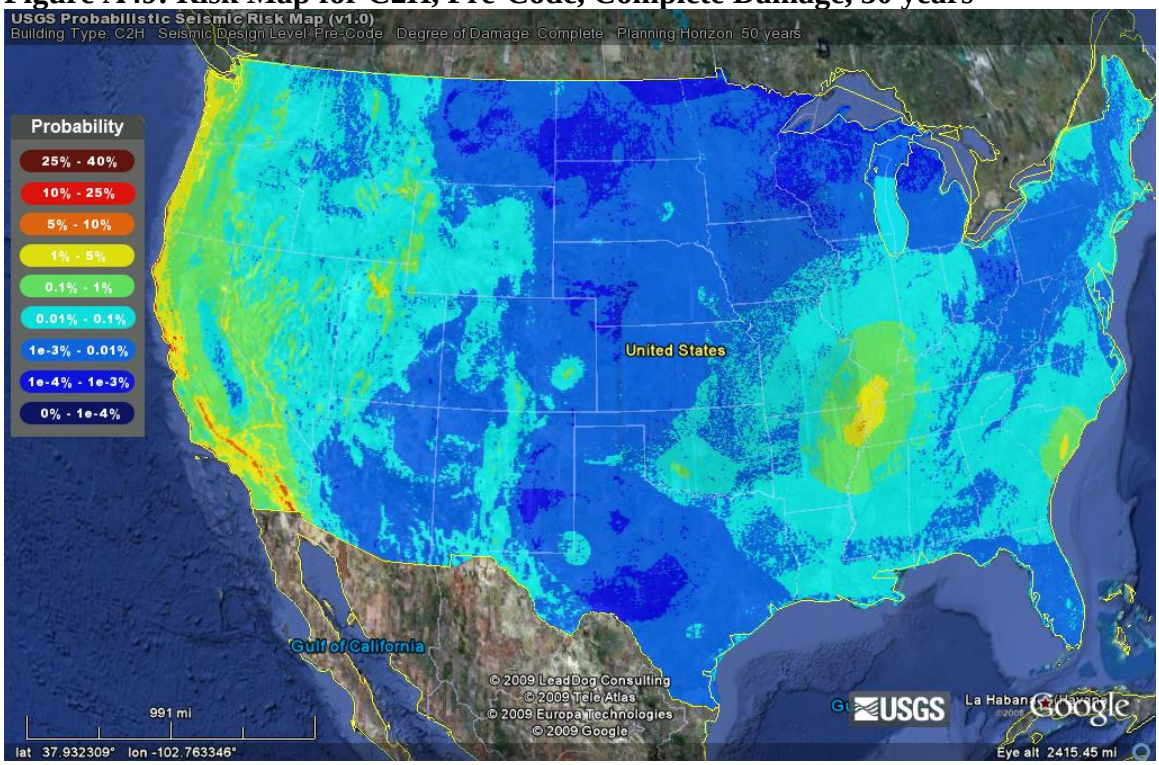

Figure A50: Risk Map for C2H, High-Code, Complete Damage, 50 years

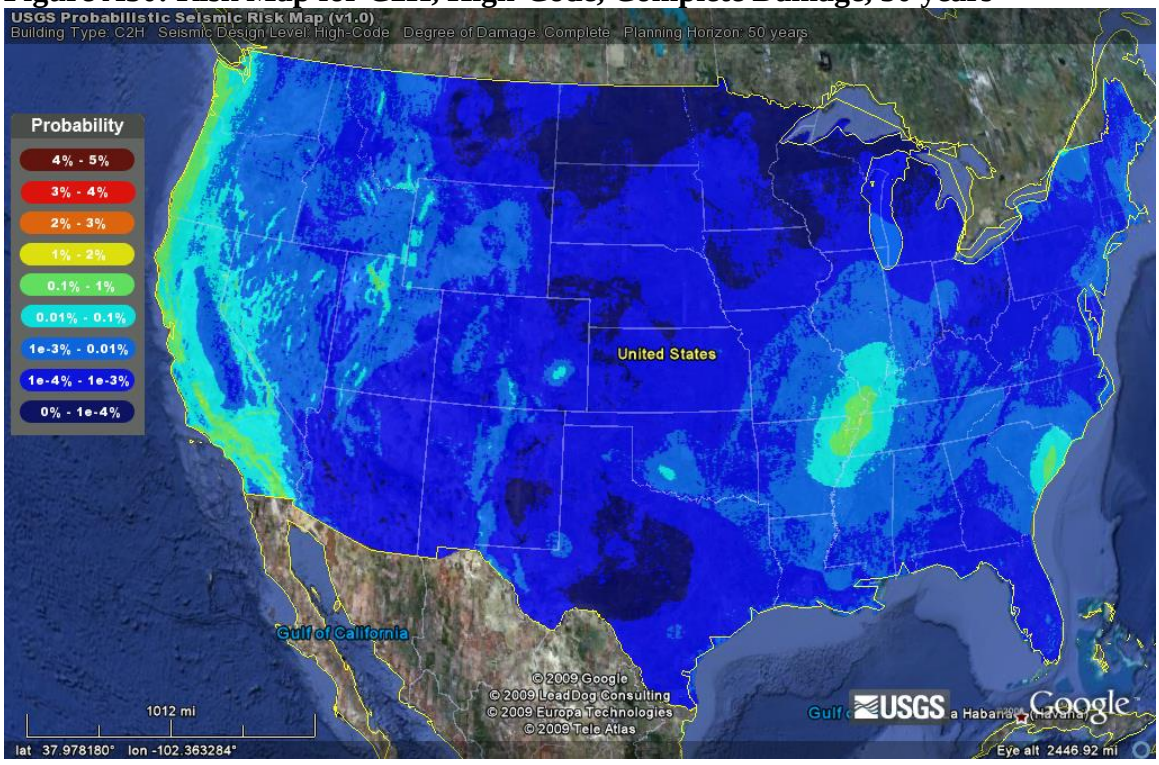

Figure A51: Difference Map for C2H, Pre- vs. High-Code, Complete Damage, 50 years

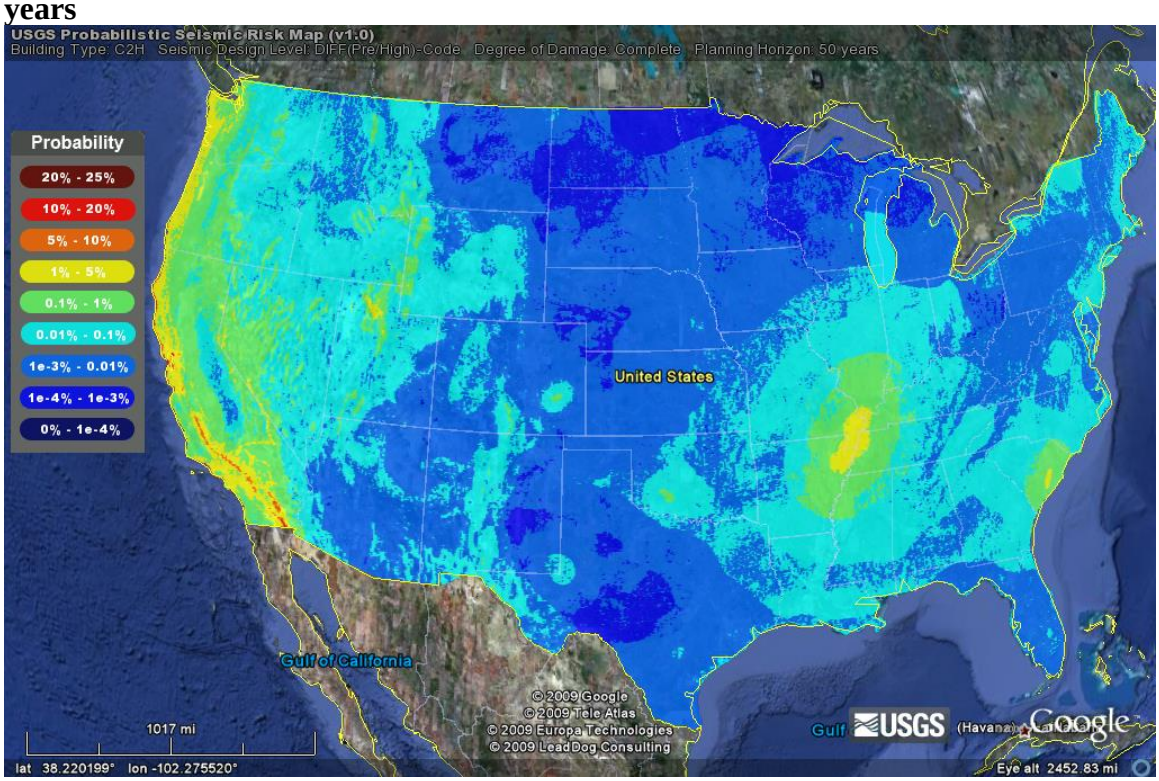

Figure A52: Expected Loss Ratio Map for C2H, Pre-Code, COM4, 1 year

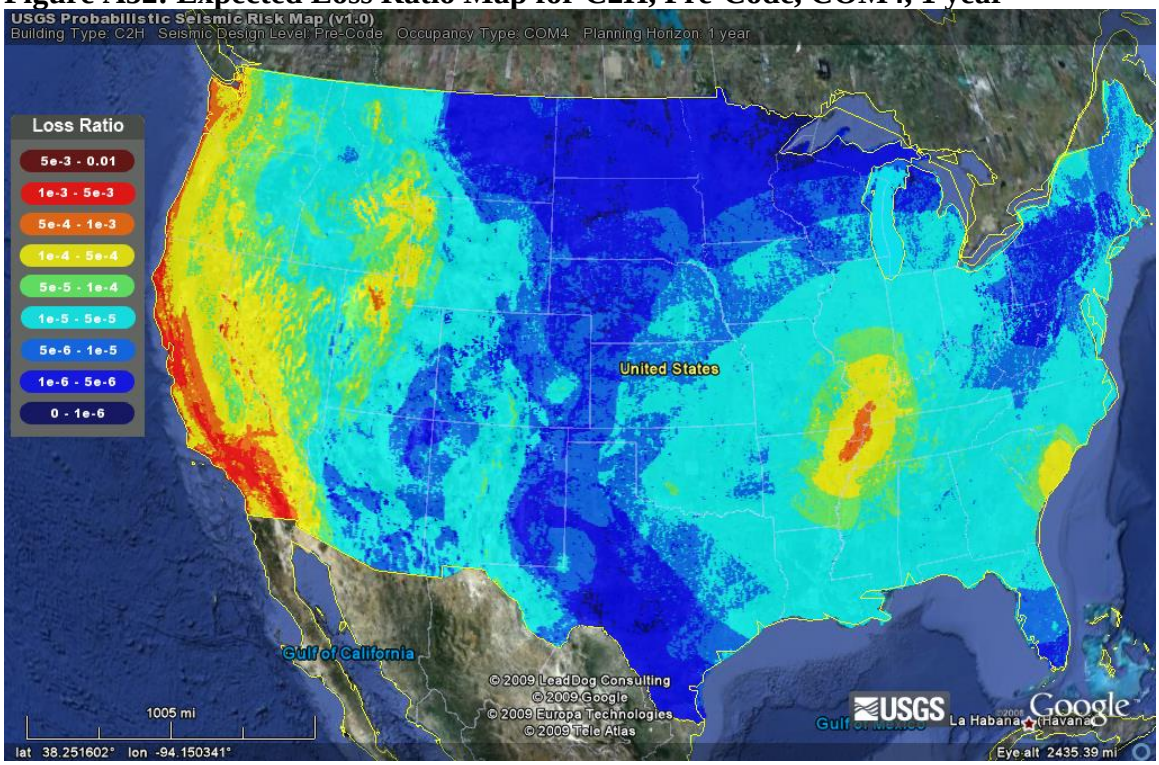

Figure A53: Expected Loss Ratio Map for C2H, High-Code, COM4, 1 year

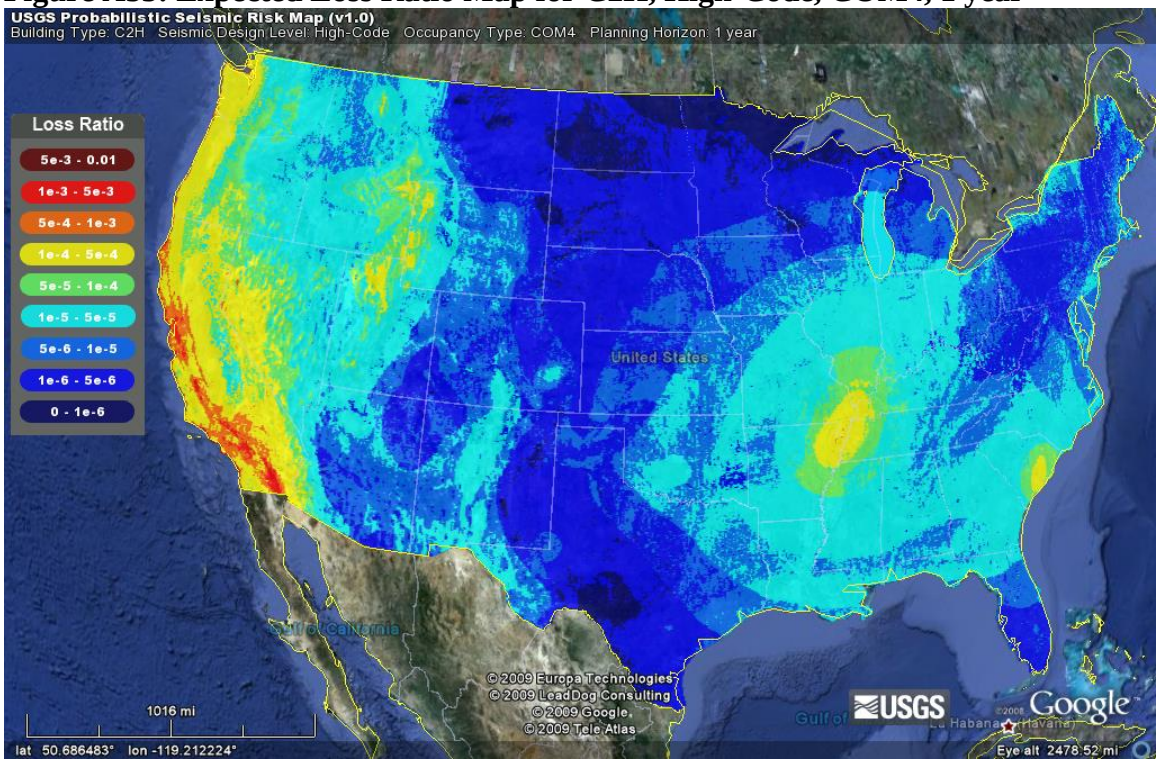

Figure A54: Expected Loss Ratio Difference Map for C2H, Pre- vs. High-Code, COM4, 1 year

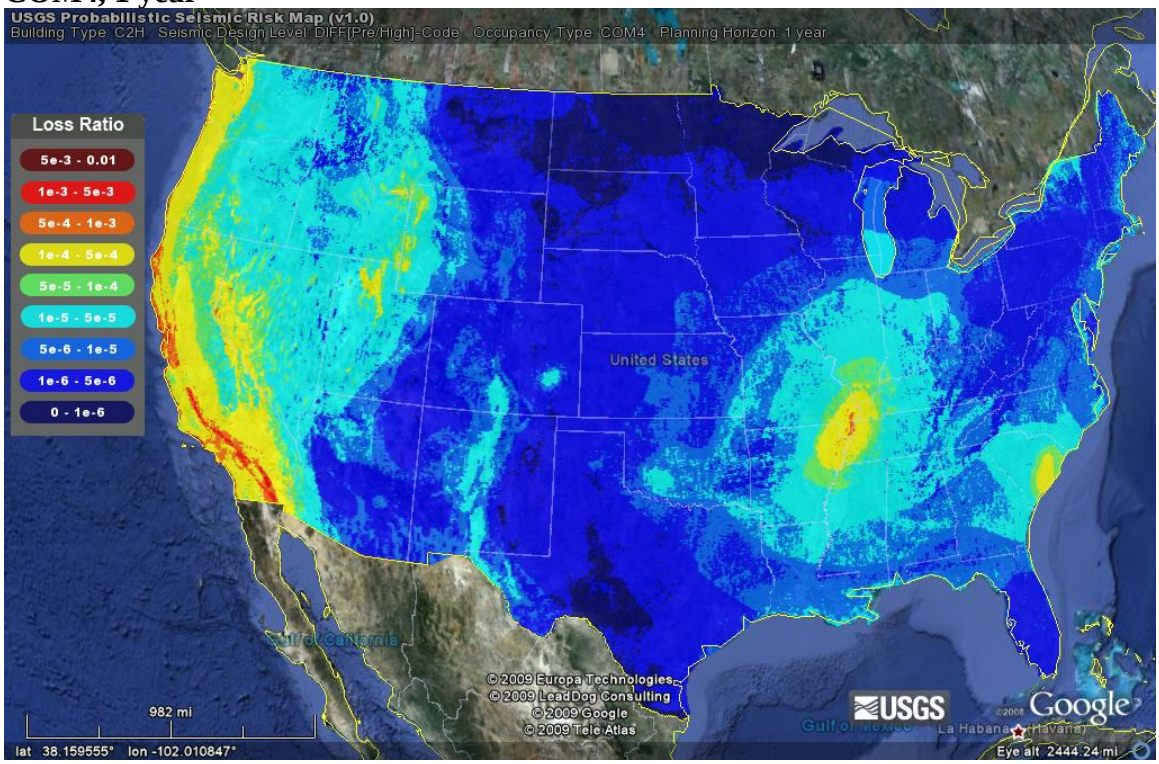

Figure A55: Curvilinear Pushover/Capacity Curves for HAZUS Concrete Buildings

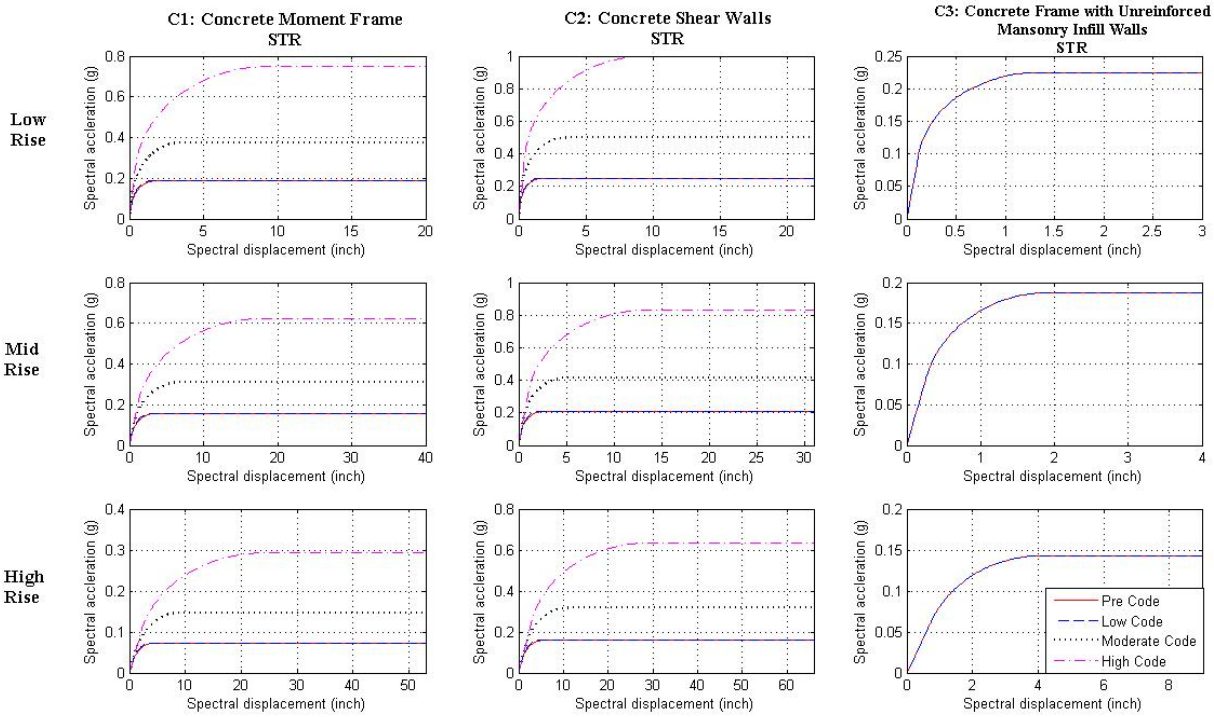

Figure A56: Multilinear Pushover/Capacity Curves for HAZUS Concrete Buildings

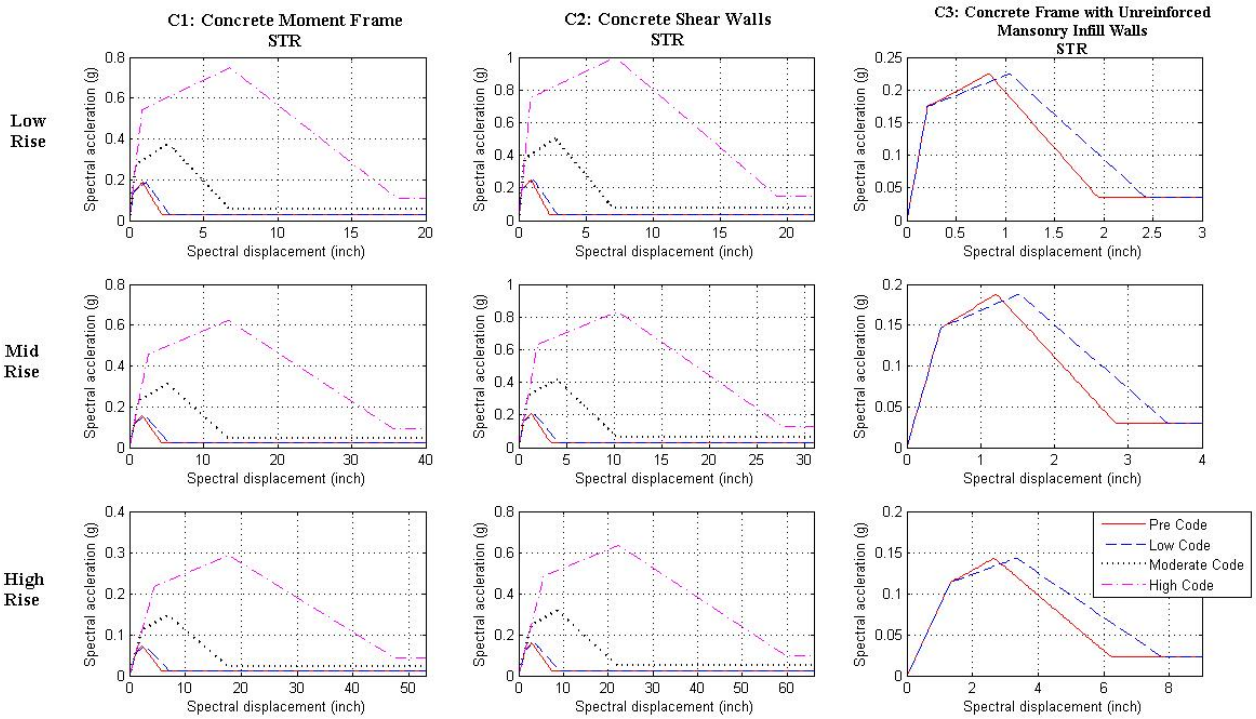

XML Files

- Inventory (filename: *NAME*_Inventory.xml)


```
<?xml version="1.0" encoding="utf-8"?>
<Inventory value="LA">
  <BDGs>
    <item SiteClass="B" T="2.0" code="Pre" index="0" lat="34.024742" lon="-
118.221034" occ="COM2" str="C2H"/>
    <item SiteClass="D" T="1.0" code="Pre" index="1" lat="34.025691" lon="-
118.222903" occ="COM2" str="C1M"/>
    <item SiteClass="C" T="2.0" code="Pre" index="2" lat="34.046528" lon="-
118.252319" occ="COM4" str="C1H"/>
    <item SiteClass="B" T="1.0" code="Pre" index="3" lat="34.052646" lon="-
118.254994" occ="COM9" str="C1M"/>
    <item SiteClass="E" T="2.0" code="Pre" index="4" lat="34.031037" lon="-
118.266206" occ="COM4" str="C1H"/>
    <item SiteClass="C" T="0.5" code="Pre" index="5" lat="34.071270" lon="-
118.198160" occ="COM2" str="C2L"/>
    <item SiteClass="C" T="2.0" code="Pre" index="6" lat="33.945742" lon="-
118.384292" occ="RES4" str="C2H"/>
```

```
    <item SiteClass="E" T="0.5" code="Pre" index="7" lat="34.047007" lon="-
118.253627" occ="COM1" str="C1L"/>
                                        ...
                                        ...
    <item SiteClass="C" T="0.5" code="Pre" index="60" lat="34.025316" lon="-
118.202715" occ="GOV1" str="C2L"/>
    <item SiteClass="C" T="0.5" code="Pre" index="61" lat="34.082252" lon="-
118.480591" occ="EDU2" str="C2L"/>
  </BDGs>
</Inventory>
```

- Fragility (filename: Fragility_*HAZUSstructure_HAZUScode_Period*.xml)

```
<?xml version="1.0" encoding="utf-8"?>
<spectral_acceleration units="seconds" value="2.0">
  <iml>
    <item index="0" value="1.000E-003"/>
    <item index="1" value="1.020E-003"/>
    <item index="2" value="1.041E-003"/>
    <item index="3" value="1.062E-003"/>
    <item index="4" value="1.083E-003"/>
            ...
            ...
    <item index="459" value="9.701E+000"/>
    <item index="460" value="9.897E+000"/>
  </iml>
  <fragility code="Moderate" name="C1H">
    <damage_state name="Slight">
      <item index="0" value="2.640E-012"/>
      <item index="1" value="3.266E-012"/>
      <item index="2" value="4.037E-012"/>
      <item index="3" value="4.986E-012"/>
      <item index="4" value="6.153E-012"/>
            ...
            ...
      <item index="459" value="1.000E+000"/>
      <item index="460" value="1.000E+000"/>
    </damage_state>
    <damage_state name="Moderate">
            ...
            ...
    </damage_state>
    <damage_state name="Extensive">
```

```
            ...
            ...
    </damage_state>
    <damage_state name="Complete">
            ...
            ...
    </damage_state>
  </fragility>
</spectral_acceleration>
```

- Vulnerability (filename: Vulnerability_*HAZUSstructure_HAZUScode_HAZUSoccupation_Period*.xml)

```
<?xml version="1.0" encoding="utf-8"?>
<spectral_acceleration units="seconds" value="2.0">
  <iml>
    <item index="0" value="1.000E-002"/>
    <item index="1" value="1.122E-002"/>
    <item index="2" value="1.259E-002"/>
    <item index="3" value="1.413E-002"/>
    <item index="4" value="1.585E-002"/>
          ...
          ...
    <item index="59" value="8.913E+000"/>
    <item index="60" value="1.000E+001"/>
  </iml>
  <vulnerability code="High" name="C1H" occupancy="COM6">
    <item index="0" value="3.529E-006"/>
    <item index="1" value="6.130E-006"/>
    <item index="2" value="1.055E-005"/>
    <item index="3" value="1.793E-005"/>
    <item index="4" value="3.002E-005"/>
          ...
          ...
    <item index="59" value="9.990E-001"/>
    <item index="60" value=" NaN"/>
  </vulnerability>
</spectral_acceleration>
```

Table A1: Legend for Tables 7 through 9. The addresses (and zip codes) have been hidden for the sake of anonymity.

Building #	Address	Zip Code	Occupancy Type	Height	Structure Type
Building 1	[redacted]	[redacted]	COM2	High	C2
Building 2	[redacted]	[redacted]	COM2	Mid	C1
Building 3	[redacted]	[redacted]	COM4	High	C1
Building 4	[redacted]	[redacted]	COM9	Mid	C1
Building 5	[redacted]	[redacted]	COM4	High	C1
Building 6	[redacted]	[redacted]	COM2	Low	C2
Building 7	[redacted]	[redacted]	RES4	High	C2
Building 8	[redacted]	[redacted]	COM1	Low	C1
Building 9	[redacted]	[redacted]	COM4	High	C2
Building 10	[redacted]	[redacted]	COM1	Low	C2
Building 11	[redacted]	[redacted]	COM2	Mid	C2
Building 12	[redacted]	[redacted]	COM1	Low	C1
Building 13	[redacted]	[redacted]	COM2	Mid	C2
Building 14	[redacted]	[redacted]	RES4	High	C2
Building 15	[redacted]	[redacted]	COM4	High	C2
Building 16	[redacted]	[redacted]	COM4	High	C1
Building 17	[redacted]	[redacted]	RES4	High	C1
Building 18	[redacted]	[redacted]	COM4	High	C1
Building 19	[redacted]	[redacted]	COM6	High	C1
Building 20	[redacted]	[redacted]	RES4	High	C1
Building 21	[redacted]	[redacted]	RES3	High	C2
Building 22	[redacted]	[redacted]	RES3	High	C1
Building 23	[redacted]	[redacted]	RES4	High	C1
Building 24	[redacted]	[redacted]	RES6	High	C2
Building 25	[redacted]	[redacted]	RES4	High	C2
Building 26	[redacted]	[redacted]	RES4	High	C1
Building 27	[redacted]	[redacted]	RES4	High	C1
Building 28	[redacted]	[redacted]	RES4	High	C1
Building 29	[redacted]	[redacted]	RES4	High	C2
Building 30	[redacted]	[redacted]	RES4	High	C1
Building 31	[redacted]	[redacted]	RES3	High	C1
Building 32	[redacted]	[redacted]	COM4	High	C1
Building 33	[redacted]	[redacted]	COM4	High	C1
Building 34	[redacted]	[redacted]	COM1	High	C2
Building 35	[redacted]	[redacted]	COM4	High	C1
Building 36	[redacted]	[redacted]	RES6	High	C2
Building 37	[redacted]	[redacted]	RES3	High	C1
Building 38	[redacted]	[redacted]	COM4	High	C2

Building 39	[redacted]	[redacted]	COM4	High	C1
Building 40	[redacted]	[redacted]	COM4	High	C1
Building 41	[redacted]	[redacted]	IND2	High	C2
Building 42	[redacted]	[redacted]	COM4	High	C1
Building 43	[redacted]	[redacted]	COM4	High	C2
Building 44	[redacted]	[redacted]	EDU2	High	C1
Building 45	[redacted]	[redacted]	COM4	High	C1
Building 46	[redacted]	[redacted]	RES4	High	C2
Building 47	[redacted]	[redacted]	COM1	Mid	C2
Building 48	[redacted]	[redacted]	COM1	High	C1
Building 49	[redacted]	[redacted]	RES3	High	C2
Building 50	[redacted]	[redacted]	RES3	High	C1
Building 51	[redacted]	[redacted]	COM4	High	C1
Building 52	[redacted]	[redacted]	IND2	High	C1
Building 53	[redacted]	[redacted]	COM4	High	C2
Building 54	[redacted]	[redacted]	COM4	High	C1
Building 55	[redacted]	[redacted]	COM4	High	C1
Building 56	[redacted]	[redacted]	RES3	High	C1
Building 57	[redacted]	[redacted]	RES3	High	C1
Building 58	[redacted]	[redacted]	COM4	High	C2
Building 59	[redacted]	[redacted]	COM4	High	C2
Building 60	[redacted]	[redacted]	IND2	High	C2
Building 61	[redacted]	[redacted]	GOV1	Low	C2
Building 62	[redacted]	[redacted]	EDU2	Low	C2

REFERENCES

Faison, H. (2008). “Magnitude 5.4 Earthquake in Los Angeles, July 29, 2008.” *PEER News,* <http://peer.berkeley.edu/news/2008/la_eq_july_2008.html> (August 05, 2009).

Federal Emergency Management Agency (2004), "NEHRP Recommended Provisions for Seismic Regulations for New Buildings and Other Structures, Part 1: Provisions," FEMA 450-1/2003 Edition, Washington, DC.

FEMA. (2006). "HAZUS-MH MR-3 Technical Manual." Federal Emergency Management Agency, Washington, D.C.

Karaca, E. and Luco, N. (2008). “Development of Hazard-Compatible Building Fragility and Vulnerability Models.” Proceedings of The 14th World Conference on Earthquake Engineering, Bejing, China.

Karaca, E. & Luco, N. (2009), "Development of Seismic Hazard Compatible Building Fragility Functions: Application to HAZUS Building Types," Under revision for publication in *Earthquake Spectra.*

Ryu, H., Luco, N., Baker, J. W., and Karaca, E. (2008). “Converting HAZUS Capacity Curves to Seismic Hazard-Compatible Building Fragility Functions: Effect of Hysteretic Models.” Proceedings of The 14th World Conference on Earthquake Engineering, Bejing, China.

“SCEDC | San Fernando Earthquake (1971).” *Southern California Earthquake Data Center Home*, <http://www.data.scec.org/chrono_index/sanfer.html> (August 05, 2009).